

**THE ROLE OF PITUITARY ADENYLATE CYCLASE-ACTIVATING
POLYPEPTIDE (PACAP) IN THE VENTROMEDIAL NUCLEUS AND ITS
ASSOCIATION WITH THE MELANOCORTIN SYSTEM IN REGULATING
ADAPTIVE THERMOGENESIS**

by

Thecla Rae McMillan

B.Sc., The University of British Columbia, 2013

THESIS SUBMITTED IN PARTIAL FULFILLMENT OF
THE REQUIREMENTS FOR THE DEGREE OF
MASTER OF SCIENCE
IN
HEALTH SCIENCES

UNIVERSITY OF NORTHERN BRITISH COLUMBIA

July 2017

© Thecla Rae McMillan, 2017

ABSTRACT

Accumulation of excess white adipose tissue in obesity has detrimental consequences for metabolic health. Activation of thermogenic adipocytes confers beneficial effects on metabolic health and is considered a potential therapeutic target for human obesity. Hormones modulating adaptive thermogenesis include melanocortins and pituitary adenylate cyclase-activating polypeptide (PACAP). In PACAP $-/-$ mice, metabolism and thermogenic capacity in response to cold is impaired. I hypothesized PACAP acts in the ventromedial nucleus of the hypothalamus, upstream of the melanocortin system, to regulate sympathetic stimulation of thermogenesis. To assess this, PACAP $+/+$ and PACAP $-/-$ mice were cold acclimated to 4°C and given daily injections of a melanocortin receptor agonist, Melanotan II (MTII), for 24 days. The effect of MTII on thermogenesis was examined by physiological, molecular, and histological analyses. Results show MTII partially rescued the impaired thermogenic capacity in PACAP $-/-$ mice as compared to PACAP $+/+$ mice, providing evidence to support our hypothesis.

TABLE OF CONTENTS

Abstract		ii
Table of Contents		iii
List of Figures		v
List of Abbreviations		xi
Chapter One	Endocrine Physiology of Obesity: Energy Homeostasis and Thermogenesis	
1.1	Obesity as a Disease	2
1.2	Causes of Obesity	3
1.3	White Adipose Tissue as a Storage and Endocrine Organ	5
1.4	Leptin: A Key Regulator in Energy Homeostasis	8
1.5	The Central Melanocortin System in Energy Homeostasis	12
1.6	Brown Adipose Tissue as a Potential Therapeutic Target for Obesity	14
1.7	Thermogenesis in Brown Adipose Tissue	16
1.8	Pituitary Adenylate Cyclase-Activating Polypeptide (PACAP): Essential for the Thermogenic Response in BAT	21
1.9	Gap in Literature: Connecting PACAP and the Melanocortin System	24
1.10	Hypothesis and Research Objectives	25
1.11	References	27
Chapter Two	Pharmacological Intervention with Melanotan II Partially Rescues the Impaired Thermogenic Capacity of PACAP $-/-$ Mice	
2.1	Introduction	37
2.2	Materials and Methods	44
2.3	Results	57
2.4	Discussion	67
2.5	References	80
2.6	Appendix	89
Chapter Three	Creating a Viral Construct for Genetic Intervention Aimed at Restoring Impaired Thermogenesis of PACAP $-/-$ Mice	
3.1	Introduction	91
3.2	Materials and Methods	98
3.3	Results	108
3.4	Discussion	110
3.5	References	118

Chapter Four	Concluding Remarks for PACAP's Association with the Melanocortin System in Regulating Adaptive Thermogenesis	
4.1	Summary	126
4.2	Significance	129
4.3	References	132

LIST OF FIGURES

- Figure 1.1.** Factors contributing to the energy balance equation. 4
- Figure 1.2.** Key adipokines and adipo-cytokines secreted by white adipose tissue. 7
TNF- α , tumor necrosis factor- α ; MCP-1, monocyte chemoattractant protein-1; IL-6, interleukin-6; PAI-1, plasminogen activator inhibitor-1. Reprinted from “The Effects of Exercise Training on Obesity-Induced Dysregulated Expression of Adipokines in White Adipose Tissue”, by T. Sakurai, J. Ogasawara, T. Kizaki, S. Sato, Y. Ishibashi, M. Takahashi et al., 2013, *International Journal Of Endocrinology*, 1-28. Copyright © 2013 Takuya Sakurai et al. Reprinted with permission from author.
- Figure 1.3.** Pathways mediating leptin action in the arcuate nucleus for its role in appetite regulation. Illustration by D. La Vine. MUTAGENETIX™, B. Beutler and colleagues, 2012, Center for the Genetics of Host Defense, UT Southwestern, Dallas, TX. Copyright © LabArchives, LLC. Reprinted with permission from author. 10
- Figure 1.4.** Multiple peptides produced from the single pro-protein, proopiomelanocortin (POMC). Illustration by R. Bowen, 2006, Colorado State University. Obtained from <http://www.vivo.colostate.edu/hbooks/pathphys/endocrine/hypopit/acth.html>. Reprinted with permission from author. 13
- Figure 1.5.** Coronal cross section of the brain showing the location of the hypothalamus and close-up five key hypothalamic nuclei involved in the regulation of energy metabolism. PVN; paraventricular nucleus, DMN; dorsomedial nucleus, LHA; lateral hypothalamic area, VMN; ventromedial nucleus, ARC; arcuate nucleus, 3V; third ventricle. Adapted from “Revisiting the Ventral Medial Nucleus of the Hypothalamus: The Roles of SF-1 Neurons in Energy Homeostasis”, by Y. Choi, T. Fujikawa, J. Lee, A. Reuter, & K. Kim, 2013, *Frontiers In Neuroscience*, 7. Copyright © 2013 Choi, Fujikawa, Lee, Reuter and Kim. Adapted with permission from author. 15
- Figure 1.6.** Histological representation differentiating WAT and BAT. WAT is unilocular with large lipid droplets (imaged at 40x), while BAT contains multilocular lipid droplets with a characteristic abundance of mitochondria (imaged at 60x using oil immersion). Images from studies in the Gray lab. 15
- Figure 1.7.** Cold-induced activation of adaptive thermogenesis in brown adipose tissue. UCP1; uncoupling protein 1. Adapted from “Activation and recruitment of brown adipose tissue by cold exposure and food ingredients in humans”, by M. Saito, T. Yoneshiro, & M. Matsushita, 2016, *Best Practice & Research Clinical Endocrinology &* 17

Metabolism, 30(4), 537-547. Copyright © 2017 Elsevier B.V. Adapted with permission from publisher.

- Figure 1.8.** Molecular mechanisms of adaptive thermogenesis at the level of brown adipocytes. Adapted from Wikipedia, 2009. Obtained from <https://en.wikipedia.org/wiki/Thermogenesis>. 19
- Figure 1.9.** Proposed pathways of neuropeptides that interact to induce adaptive thermogenesis in BAT in response to cold exposure. VMN; ventromedial nucleus, PACAP; pituitary adenylate cyclase-activating polypeptide, MC; melanocortin system, SNA; sympathetic nerve activity, BAT; brown adipose tissue. Images adapted from “Revisiting the Ventral Medial Nucleus of the Hypothalamus: The Roles of SF-1 Neurons in Energy Homeostasis”, by Y. Choi, T. Fujikawa, J. Lee, A. Reuter, & K. Kim, 2013, *Frontiers In Neuroscience*, 7. Copyright © 2013 Choi, Fujikawa, Lee, Reuter and Kim. Adapted with permission from author. 23
- Figure 2.1.** Sympathetic and endocrine control of BAT thermogenesis. β AR; beta-adrenergic receptor, NE; norepinephrine, NP; natriuretic peptide, T4; thyroxine, UCP1; uncoupling protein 1, WAT; white adipose tissue. Adapted from “Activation and recruitment of brown adipose tissue by cold exposure and food ingredients in humans”, by M. Saito, T. Yoneshiro, & M. Matsushita, 2016, *Best Practice & Research Clinical Endocrinology & Metabolism*, 30(4), 537-547. Copyright © 2017 Elsevier B.V. Adapted with permission from publisher. 38
- Figure 2.2.** Proposed pathways of interaction for adaptive thermogenesis in BAT in response to cold exposure. VMN; ventromedial nucleus, PACAP; pituitary adenylate cyclase-activating polypeptide, MC; melanocortin system, SNA; sympathetic nerve activity, BAT; brown adipose tissue. Images adapted from “Revisiting the Ventral Medial Nucleus of the Hypothalamus: The Roles of SF-1 Neurons in Energy Homeostasis”, by Y. Choi, T. Fujikawa, J. Lee, A. Reuter, & K. Kim, 2013, *Frontiers In Neuroscience*, 7. Copyright © 2013 Choi, Fujikawa, Lee, Reuter and Kim. Adapted with permission from author. 45
- Figure 2.3.** Schematic of methodology over the course of the 6-week experiment. 48
- Figure 2.4.** Methodological steps used to analyze BAT sections for lipid area at 60x oil immersion. A. Images were converted to grayscale. B. Contrast was maximized. C. Segments that were not brown adipocytes were selectively deleted (indicated as red). D. Image was binarized and “white” area counted as lipid. 54

Figure 2.5.	Methodological steps used to determine cell area counts in histological sections of gWAT imaged at 20x. A. Images were converted to grayscale. B. Differential contrast was maximized. C. Images were binarized. D. Adipocytes not entirely displayed within the field of view were excluded from analyses.	56
Figure 2.6.	Body mass of PBS WT, PBS KO, MTII WT, and MTII KO mice over the course of the experiment. Treatment with vehicle (PBS) or MTII began on Day 7. Data are mean \pm SEM. Two-way ANOVA, $p > 0.05$.	59
Figure 2.7.	Difference of fat and lean mass as a percentage of total mass in PBS WT, PBS KO, MTII WT, and MTII KO mice pre and post 4°C cold challenge. Data are mean \pm SEM. Two-way ANOVA, $p > 0.05$.	59
Figure 2.8.	Percent tissue mass per total body mass of different tissue types in PBS WT, PBS KO, MTII WT, and MTII KO mice after 4-week 4°C cold challenge. Data are mean \pm SEM. Unpaired t-tests. * $p < 0.05$ indicates a genotype effect within the same treatment.	60
Figure 2.9.	A. Norepinephrine induced thermogenesis in cold-acclimated PBS WT, PBS KO, MTII WT, and MTII KO mice. B. Mean basal metabolic rate (BMR) and maximal metabolic rate (MMR) of cold-acclimated PBS WT, PBS KO, MTII WT, and MTII KO mice. Data are expressed as mean \pm SEM. Two-way ANOVA. * $p < 0.05$ indicates a genotype effect within the same treatment.	62
Figure 2.10.	Respiratory exchange ratio (RER) of cold-acclimated PBS WT, PBS KO, MTII WT, and MTII KO mice. Statistical significance ($p < 0.05$) between PBS WT and PBS KO at 8 and 10 minutes and between MTII WT and MTII KO at 2, 4 and 6 minutes. Two-way ANOVA.	63
Figure 2.11.	Gene expression in BAT of cold-acclimated PBS WT, PBS KO, MTII WT, and MTII KO mice. Target gene expression was normalized to two reference genes: RPL19 and PPIA. Data are expressed as \pm SEM. One-way ANOVA for each gene, $p > 0.05$.	65
Figure 2.12.	A. Average percent lipid area/field of view in cold-acclimated PBS WT, PBS KO, MTII WT, and MTII KO mice. B. Average numbers of nuclei per ROI in cold-acclimated PBS WT, PBS KO, MTII WT, and MTII KO mice. Data are expressed as \pm SEM. One-way ANOVA, $p > 0.05$.	66
Figure 2.13.	Number of cells within each cell area bin (μm^3) in cold-acclimated PBS WT or MTII WT mice. Data are expressed as \pm SEM. Unpaired t-tests, $p > 0.05$.	68

- Figure 2.14.** Representative images of hematoxylin and eosin-stained gWAT observed at 4x and 20x in cold-acclimated PBS WT (A), PBS KO (B), MTII WT (C), and MTII KO mice (D). 69
- Figure S2.1.** PCR assessment of PACAP genotype in *Mus musculus*. Electrophoresis performed on ethidium bromide stained 1.5% agarose gel at 100V for 20 minutes. Each well represents a different animal. (+/+) denotes PACAP wildtype, (+/-) PACAP heterozygote, and (-/-) PACAP knockout. 89
- Figure S2.2.** Assessment of RNA integrity of isolated *Mus musculus* brown adipose tissue (BAT) with electrophoresis on an ethidium bromide stained 1.5% agarose gel at 100V for 30 minutes. Each well represents a different BAT sample. The top band indicates intact 28S rRNA and the bottom band indicates intact 18S rRNA. 89
- Figure 3.1.** A. Plasmid map for pscAAV-GFP (Addgene Plasmid #32396). Image courtesy of John T. Gray. B. The CMV promoter within pscAAV-GFP was replaced with the SF1 promoter (pscAAV-SF1-GFP) with the goal of expressing GFP specifically in the VMN of the hypothalamus, a region of the brain known to specifically express SF1. Virus will be delivered to the brain via stereotaxic injection into the VMN. Adapted with permission from the author. Source: <https://www.addgene.org/32396/>. Accessed May 4, 2017. 99
- Figure 3.2.** Plasmid map for pGEM®-T Vector (Promega). SF1 insert is ligated into the lacZ gene by attaching to overhanging thymine nucleotides, disrupting the lacZ gene. Accessed from <https://www.promega.ca/products/pcr/pcr-cloning/pgem-t-vector-systems/>. Copyright © 2017 Promega Corporation. Image reproduced with permission from the corporation. 104
- Figure 3.3.** Location of lambda and bregma as defined by Dr. George Paxinos. Interaural line corresponds with the placement of the ear bars. Reproduced from “The rat brain in stereotaxic coordination”, by G. Paxinos, & C. Watson, 1998, 1st Edition, p. 11. Copyright © 2017 Academic Press/Elsevier. Reproduced with permission from publisher. 107
- Figure 3.4.** A. Stereotaxic administrations are given using x, y, and z coordinates to a specific location and depth. B. Location of injection into the VMN of the hypothalamus. Illustrations by Encapsula NanoSciences LLC, Brentwood, TN. Copyright © 2014 Encapsula NanoSciences LLC. Obtained from <https://www.clodrosome.com/animal-injection/>. Adapted with permission from Encapsula NanoSciences. 107

- Figure 3.5.** A section of nucleotides matching from NCBI's BLAST between the pscAAV-GFP plasmid sequence provided from Addgene (Query) and the isolated plasmid (Sbjct) sequenced using M13 Reverse primer. Yellow indicates AvrII RE site (5' CCT AGG 3') and red indicates BspEI RE site (5' TCC GGA 3'). A small section of the isolated plasmid DNA was unreadable (indicated by "N") using M13 Reverse primer. A matching sequence was confirmed using M13 Forward primer (results not shown). 109
- Figure 3.6.** NCBI's BLAST search of the sequence obtained from SF1-pGEM®-T Vector (Sbjct) using T7 primer revealed a match to a section of the *Mus musculus* strain C57BL/6J, chromosome 2, GRCm38.p4 (Query): the region of the mouse genome that houses the SF1 promoter. Yellow indicates AvrII RE site (5' CCT AGG 3') and red indicates BspEI RE site (5' TCC GGA 3') added to the PCR-amplified SF1. 111
- Figure 3.7.** A. Coronal cross section of the brain showing the location of the hypothalamus and close-up five key hypothalamic nuclei involved in the regulation of energy metabolism. PVN; paraventricular nucleus, DMN; dorsomedial nucleus, LHA; lateral hypothalamic area, VMN; ventromedial nucleus, ARC; arcuate nucleus, 3V; third ventricle. Adapted from "Revisiting the Ventral Medial Nucleus of the Hypothalamus: The Roles of SF-1 Neurons in Energy Homeostasis", by Y. Choi, T. Fujikawa, J. Lee, A. Reuter, & K. Kim, 2013, *Frontiers In Neuroscience*, 7. Copyright © 2013 Choi, Fujikawa, Lee, Reuter and Kim. Adapted with permission from author. B. Dorsal view of the mouse brain. C. Ventral view of the mouse brain (box indicates hypothalamus). D. Blue dye observed in the hypothalamus. E. Anterior coronal section through the hypothalamus; blue dye observed in the 3V and surrounding hypothalamic tissues. F. Middle coronal section through the hypothalamus; dye localized along the 3V. G. Posterior coronal section through the hypothalamus; dye localized further dorsal along the 3V. 112
- Figure 3.8.** Middle coronal cross section through the hypothalamus of *Mus musculus* stereotaxically injected with 5x loading dye. Ruler shows 1mm increments. 114
- Figure 3.9.** The CMV promoter replaced with the SF1 promoter, and the GFP gene replaced with the PACAP gene (pscAAV-SF1-PACAP) with the goal of expressing PACAP specifically in the VMN of the hypothalamus, a region of the brain known to specifically express SF1. Virus will be delivered to the brain via stereotaxic injection into the VMN. Adapted with permission from the author. Source: <https://www.addgene.org/32396/>. Accessed May 4, 2017. 117

Figure 4.1. Hypothesized pathways of interaction for adaptive thermogenesis in BAT in response to cold exposure. VMN; ventromedial nucleus, PACAP; pituitary adenylate cyclase-activating polypeptide, MC; melanocortin system, SNA; sympathetic nerve activity, BAT; brown adipose tissue. Images adapted from “Revisiting the Ventral Medial Nucleus of the Hypothalamus: The Roles of SF-1 Neurons in Energy Homeostasis”, by Y. Choi, T. Fujikawa, J. Lee, A. Reuter, & K. Kim, 2013, *Frontiers In Neuroscience*, 7. Copyright © 2013 Choi, Fujikawa, Lee, Reuter and Kim. Adapted with permission from author.

127

LIST OF ABBREVIATIONS

α -MSH	Alpha Melanocyte-Stimulating Hormone
β 3-AR	Beta-3 Adrenergic Receptor
3V	Third Ventricle
Amp	Ampicillin
ANOVA	Analysis of Variance
ARC	Arcuate Nucleus
ATP	Adenosine Triphosphate
BAT	Brown Adipose Tissue
BBB	Blood Brain Barrier
BMR	Basal Metabolic Rate
CMV	Cytomegalovirus
DMN	Dorsomedial Nucleus
FA	Fatty Acid
FFA	Free Fatty Acid
GFP	Green Fluorescent Protein
GPCR	G Protein-Coupled Receptors
gWAT	Gonadal White Adipose Tissue
HSL	Hormone Sensitive Lipase
ICV	Intracerebroventricular
ingWAT	Inguinal White Adipose Tissue
KO	Knock Out
LB	Luria Broth
LHA	Lateral Hypothalamic Area

MCR	Melanocortin Receptor
MMR	Maximal Metabolic Rate
MTII	Melanotan II
NE	Norepinephrine
PACAP	Pituitary Adenylate Cyclase-Activating Polypeptide
PBS	Phosphate-Buffered Saline
PCR	Polymerase Chain Reaction
POMC	Pro-opiomelanocortin
PVN	Paraventricular Nucleus
RE	Restriction Enzyme
RER	Respiratory Exchange Ratio
scAAV9	Self-Complimentary Adeno-Associated Virus Serotype 9
SEM	Standard Error Mean
SF1	Steroidogenic Factor 1
SNA	Sympathetic Nerve Activity
UCP1	Uncoupling Protein 1
VMN	Ventromedial Nucleus
WAT	White Adipose Tissue
WT	Wild Type

CHAPTER 1

Endocrine Physiology of Obesity: Energy Homeostasis and Thermogenesis

1.1 OBESITY AS A DISEASE

Obesity is a disease characterized by increased white adipose tissue (WAT) mass resulting from both adipocyte hyperplasia and cellular hypertrophy (Galic, Oakhill, & Steinberg, 2010; Lee, & Shao, 2014). With chronic food abundance and the change to sedentary work practices and lifestyles in modern society, the prevalence of adult obesity has more than doubled worldwide since 1980 (Finucane et al., 2011). In 2014, it was estimated that 39% of the world's adult population was overweight, defined by the World Health Organization (WHO) as a person with a body mass index (BMI) (body mass (kg)/height (m)²) greater than or equal to 25 (Lee, & Shao, 2014; WHO, 2016; Yeo, & Heisler, 2012). Overweight and obesity affects all age and socioeconomic groups and poses a substantial economic burden on society and health care systems due to increased risk of developing chronic disease such as cardiovascular disease, type 2 diabetes, arthritis, hypertension, stroke, and some forms of cancer (Lidell, Betz, & Enerbäck, 2014; WHO, 2016). In addition, while the prevalence of obesity continues to rise, so too does the stigma (Lidell et al., 2014). Negative stereotypes that persons with obesity are lazy, lacking self-discipline, or unmotivated may translate into inequalities in health care, education and employment (Canadian Obesity Network, 2016). Research has shown that body weight is determined by both environmental and genetic factors. Genetically, body weight is a polygenic factor, similar to height, skin, eye, and hair color, indicating that the development of obesity is influenced by more than a person's motivation, self-control, and lifestyle (Hinney, Vogel, & Hebebrand, 2010). A person's genetic predisposition to the disease can result from pathophysiological changes that lead to increased efficiency in energy metabolism and a state of chronic positive energy balance (Choquet, & Meyre, 2011; Walley, 2006). The consequences of overweight and obesity range from decreased overall quality of life to

premature death; indicating the necessity to understand the causes of obesity such that it can be prevented and treated effectively (Centre for Disease Control, 2016; Galic et al., 2010; WHO, 2016).

1.2 CAUSES OF OBESITY

Obesity is determined by both genetic makeup and environmental factors (Farooqi & O’Rahilly, 2006; Hinney, Vogel, & Hebebrand, 2010). The cause of obesity can be explained by a homeostatic imbalance in energy metabolism and impaired adipose tissue function (Harwood, 2012). Metabolic homeostasis is achieved when energy intake matches energy output. Energy intake consists of food consumption while energy expenditure includes basal metabolic rate, waste production, physical activity, and thermogenesis (Figure 1.1), which will be a major focus of the research in Chapters 2 and 3 and discussed in detail below.

When energy intake chronically exceeds energy expenditure, adipose tissue expands both in mass and size due to an increase in the number of cells and the size of the adipocytes, which increase as triglycerides accumulate within (Fonseca-Alaniz, Takada, Alonso-Vale, & Lima, 2007; Harwood, 2012). Research has shown that adipose tissue itself plays an important role in the maintenance of metabolic homeostasis. In obesity, WAT is dysfunctional with a change in the production of adipocyte-derived factors including adipokines (discussed below), free fatty acids (FFAs), and cytokines that control metabolic homeostasis of a variety of tissues on a molecular level (Greenberg, & Obin, 2006; Lee, & Shao, 2014). It is this dysfunctional WAT that is found to be associated with an increased risk for the chronic diseases listed above in obesity (Lee, & Shao, 2014). Thus, research into the biological mechanisms linking adipocyte function with energy homeostasis will shed light on the biological complexities of obesity and may lead to innovative therapeutic

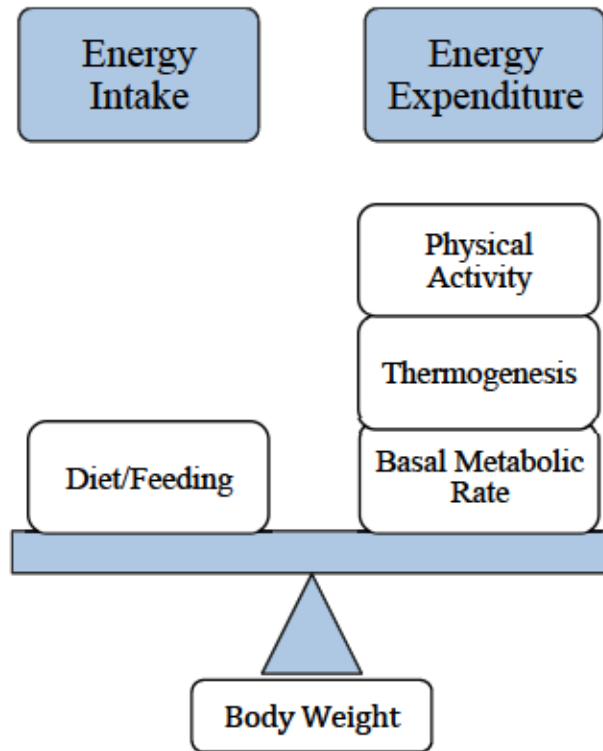


Figure 1.1. Factors contributing to the energy balance equation.

treatments for this disease. Further evidence for a key role of adipose tissue in the maintenance of energy homeostasis will be discussed here.

1.3 WHITE ADIPOSE TISSUE AS A STORAGE AND ENDOCRINE ORGAN

WAT is comprised predominantly of white adipocytes; a cell type specialized in storing energy as triglycerides. WAT also contains macrophages, fibroblasts, and preadipocytes held together by loose connective tissue and is highly vascularized and innervated by the autonomic nervous system (Ahima, 2006). It acts as a thermal insulator by reducing heat loss through the skin, and as a protective layer around organs and muscle groups where it softens impact to ensure proper functioning of these tissues without the loss of integrity (Harwood, 2012).

WAT has long been known for its role as an energy reservoir, involved in both lipid and glucose metabolism. In periods of caloric abundance, consumed glucose and lipids stimulate insulin release from the pancreas, which promotes uptake of FFAs in the liver and WAT where they are combined with glycerol to form triglycerides (Galic et al., 2010). Additionally, excess glucose is stored as triglycerides in the liver and WAT through the process of lipogenesis (Galic et al., 2010). During energy shortage or periods of fasting, insulin levels fall and stimulate lipolysis in WAT, resulting in glycerol and FFAs that supply gluconeogenic and oxidative pathways in the liver where glycogen breakdown occurs to increase circulating glucose levels, therefore supplying the brain and vital organs with energy (Galic et al., 2010; Harwood, 2012; Lee, & Shao, 2014; Vázquez-Vela, Torres, & Tovar, 2008).

Gavrilova et al. (2000) demonstrated the critical importance of white adipose tissue in metabolic homeostasis with their mouse model of lipotrophic diabetes, known as the A-ZIP/F-1 mouse line. The mouse line was generated by targeting an adipocyte-specific

transgene that expresses a dominant-negative protein, known as A-ZIP/F, resulting in the inhibition of adipocyte-specific proteins and DNA binding (Moitra et al., 1998). The result was mice that had virtually no WAT. The mice developed characteristics similar to those of humans with severe lipotrophic diabetes, including insulin resistance, hyperglycemia, hyperlipidemia, and fatty livers. Transplantation of healthy WAT into the A-ZIP/F-1 mice reversed the phenotype, and resulted in normoglycemic mice with lowered insulin levels, decreased serum triacylglycerols, decreased hepatic gluconeogenesis, and decreased amounts of fat deposited in the liver. These beneficial effects were dependent on the presence of transplanted WAT and thus it became evident that the lack of WAT is metabolically detrimental (Gavrilova et al., 2000). These results provided a compelling platform for the argument that adipose tissue plays an important role in maintaining homeostasis on a molecular level, as suggested above. In fact, research has shown that WAT effectively communicates with the body and brain through the secretion of greater than 50 adipocyte-specific factors that include hormones and cytokines (Figure 1.2) (Galic et al., 2010; Harwood, 2012; Lee, & Shao, 2014; Sakurai et al., 2013). These adipocyte-specific factors, known as adipokines, act on both central and peripheral organs such as the liver, pancreas, brain, and skeletal muscle to control diverse metabolic processes including energy expenditure, lipid metabolism, food intake, and inflammation (Harwood, 2012). The discovery of adipokines led to the now widely accepted and recognized role of WAT as a major endocrine organ, in contrast to its early classification as a passive, metabolically inactive organ that simply acted as a storage reservoir for energy (Galic et al., 2010; Greenberg, & Obin, 2006; Harwood, 2012; Lee, & Shao, 2014; Trayhurn, 2005; Vázquez-Vela et al., 2008). In the majority of cases of overweight or obesity, adipose tissue is characterized by profound histological and biochemical changes associated with

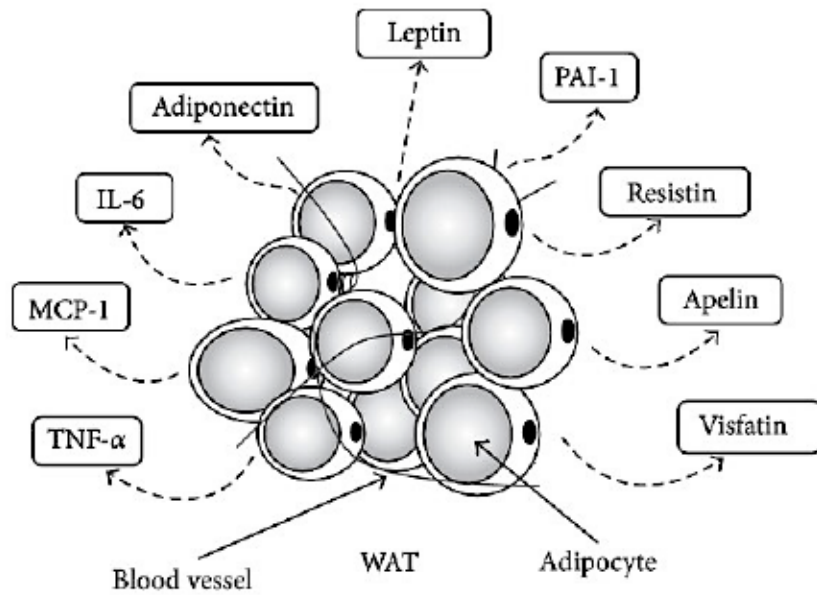


Figure 1.2. Key adipokines and adipo-cytokines secreted by white adipose tissue. TNF- α , tumor necrosis factor- α ; MCP-1, monocyte chemoattractant protein-1; IL-6, interleukin-6; PAI-1, plasminogen activator inhibitor-1. Reprinted from “The Effects of Exercise Training on Obesity-Induced Dysregulated Expression of Adipokines in White Adipose Tissue”, by T. Sakurai, J. Ogasawara, T. Kizaki, S. Sato, Y. Ishibashi, M. Takahashi et al., 2013, *International Journal Of Endocrinology*, 1-28. Copyright © 2013 Takuya Sakurai et al. Reprinted with permission from author.

dysregulation of adipokine secretion, lipotoxicity, and inflammation; all of which contribute to metabolic dysfunction (Ahima, 2006; Greenberg, & Obin, 2006). Although not *directly* part of the research in this thesis, the metabolic function of one of the most well studied adipokines, leptin, will be discussed here for further background. Of particular interest will be leptin's action on one of the systems of interest for this thesis; the melanocortin system, discussed in detail below.

1.4 LEPTIN: A KEY REGULATOR IN ENERGY HOMEOSTASIS

Leptin, the first adipocyte hormone to be identified, is produced mainly by adipocytes and crosses the blood-brain barrier to bind leptin receptors in the hypothalamus (Yeo, & Heisler, 2012). Leptin is also produced at low levels by the stomach, placenta, bone, skeletal muscle, and other tissues, although the target in these cases is likely to be local and therefore paracrine in action rather than endocrine (Trayhurn, 2005). Zhang et al. (1994) first identified leptin while studying obese mice with a naturally occurring genetic mutation in the *ob* gene (*ob/ob*). Without the *ob* gene, which was found to code for leptin (named by Halaas et al. in 1995), the mice were morbidly obese and diabetic due to severe hyperphagia and decreased energy expenditure. When treated with regular injections of leptin into the brain, the *ob/ob* mice reduced their food intake, increased their metabolic rate, and lost weight (Greenberg, & Obin, 2006). Although analogous genetic mutations in humans are extremely rare, the clinical presentation of patients with genetic mutations in the leptin gene or its receptor is very similar to the phenotype of the *ob/ob* mice and leptin therapy is beneficial in these cases (Farooqi, & O'Rahilly, 2006). These seminal findings exhibited the importance of leptin as a key regulator of energy balance, and introduced the idea that adipose tissue was an important endocrine organ involved in regulating whole body energy metabolism. Classic pathways of

leptin action in the brain and its effects on feeding behavior have been well elucidated and the best-described pathways are depicted in Figure 1.3.

Briefly, leptin acts on the melanocortin axis (discussed in detail below), positively regulating neurons within the arcuate nucleus (ARC) that express pro-opiomelanocortin (POMC) and cocaine- and-amphetamine regulated transcripts (CART). POMC then undergoes post-translational modification and is processed into alpha melanocyte-stimulating hormone (α -MSH), which then binds melanocortin 4 receptors (MC4R) to inhibit food intake (How, 2016; Yeo, & Heisler, 2012). Furthermore, leptin negatively regulates the MC4R antagonist agouti-related protein (AGRP) and neuropeptide Y (NPY) whose normal functions are to increase food intake, therefore further inhibiting food intake (How, 2016; Tabeta, & Beutler, 2012). Although leptin's role in appetite regulation through the modulation of the melanocortin system in the ARC has been extensively studied, it is apparent that the ARC cannot explain all aspects of leptin function (Bingham et al., 2008). For example, when leptin receptors were specifically deleted in POMC neurons, mouse body weights increased to only 18% of that observed in mice with complete lack of leptin receptors (Balthasar et al., 2004). This suggests that leptin acts elsewhere to control energy homeostasis, and that its function in other brain regions should be considered (Balthasar et al., 2004). As such, leptin has been shown to enhance energy expenditure by increasing thermogenesis, fatty acid (FA) oxidation, and plasma glucose levels (Havel, 2002). Acting in the ventromedial hypothalamus (VMN), leptin increases sympathetic nerve activity by means of the melanocortin system, resulting in activated thermogenesis (further discussed in Chapter 3) (Butler, & Cone, 2002; Hwa et al., 1996; Satoh et al., 1999; Scarpace, Matheny, Pollock, & Tumer, 1997; Voss-Andreae et al., 2007). Importantly, this mechanism will be further discussed throughout this thesis. Other

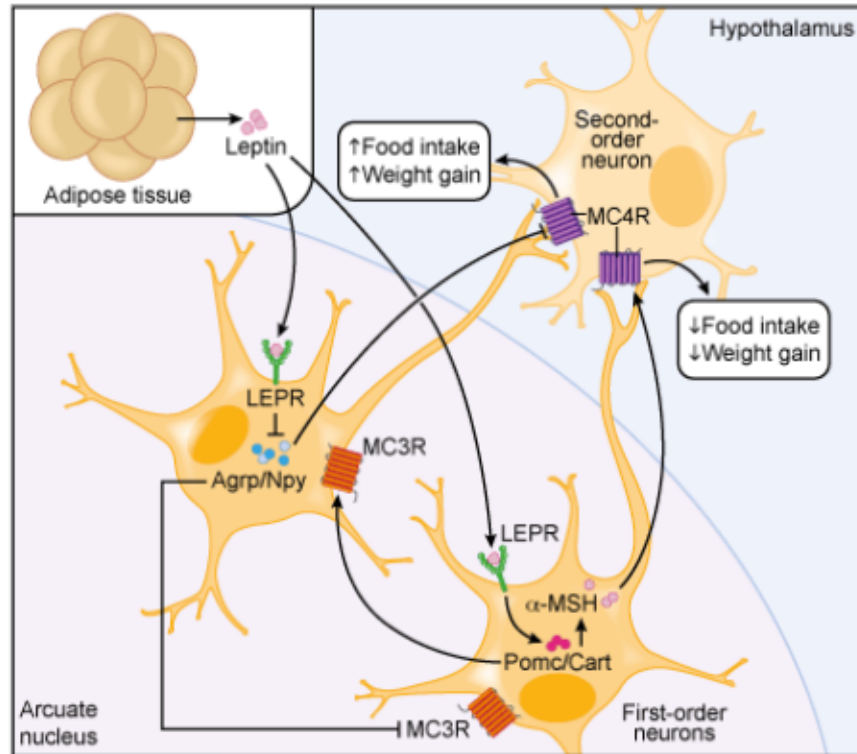


Figure 1.3. Pathways mediating leptin action in the arcuate nucleus for its role in appetite regulation. Illustration by D. La Vine. MUTAGENETIX™, B. Beutler and colleagues, 2012, Center for the Genetics of Host Defense, UT Southwestern, Dallas, TX. Copyright © LabArchives, LLC. Reprinted with permission from author.

functions of leptin include acting as a major signal to the reproductive system and as a factor in the immune system (Flier, 2004; Havel, 2002; Trayhurn, & Beattie, 2001).

Circulating leptin levels increase linearly with weight gain and decrease with weight loss or during fasting, proportional to adipose tissue mass. In healthy humans, leptin production is stimulated by adipocyte glucose metabolism in the postprandial state to reduce feeding behavior (Fonseca-Alaniz et al., 2007; Mueller et al., 1998). During fasting, both leptin and insulin decrease which stimulates appetite, inhibits sympathetic nerve activity, inhibits thermogenesis and suppresses the action of reproductive hormones, growth hormones and thyroid hormones (Ahima, 2006; Harwood, 2012). Whereas decreases in leptin inhibit food intake and food seeking behaviors, increases in leptin associated with overfeeding or obesity appear to have substantially less of a biological impact (Havel, 2002). For example, administering leptin to obese humans without leptin deficiency induces variable, modest, or no weight loss (Havel, 2002). Despite having high levels of leptin, which intuitively should reduce food intake and body fat, people with obesity maintain high levels of adipose tissue (Galic et al., 2010). The proposed reasoning for this phenomenon is leptin resistance, particularly in metabolically active tissues such as skeletal muscle (Westerterp-Platenga, Saris, Huckshorn, & Campfield, 2001). Therefore, the major role of leptin appears not to be as a restraint to limit energy intake and obesity, but rather an endocrine factor that allowed physiological adaptation to reduced energy intake in times of decreased nutrient availability and reduced body fat stores (Havel, 2002). Whether leptin resistance is the cause or consequence of obesity is yet to be identified, and while the metabolic effects of leptin on target tissues are robust, the precise mechanism by which it is secreted from the adipocyte remains elusive (Ahima, 2006; Stern, Rutkowski, & Scherer, 2016). Further investigation into the developmental origins and biological mechanisms of leptin is pertinent for potential

therapeutic targeting (Peirce, Carobbio, & Vidal-Puig, 2014; Stern et al., 2016). As mentioned above, however, one of the key mediators of leptin action is the melanocortin system, which will be discussed here (Butler, & Cone, 2002; Voss-Andreae et al., 2007).

1.5 THE CENTRAL MELANOCORTIN SYSTEM IN ENERGY HOMEOSTASIS

The central pathways mediating the melanocortin system's role in energy homeostasis is well characterized (Cone, 1999; Cone, 2005; Ellacott, & Cone, 2006). It detects and integrates a variety of neuronal, hormonal, and nutritional metabolic signals such as leptin (discussed above), insulin, glucose, and serotonin to influence energy metabolism (Jeong, Kim, & Lee, 2014). Melanocortins, such as α -MSH and β -endorphin, are a family of small peptides that originate from the POMC precursor (Figure 1.4) (Bowen, 2006).

Greenman et al. (2013) showed that mice with postnatal ablation of POMC neurons in the ARC in the hypothalamus resulted in an obese phenotype with reduced energy expenditure, similar to that observed in leptin-deficient animal models. POMC gene deletion and gene mutations have also shown to be highly correlated with obesity development in humans (Dubern et al., 2008; Challis et al., 2004; Krude et al., 1999; Yaswen, Diehl, Brennan, & Hochgeschwender, 1999). Additionally, when POMC is overexpressed in the ARC either by virus-associated gene delivery or genetic modification in leptin deficient animals, they were protected from the development of obesity (Li, Mobbs, & Scarpance, 2003; Mizuno, Kelly, Pasinetti, Roberts, & Mobbs, 2003). These studies demonstrate a clear role of the central POMC system in metabolic regulation.

Melanocortin receptor expression and function in the mammalian brain have been well elucidated since the 1990's (Cone, 1999; Jeong, Kim, & Lee, 2014). In genetically altered animals lacking the gene for melanocortin receptor types 3 and 4 (MC3R and MC4R, respectively), an obese phenotype ensues, providing evidence for the involvement of

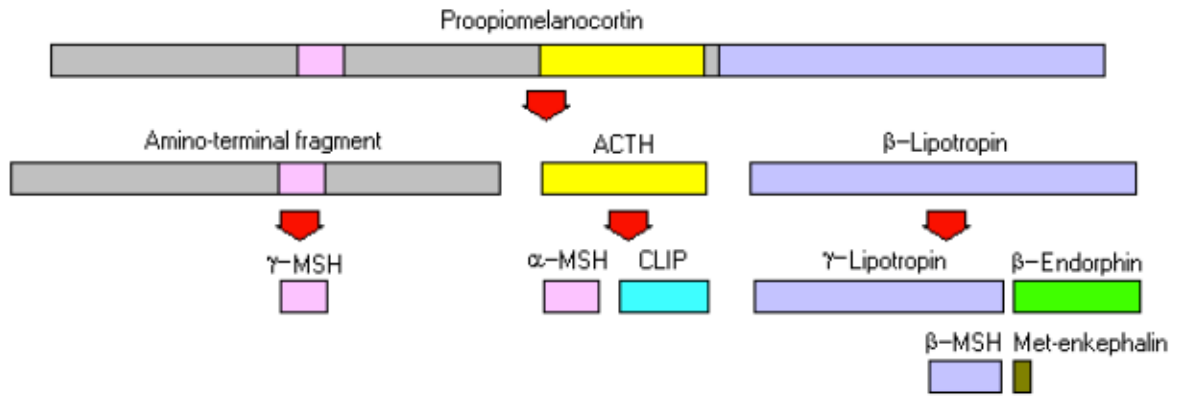


Figure 1.4. Multiple peptides produced from the single pro-protein, proopiomelanocortin (POMC). Illustration by R. Bowen, 2006, Colorado State University. Obtained from <http://www.vivo.colostate.edu/hbooks/pathphys/endocrine/hypopit/acth.html>. Reprinted with permission from author.

melanocortins in the regulation of energy metabolism (Cone, 1999). MC3Rs and MC4Rs are found in several brain regions in the hypothalamus known for the regulation of energy intake processes such as feeding, and energy output processes such as thermogenesis, including the paraventricular nucleus (PVN), the arcuate nucleus (ARC) (discussed earlier in terms of leptin regulation), the ventromedial nucleus (VMN) (the brain region of interest for Chapter 3), the lateral hypothalamic area (LHA), and dorsomedial nucleus (DMN) (Figure 1.5) (Cone, 1999). The research presented in this thesis relates to the melanocortin system's role in energy *output* through the activation of thermogenesis in brown adipose tissue (BAT).

1.6 BROWN ADIPOSE TISSUE AS A POTENTIAL THERAPEUTIC TARGET FOR OBESITY

Brown adipose tissue (BAT) has been well characterized in rodents and other small mammals (Haney et al., 2002). In humans, BAT was thought to exist predominantly in the interscapular region in infants only and was rapidly lost postnatally such that only vestigial amounts remained later in life (Haney et al., 2002; Nedergaard, Bengtsson, & Cannon, 2007). In 2007, however, it was shown that brown adipocytes reside in the cervical and supraclavicular regions in human adults (Bartelt, & Heeren, 2013; Haney et al., 2002). Similar to WAT, BAT is capable of accumulating and storing lipids. However, BAT is distinct from WAT in that its adipocytes contain an abundance of mitochondria (Figure 1.6) that are enriched with a specialized protein called uncoupling protein 1 (UCP1), which uncouples substrate oxidation from adenosine triphosphate (ATP) production such that heat is produced (Lidell et al., 2014; Peirce et al., 2014). This process of heat production is the major role of BAT and is known as adaptive thermogenesis (discussed below).

Interestingly, as a result of thermogenic stimuli, brown-like adipocytes are observed in some WAT regions: a process known as “browning” of WAT (Bartelt, & Heeren, 2013).

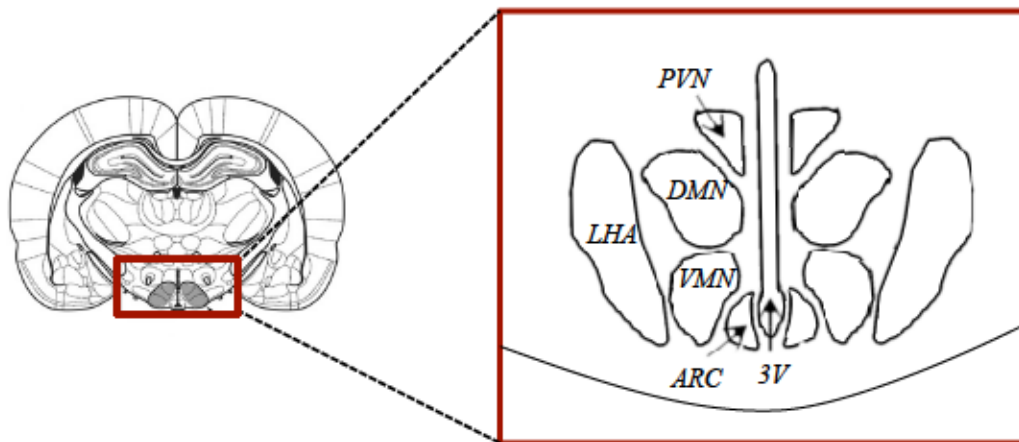
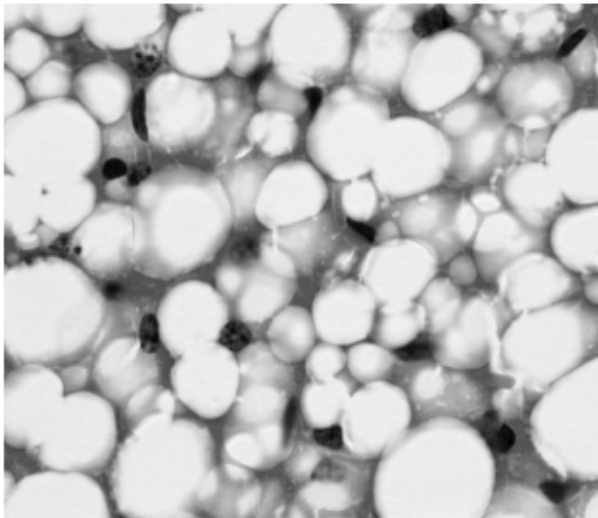


Figure 1.5. Coronal cross section of the brain showing the location of the hypothalamus and close-up five key hypothalamic nuclei involved in the regulation of energy metabolism. PVN; paraventricular nucleus, DMN; dorsomedial nucleus, LHA; lateral hypothalamic area, VMN; ventromedial nucleus, ARC; arcuate nucleus, 3V; third ventricle. Adapted from “Revisiting the Ventral Medial Nucleus of the Hypothalamus: The Roles of SF-1 Neurons in Energy Homeostasis”, by Y. Choi, T. Fujikawa, J. Lee, A. Reuter, & K. Kim, 2013, *Frontiers In Neuroscience*, 7. Copyright © 2013 Choi, Fujikawa, Lee, Reuter and Kim. Adapted with permission from author.

White Adipose Tissue



Brown Adipose Tissue

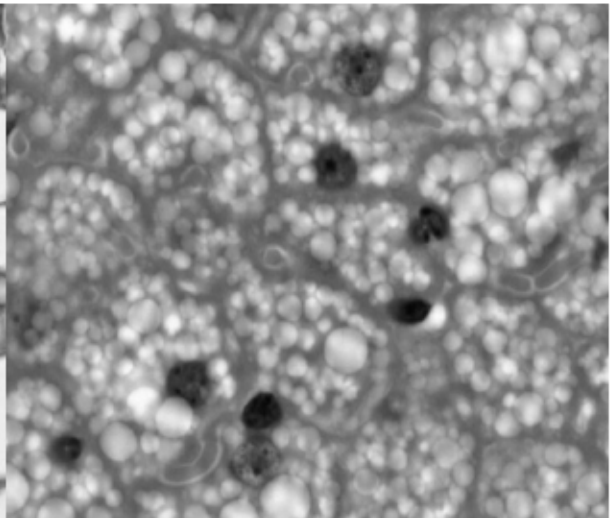


Figure 1.6. Histological representation differentiating WAT and BAT. WAT is unilocular with large lipid droplets (imaged at 40x), while BAT contains multilocular lipid droplets with a characteristic abundance of mitochondria (imaged at 60x using oil immersion). Images from studies in the Gray lab.

Although these adipocytes are capable of undergoing adaptive thermogenesis, their lineage is closer to that of white adipocytes than brown adipocytes (Bartelt, & Heeren, 2013; Giralt, & Villaroya, 2013). These adipocytes are referred to as beige, brite (brown in white), or inducible adipocytes (Giralt, & Villaroya, 2013). For the remainder of this thesis, they will be referred to as beige adipocytes. Although the activation of BAT and the browning process in WAT share common pathways of induction the focus here will be on brown adipocytes and BAT, while acknowledging that other thermogenic adipocytes exist and are currently under intense study (Giralt, & Villaroya, 2013). The relevance of BAT will be discussed in terms of energy metabolism, as evidence suggests that obesity may in part be determined by reduced energy expenditure (Flier, 2004).

1.7 THERMOGENESIS IN BROWN ADIPOSE TISSUE

Thermoeffector mechanisms exist for both heat and cold defense. These include thermoregulatory behaviors to increase or decrease the amount of heat loss, cutaneous vasodilation or constriction, evaporative cooling (sweating) or heat production (thermogenesis) (Morrison, 2016). Thermogenesis, a component of the 'energy out' aspect of the energy balance equation (total body energy = energy in – energy out), is the behavioral and autonomic increase in body temperature in response to cold stress or overfeeding to preserve energy homeostasis (Morrison, 2016). Upon cold stimulation in rodents and human adults, thermogenesis is initially mediated by shivering in skeletal muscle that produces heat through mechanical work (Morrison, 2016). After prolonged cold stimulation, shivering subsides while non-shivering, or adaptive thermogenesis increases in brown (and beige) adipocytes that are activated by efferent signals from the hypothalamus via sympathetic nerve innervation (Figure 1.7) (Blondin et al., 2014; Lidell et al., 2014; Peirce et al., 2014). The sympathetic neural input promotes mitochondria oxidation that shunts proton fluxes into

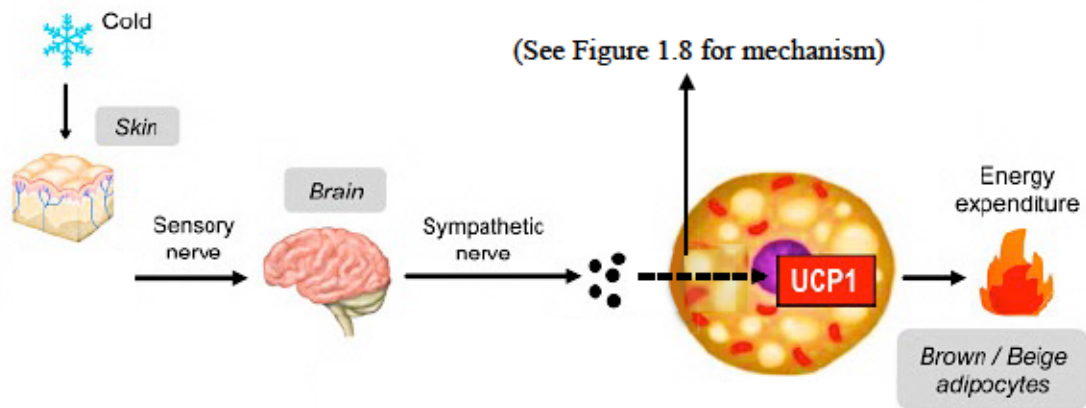


Figure 1.7. Cold-induced activation of adaptive thermogenesis in brown adipose tissue. UCP1; uncoupling protein 1. Adapted from “Activation and recruitment of brown adipose tissue by cold exposure and food ingredients in humans”, by M. Saito, T. Yoneshiro, & M. Matsushita, 2016, *Best Practice & Research Clinical Endocrinology & Metabolism*, 30(4), 537-547. Copyright © 2017 Elsevier B.V. Adapted with permission from publisher.

heat production via the specialized protein UCP1 (Figure 1.7). The unique capacity to undergo the energetically expensive process of adaptive thermogenesis has brought BAT into the limelight as a potential therapeutic target in pathological states of energy dysfunction, including obesity (Chechi, Carpentier, & Richard, 2013; Lidell et al., 2014; Saito, 2013).

Norepinephrine (NE) released by the postganglionic sympathetic neurons is the primary neurotransmitter that activates thermogenesis in brown adipocytes in response to cold (Chechi et al., 2013; Lidell et al., 2014; Hawke et al., 2009). NE binds to the β 3-adrenergic G protein-coupled receptors (GPCRs), which activates the G protein alpha-subunit and phosphorylates adenylate cyclase (Figure 1.8). This enzyme converts ATP to cyclic adenosine monophosphate (cAMP) that activates protein kinase A (PKA). PKA acts on downstream messenger proteins such as hormone-sensitive lipase (HSL), which induces lipolysis that generates FFA's, serving two roles: activating UCP1 which is only found on the inner mitochondrial membrane of brown adipocytes, and undergoing FA catabolism via β -oxidation to fuel thermogenesis (Chechi et al., 2013; Lidell et al., 2014; Hawke et al., 2009). Activated UCP1 uncouples oxidative phosphorylation from ATP generation by bypassing ATP synthase and enabling the reflux of protons across the inner mitochondrial membrane down the proton gradient. It is this proton leak, or disruption of the proton gradient, that generates heat and results in whole-body energy expenditure (Chondronikola et al., 2016; Lidell et al., 2014).

Evidence for the role of BAT in energy expenditure has been shown experimentally in animal and human models. When BAT is ablated genetically in mice, obesity ensues (Lowell et al., 1993). However, when BAT is regenerated in these transgenic mice, obesity resolves (Lowell et al., 1993). Genetic overexpression of UCP1 in mice has also been shown to mitigate obesity induced by a high-fat diet, providing evidence that enhancing thermogenic

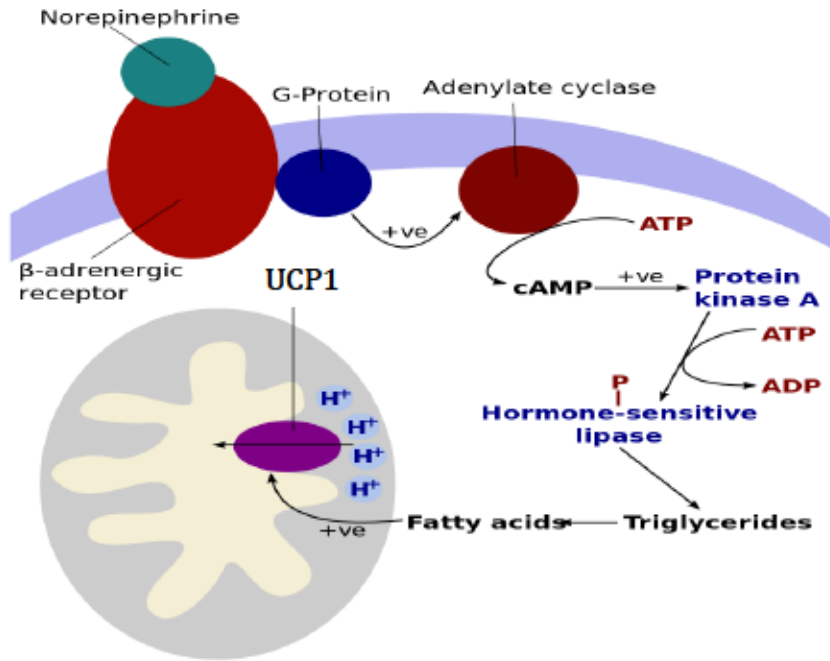


Figure 1.8. Molecular mechanisms of adaptive thermogenesis at the level of brown adipocytes. Adapted from Wikipedia, 2009. Obtained from <https://en.wikipedia.org/wiki/Thermogenesis>.

potential via increased UCP1 activity is able to alter body weight in mice and thus elicits potential as a therapy to regulate body weight in humans (Kopecky et al., 1995). Mice lacking UCP1 fail to demonstrate an obesogenic effect at room temperature (23°C), yet in thermoneutrality (30°C; the optimal temperature at which normal body temperature can be maintained for mice), obesity develops (Enerbäck et al., 1997; Feldmann, Golozoubova, Cannon, & Nedergaard, 2009). These results can be explained by the demand for the mice to compensate with shivering at colder temperatures and demonstrates that ambient temperature is a determinant for metabolic studies.

Just as WAT can undergo adaptive and dynamic changes during periods of prolonged starvation or overfeeding, so too can BAT in response to cold or thermoneutrality (Bartelt, & Heeren, 2013). For example, both UCP1 expression and BAT mass are increased in mice housed at colder temperatures when compared to mice housed at thermoneutrality (Lim et al., 2012; Yoo et al., 2014). Human studies have also demonstrated that BAT plays a physiologically significant role in thermoregulation as observed by increased BAT activity during mild cold exposure, and with the observation that BAT activity is highly correlated with BMI such that BAT activity decreases as BMI increases (Chen et al., 2013; Chondronikola et al., 2016; Vijgen et al., 2011). In addition, both BAT activity and mass decline in older individuals, which may be associated with the accumulation of body fat observed with aging (Pfannenbergh et al., 2010; Wang et al., 2015; Yoneshiro et al., 2011). Precise mechanisms of BAT activation and modulation continue to be studied and necessitate further elucidation before BAT can be targeted for therapeutics. Increasing information on some of the classic hormones, proteins, endocrine factors, and pathways regulating BAT function are becoming known, including endocrine pathways involving thyroid hormones, bone morphogenetic proteins, natriuretic peptides, and the melanocortin system (discussed

above) (Chechi et al., 2013; Koojiman et al., 2014; Labbé et al., 2015). The Gray lab, and thus this research, is interested in a novel hormone deemed essential for the adaptive thermogenic response of BAT to cold exposure called pituitary adenylate cyclase-activating polypeptide (PACAP) and will be discussed here (Rudecki, & Gray, 2016).

1.8 PITUITARY ADENYLATE CYCLASE-ACTIVATING POLYPEPTIDE (PACAP): ESSENTIAL FOR THE THERMOGENIC RESPONSE IN BAT

Discovered in 1989, PACAP is widely expressed in the brain and peripheral organs, notably in the gonads, adrenal glands, pancreas, respiratory and urogenital tracts, and involved in an array of physiological functions including modulation of immune and inflammatory responses, dilation of vessels and bronchi, psychomotor control, the stress response and energy metabolism (Miyata et al., 1989; Vaudry et al., 2009; Xu et al., 2016). Receptors are located in the lungs, liver, testis, adrenal gland, and pancreatic islets and are particularly abundant in the brain, especially in the DMN, PVN, ARC, LHA, and VMN of the hypothalamus (Figure 1.5) (Hashimoto et al., 1996; Nakata, Shioda, Oka, Maruyama, & Yada, 1999). PACAP is known for its pleiotropic biological actions and its role as a master stress regulator (Rudecki, & Gray, 2016). Here, the focus will be on its role in thermogenic stress and energy metabolism.

Expressed in the pancreatic nerve fibers and islets, PACAP potently augments glucose-induced insulin secretion by acting on pancreatic beta-cells and is thus considered a regulator of glucose metabolism (Nakata et al., 1999; Nakata et al., 2004). It also promotes feeding behavior by activating neurons in the ARC (discussed above), known as the hypothalamic feeding center, and induces lipolysis in WAT (Nakata, & Yada, 2007; Rudecki, & Gray, 2016). It has been shown that leptin signaling enhances PACAP expression in steroidogenic factor 1 (SF1) cells of the VMN and strong evidence suggests that PACAP

forms an important downstream component of the acute effects of leptin on energy balance. For example, PACAP mRNA levels were significantly reduced in leptin-deficient mice and were restored with exogenous leptin treatments (Hawke et al., 2009). Further neuroanatomical mapping is required to further elucidate the interactions between leptin and PACAP; however, proposed interactions are shown in Figure 1.9. Additional interactions involved in this mechanism will be further discussed here.

Both pharmacological and genetic evidence exists for PACAP's essential role in thermogenesis. Although PACAP and its receptors are highly expressed in the PVN and the VMN, the VMN is known to be a region of the hypothalamus important for the regulation of energy homeostasis by integrating behavioral and metabolic mechanisms. Normal VMN functions include decreasing food intake in response to satiety and increasing energy expenditure, as obesity ensues with VMN lesions (Resch et al., 2011). When PACAP is injected directly into the VMN of healthy, wildtype mice, food intake is significantly reduced, core body temperature and spontaneous locomotor activity is increased, and BAT UCP1 mRNA expression is increased (Hawke et al., 2009; Resch et al., 2011). These effects were not observed when PACAP was injected into the PVN, suggesting the VMN as a major center for PACAP-mediated thermogenesis (Resch et al., 2011; Resch et al., 2013). Using PACAP^{-/-} mice generated by Gray, Cummings, Jirik, & Sherwood (2001) the Gray lab is exploring PACAP's role specifically in the VMN in activating BAT thermogenesis and this will be the focus of the research presented in Chapter 3.

Genetically, without the PACAP gene, PACAP^{-/-} mice display high mortality rates (89%) when raised at 21°C as compared to those raised at 24°C (24%), (Adams et al., 2008; Gray et al., 2001; Gray, Yamaguchi, Vencova, & Sherwood, 2002). These mice are sensitive to a 4°C cold challenge, displaying reduced levels of NE and β -adrenergic receptors, and

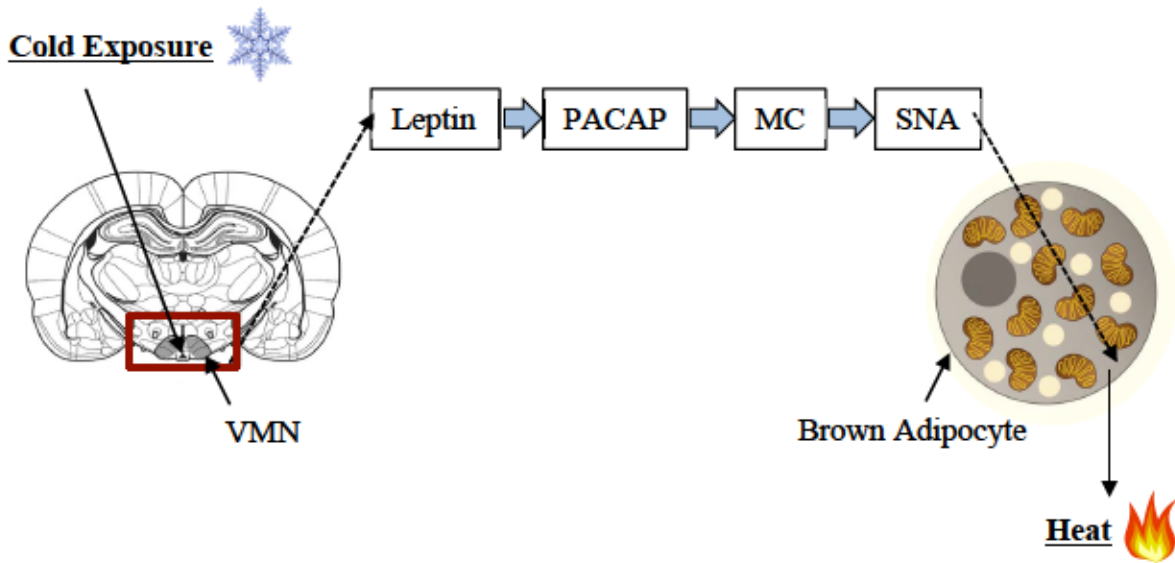


Figure 1.9. Proposed pathways of neuropeptides that interact to induce adaptive thermogenesis in BAT in response to cold exposure. VMN; ventromedial nucleus, PACAP; pituitary adenylate cyclase-activating polypeptide, MC; melanocortin system, SNA; sympathetic nerve activity, BAT; brown adipose tissue. Images adapted from “Revisiting the Ventral Medial Nucleus of the Hypothalamus: The Roles of SF-1 Neurons in Energy Homeostasis”, by Y. Choi, T. Fujikawa, J. Lee, A. Reuter, & K. Kim, 2013, *Frontiers In Neuroscience*, 7. Copyright © 2013 Choi, Fujikawa, Lee, Reuter and Kim. Adapted with permission from author.

impaired upregulation of UCP1 with cold exposure (Diané et al., 2014; Gray et al., 2002). These findings indicate PACAP's role as a critical hormone regulator of BAT thermogenesis (Adams et al., 2008; Gray et al., 2001; Gray et al., 2002).

1.9 GAP IN LITERATURE: CONNECTING PACAP AND THE MELANOCORTIN SYSTEM

As stated above, the central melanocortin system plays a critical role in regulating energy expenditure whereby α -MSH acts on the MC4R to regulate thermogenesis via the sympathetic nervous system (Fan et al., 2005; Vaughan, Shrestha, & Bartness, 2011; Voss-Andreae et al., 2007). Although molecular and physiological mechanisms of PACAP's involvement in BAT activation remain unclear, some evidence exists to suggest PACAP interacts with the melanocortin system to activate BAT thermogenesis (Tanida, Shintani, & Hashimoto, 2011). This potential association and gap in the literature is the focus of the research for Chapter 2.

Research has shown that both PACAP $-/-$ and melanocortin 4-receptor (MC4R) $-/-$ mice have impaired thermogenesis and it is hypothesized that PACAP and the melanocortin system are connected in activating BAT thermogenesis (Berghlund et al., 2014; Diané et al., 2014; Fan, Voss-Andreae, Cao, & Morrison, 2005; Gray et al., 2002; Voss-Andreae et al., 2007). It is clear that BAT activation unequivocally occurs by sympathetic nerve activity (SNA) initiated at the level of the hypothalamus, whereby the central sympathetic outflow circuits to BAT have been revealed by injecting a retrograde viral transneuronal tract tracer into the tissue (Bamshad, Song, & Bartness, 1999; Bartness, Vaughan, & Song, 2010). However, the mechanisms by which the hypothalamic nuclei activating BAT are not precisely known. Interestingly, a high degree of colocalization of MC4R mRNA is found on the neurons along the neuronal tract where the viral tracer is detected (Bartness, Vaughan, &

Song, 2010). Additionally, when MC4R agonist Melanotan II (MTII) was stereotaxically injected into the VMN, similar results were observed to those with pharmacological injections of PACAP into the VMN; an increase in energy expenditure and thermogenesis, suggesting that PACAP and the melanocortin system may share a common pathway in activating BAT thermogenesis (Gavini, Jones, & Novak, 2016). Tanida, Shintani, & Hashimoto (2011) conducted further research into the connection between PACAP and the melanocortin system where they monitored neural response in BAT as opposed to thermogenic markers. They performed intracerebroventricular injections of an MC4R antagonist, followed by PACAP, and compared the neural response in BAT to those without the antagonist injection. Without the antagonist, PACAP injections showed increased neural activity to BAT. However, when the MC4R antagonist was injected before PACAP, very little sympathetic nerve activity was observed at the level of BAT (Tanida, Shintani, & Hashimoto 2011). This provides evidence to suggest that PACAP acts upstream of the melanocortin system in activating BAT (as proposed in Figure 1.9). Further research is necessary to support these results, which will be presented in Chapter 2.

1.10 HYPOTHESIS AND RESEARCH OBJECTIVES

I hypothesize that PACAP acts upstream from the melanocortin system to regulate SNA to stimulate adaptive thermogenesis in BAT. Moreover, I hypothesize that the cold sensitivity of PACAP *-/-* mice may be due to the absence of PACAP signaling within the VMN specifically (Figure 1.9).

The objectives of this research are:

1. To determine if the impaired thermogenesis in PACAP *-/-* mice can be rescued pharmacologically with a melanocortin agonist, Melanotan II (MTII), and thus provide evidence using a genetic model of PACAP deficiency for the

connection between PACAP and the melanocortin system in regulating thermogenesis in BAT

2. To create an adenoviral construct that expresses GFP under the regulation of the SF1 promoter to act as a control vector to be used in stereotaxic surgery, thus ensuring VMN-specific expression of the vector
3. To devise a protocol for stereotaxic injections which reaches the VMN in live animals

Results obtained from objectives 2 and 3 act as preliminary steps following future objective:

4. To create an adenoviral construct for VMN specific expression of PACAP to determine if the impaired thermogenesis in PACAP $-/-$ mice can be genetically rescued by transgenic expression of PACAP in the VMN only, thus determining the importance of VMN PACAP in regulating thermogenesis

The work is presented in self-contained chapters. The focus of Chapter 2 is to determine the pathway connecting PACAP and the melanocortin system in activating thermogenesis in BAT. This was achieved by injecting PACAP $-/-$ mice with a pharmacological MC4R agonist in attempt to rescue impaired thermogenesis in PACAP $-/-$ mice. Methodology of assessing the physiological and biochemical markers for thermogenic response is discussed in detail in Chapter 2. Chapter 3 focuses on the creation of an adenoviral control construct to be used as the initial step in the genetic reintroduction of PACAP specifically in the VMN to determine its role in BAT thermogenesis activation. This chapter also includes development of a stereotaxic protocol for injection of the adenovirus into the VMN of mice to achieve VMN specific expression of PACAP. Chapter 4 connects Chapters 2 and 3, providing a conclusion and significance for research in this area.

1.11 REFERENCES

- About Obesity in Canada - Canadian Obesity Network.* (2016). *Obesitynetwork.ca*. Retrieved 2 June 2016, from <http://www.obesitynetwork.ca/obesity-in-canada>
- Adams, B., Gray, S., Isaac, E., Bianco, A., Vidal-Puig, A., & Sherwood, N. (2008). Feeding and Metabolism in Mice Lacking Pituitary Adenylate Cyclase-Activating Polypeptide. *Endocrinology*, *149*(4), 1571-1580. <http://dx.doi.org/10.1210/en.2007-0515>
- Adult Obesity Facts | Overweight & Obesity | CDC.* (2016). *Cdc.gov*. Retrieved 2 June 2016, from <http://www.cdc.gov/obesity/data/adult.html>
- Ahima, R. (2006). Adipose Tissue as an Endocrine Organ. *Obesity*, *14*, 242S-249S. <http://dx.doi.org/10.1038/oby.2006.317>
- Balthasar, N., Coppari, R., McMinn, J., Liu, S., Lee, C., & Tang, V. et al. (2004). Leptin Receptor Signaling in POMC Neurons Is Required for Normal Body Weight Homeostasis. *Neuron*, *42*(6), 983-991. <http://dx.doi.org/10.1016/j.neuron.2004.06.004>
- Bamshad, M., Song, C., & Bartness, T. (1999). CNS origins of the sympathetic nervous system outflow to brown adipose tissue. *Am J Physiol*, *276*(6 Pt 2), R1569-78.
- Bartelt, A. & Heeren, J. (2013). Adipose tissue browning and metabolic health. *Nat Rev Endocrinol*, *10*(1), 24-36. <http://dx.doi.org/10.1038/nrendo.2013.204>
- Bartness, T., Vaughan, C., & Song, C. (2010). Sympathetic and sensory innervation of brown adipose tissue. *Int J Obes Relat Metab Disord*, *34*, S36-S42. <http://dx.doi.org/10.1038/ijo.2010.182>
- Berglund, E., Liu, T., Kong, X., Sohn, J., Vong, L., & Deng, Z. et al. (2014). Melanocortin 4 receptors in autonomic neurons regulate thermogenesis and glycemia. *Nature Neuroscience*, *17*(7), 911-913. <http://dx.doi.org/10.1038/nn.3737>
- Bingham, N., Anderson, K., Reuter, A., Stallings, N., & Parker, K. (2008). Selective Loss of Leptin Receptors in the Ventromedial Hypothalamic Nucleus Results in Increased Adiposity and a Metabolic Syndrome. *Endocrinology*, *149*(5), 2138-2148. <http://dx.doi.org/10.1210/en.2007-1200>
- Blondin, D., Labbé, S., Phoenix, S., Guérin, B., Turcotte, É., & Richard, D. et al. (2014). Contributions of white and brown adipose tissues and skeletal muscles to acute cold-induced metabolic responses in healthy men. *J Physiol*, *593*(3), 701-714. <http://dx.doi.org/10.1113/jphysiol.2014.283598>
- Bowen, R. (2006). Adrenocorticotrophic Hormone (ACTH, corticotropin). In R. Bowen, *Pathophysiology of the Endocrine System* (1st ed.). Colorado. Retrieved from <http://www.vivo.colostate.edu/hbooks/pathophys/endocrine/hypopit/acth.html>

- Butler, A., & Cone, R. (2002). The melanocortin receptors: Lessons from knockout models. *Neuropeptides*, 36(2-3), 77-84. <http://dx.doi.org/10.1054/npep.2002.0890>
- Challis, B., Coll, A., Yeo, G., Pinnock, S., Dickson, S., & Thresher, R. et al. (2004). Mice lacking pro-opiomelanocortin are sensitive to high-fat feeding but respond normally to the acute anorectic effects of peptide-YY3-36. *Proceedings Of The National Academy Of Sciences*, 101(13), 4695-4700. <http://dx.doi.org/10.1073/pnas.0306931101>
- Chechi, K., Carpentier, A., & Richard, D. (2013). Understanding the brown adipocyte as a contributor to energy homeostasis. *Trends In Endocrinology & Metabolism*, 24(8), 408-420. <http://dx.doi.org/10.1016/j.tem.2013.04.002>
- Chen, K., Brychta, R., Linderman, J., Smith, S., Courville, A., & Dieckmann, W. et al. (2013). Brown Fat Activation Mediates Cold-Induced Thermogenesis in Adult Humans in Response to a Mild Decrease in Ambient Temperature. *The Journal Of Clinical Endocrinology & Metabolism*, 98(7), E1218-E1223. <http://dx.doi.org/10.1210/jc.2012-4213>
- Choi, Y., Fujikawa, T., Lee, J., Reuter, A., & Kim, K. (2013). Revisiting the Ventral Medial Nucleus of the Hypothalamus: The Roles of SF-1 Neurons in Energy Homeostasis. *Frontiers In Neuroscience*, 7. <http://dx.doi.org/10.3389/fnins.2013.00071>
- Chondronikola, M., Volpi, E., Børsheim, E., Porter, C., Saraf, M., & Annamalai, P. et al. (2016). Brown Adipose Tissue Activation Is Linked to Distinct Systemic Effects on Lipid Metabolism in Humans. *Cell Metabolism*, 23(6), 1200-1206. <http://dx.doi.org/10.1016/j.cmet.2016.04.029>
- Choquet, H. & Meyre, D. (2011). Genetics of Obesity: What have we Learned?. *CG*, 12(3), 169-179. <http://dx.doi.org/10.2174/138920211795677895>
- Cone, R. (1999). The Central Melanocortin System and Energy Homeostasis. *Trends In Endocrinology & Metabolism*, 10(6), 211-216. [http://dx.doi.org/10.1016/s1043-2760\(99\)00153-8](http://dx.doi.org/10.1016/s1043-2760(99)00153-8)
- Cone, R. (2005). Anatomy and regulation of the central melanocortin system. *Nature Neuroscience*, 8(5), 571-578. <http://dx.doi.org/10.1038/nn1455>
- Diané, A., Nikolic, N., Rudecki, A., King, S., Bowie, D., & Gray, S. (2014). PACAP is essential for the adaptive thermogenic response of brown adipose tissue to cold exposure. *Journal Of Endocrinology*, 222(3), 327-339. <http://dx.doi.org/10.1530/joe-14-0316>
- Dubern, B., Lubrano-Berthelier, C., Mencarelli, M., Ersoy, B., Frelut, M., & Bouglé, D. et al. (2008). Mutational Analysis of the Pro-opiomelanocortin Gene in French Obese Children Led to the Identification of a Novel Deleterious Heterozygous Mutation Located in the α -Melanocyte Stimulating Hormone Domain. *Pediatr Res*, 63(2), 211-216. <http://dx.doi.org/10.1203/pdr.0b013e31815ed62b>

- Ellacott, K. & Cone, R. (2006). The role of the central melanocortin system in the regulation of food intake and energy homeostasis: lessons from mouse models. *Philosophical Transactions Of The Royal Society B: Biological Sciences*, 361(1471), 1265-1274. <http://dx.doi.org/10.1098/rstb.2006.1861>
- Enerbäck, S., Jacobsson, A., Simpson, E., Guerra, C., Yamashita, H., Harper, M., & Kozak, L. (1997). Mice lacking mitochondrial uncoupling protein are cold-sensitive but not obese. *Nature*, 387(6628), 90-94. <http://dx.doi.org/10.1038/387090a0>
- Fan, W., Voss-Andreae, A., Cao, W., & Morrison, S. (2005). Regulation of thermogenesis by the central melanocortin system. *Peptides*, 26(10), 1800-1813. <http://dx.doi.org/10.1016/j.peptides.2004.11.033>
- Farooqi, I. & O'Rahilly, S. (2006). Genetics of Obesity in Humans. *Endocrine Reviews*, 27(7), 710-718. <http://dx.doi.org/10.1210/er.2006-0040>
- Feldmann, H., Golozoubova, V., Cannon, B., & Nedergaard, J. (2009). UCP1 Ablation Induces Obesity and Abolishes Diet-Induced Thermogenesis in Mice Exempt from Thermal Stress by Living at Thermoneutrality. *Cell Metabolism*, 9(2), 203-209. <http://dx.doi.org/10.1016/j.cmet.2008.12.014>
- Finucane, M., Stevens, G., Cowan, M., Danaei, G., Lin, J., & Paciorek, C. et al. (2011). National, regional, and global trends in body-mass index since 1980: systematic analysis of health examination surveys and epidemiological studies with 960 country-years and 9.1 million participants. *The Lancet*, 377(9765), 557-567. [http://dx.doi.org/10.1016/s0140-6736\(10\)62037-5](http://dx.doi.org/10.1016/s0140-6736(10)62037-5)
- Flier, J. (2004). Obesity Wars: Molecular Progress Confronts an Expanding Epidemic. *Cell*, 116(2), 337-350. [http://dx.doi.org/10.1016/s0092-8674\(03\)01081-x](http://dx.doi.org/10.1016/s0092-8674(03)01081-x)
- Fonseca-Alaniz, M., Takada, J., Alonso-Vale, M., & Lima, F. (2007). Adipose tissue as an endocrine organ: from theory to practice. *J Pediatr (Rio J)*, 0(0). <http://dx.doi.org/10.2223/jped.1709>
- Galic, S., Oakhill, J., & Steinberg, G. (2010). Adipose tissue as an endocrine organ. *Molecular And Cellular Endocrinology*, 316(2), 129-139. <http://dx.doi.org/10.1016/j.mce.2009.08.018>
- Gavini, C., Jones, W., & Novak, C. (2016). Ventromedial hypothalamic melanocortin receptor activation: regulation of activity energy expenditure and skeletal muscle thermogenesis. *The Journal Of Physiology*, 594(18), 5285-5301. <http://dx.doi.org/10.1113/jp272352>
- Gavrilova, O., Marcus-Samuels, B., Graham, D., Kim, J., Shulman, G., & Castle, A. et al. (2000). Surgical implantation of adipose tissue reverses diabetes in lipoatrophic mice. *Journal Of Clinical Investigation*, 105(3), 271-278. <http://dx.doi.org/10.1172/jci7901>

- Giralt, M., & Villarroya, F. (2013). White, Brown, Beige/Brite: Different Adipose Cells for Different Functions?. *Endocrinology*, *154*(9), 2992-3000. <http://dx.doi.org/10.1210/en.2013-1403>
- Gray, S., Cummings, K., Jirik, F., & Sherwood, N. (2001). Targeted Disruption of the Pituitary Adenylate Cyclase-Activating Polypeptide Gene Results in Early Postnatal Death Associated with Dysfunction of Lipid and Carbohydrate Metabolism. *Molecular Endocrinology*, *15*(10), 1739-1747. <http://dx.doi.org/10.1210/mend.15.10.0705>
- Gray, S., Yamaguchi, N., Vencova, P., & Sherwood, N. (2002). Temperature-Sensitive Phenotype in Mice Lacking Pituitary Adenylate Cyclase-Activating Polypeptide. *Endocrinology*, *143*(10), 3946-3954. <http://dx.doi.org/10.1210/en.2002-220401>
- Greenberg, A. & Obin, M. (2006). Obesity and the role of adipose tissue in inflammation and metabolism. *The American Journal Of Clinical Nutrition*, *83*, 461-465.
- Greenman, Y., Kuperman, Y., Drori, Y., Asa, S., Navon, I., & Forkosh, O. et al. (2013). Postnatal Ablation of POMC Neurons Induces an Obese Phenotype Characterized by Decreased Food Intake and Enhanced Anxiety-Like Behavior. *Molecular Endocrinology*, *27*(7), 1091-1102. <http://dx.doi.org/10.1210/me.2012-1344>
- Halaas, J., Gajiwala, K., Maffei, M., Cohen, S., Chait, B., & Rabinowitz, D. et al. (1995). Weight-reducing effects of the plasma protein encoded by the obese gene. *Science*, *269*(5223), 543-546. <http://dx.doi.org/10.1126/science.7624777>
- Hany, T., Gharehpapagh, E., Kamel, E., Buck, A., Himms-Hagen, J., & von Schulthess, G. (2002). Brown adipose tissue: a factor to consider in symmetrical tracer uptake in the neck and upper chest region. *European Journal Of Nuclear Medicine And Molecular Imaging*, *29*(10), 1393-1398. <http://dx.doi.org/10.1007/s00259-002-0902-6>
- Harwood, H. (2012). The adipocyte as an endocrine organ in the regulation of metabolic homeostasis. *Neuropharmacology*, *63*(1), 57-75. <http://dx.doi.org/10.1016/j.neuropharm.2011.12.010>
- Hashimoto, H., Nogi, H., Mori, K., Ohishi, H., Shigemoto, R., & Yamamoto, K. et al. (1996). Distribution of the mRNA for a pituitary adenylate cyclase-activating polypeptide receptor in the rat brain: An in situ hybridization study. *The Journal Of Comparative Neurology*, *371*(4), 567-577. [http://dx.doi.org/10.1002/\(sici\)1096-9861\(19960805\)371:4<567::aid-cne6>3.3.co;2-m](http://dx.doi.org/10.1002/(sici)1096-9861(19960805)371:4<567::aid-cne6>3.3.co;2-m)
- Havel, P. (2002). Control of energy homeostasis and insulin action by adipocyte hormones: leptin, acylation stimulating protein, and adiponectin. *Current Opinion In Lipidology*, *13*(1), 51-59. <http://dx.doi.org/10.1097/00041433-200202000-00008>
- Hawke, Z., Ivanov, T., Bechtold, D., Dhillon, H., Lowell, B., & Luckman, S. (2009). PACAP Neurons in the Hypothalamic Ventromedial Nucleus Are Targets of Central Leptin

- Signaling. *Journal Of Neuroscience*, 29(47), 14828-14835.
<http://dx.doi.org/10.1523/jneurosci.1526-09.2009>
- Hinney, A., Vogel, C., & Hebebrand, J. (2010). From monogenic to polygenic obesity: recent advances. *European Child & Adolescent Psychiatry*, 19(3), 297-310.
<http://dx.doi.org/10.1007/s00787-010-0096-6>
- How, S. (2016). *Satiety Gene Variants as Markers for Obesity*. *Utar.edu.my*. Retrieved 5 August 2016, from
<http://www.utar.edu.my/contentRandD.jsp?catid=9&contentid=417&2ndcontentid=1957>
- Hwa, J., Ghibaudi, L., Compton, D., Fawzi, A., & Strader, C. (1996). Intracerebroventricular Injection of Leptin Increases Thermogenesis and Mobilizes Fat Metabolism in ob/obMice. *Hormone And Metabolic Research*, 28(12), 659-663.
<http://dx.doi.org/10.1055/s-2007-979873>
- Jeong, J., Kim, J., & Lee, B. (2014). Participation of the central melanocortin system in metabolic regulation and energy homeostasis. *Cell. Mol. Life Sci.*, 71(19), 3799-3809.
<http://dx.doi.org/10.1007/s00018-014-1650-z>
- Kooijman, S., Boon, M., Parlevliet, E., Geerling, J., van de Pol, V., & Romijn, J. et al. (2014). Inhibition of the central melanocortin system decreases brown adipose tissue activity. *The Journal Of Lipid Research*, 55(10), 2022-2032.
<http://dx.doi.org/10.1194/jlr.m045989>
- Kopecky, J., Clarke, G., Enerbäck, S., Spiegelman, B., & Kozak, L. (1995). Expression of the mitochondrial uncoupling protein gene from the aP2 gene promoter prevents genetic obesity. *Journal Of Clinical Investigation*, 96(6), 2914-2923.
<http://dx.doi.org/10.1172/jci118363>
- Krude, H., Bierbermann, H., Luck, W., Horn, R., Brabant, G., & Gruters, A. (1999). Severe Early-Onset Obesity, Adrenal Insufficiency and Red Hair Pigmentation Caused by POMC Mutations in Humans. *Nat Genet*, 19(2), 155-7.
- Labbé, S., Caron, A., Lanfray, D., Monge-Rofarello, B., Bartness, T., & Richard, D. (2015). Hypothalamic control of brown adipose tissue thermogenesis. *Front. Syst. Neurosci.*, 9.
<http://dx.doi.org/10.3389/fnsys.2015.00150>
- Lee, B. & Shao, J. (2014). Adiponectin and energy homeostasis. *Rev Endocr Metab Disord*, 15(2), 149-156. <http://dx.doi.org/10.1007/s11154-013-9283-3>
- Li, G., Mobbs, C., & Scarpace, P. (2003). Central Pro-opiomelanocortin Gene Delivery Results in Hypophagia, Reduced Visceral Adiposity, and Improved Insulin Sensitivity in Genetically Obese Zucker Rats. *Diabetes*, 52(8), 1951-1957.
<http://dx.doi.org/10.2337/diabetes.52.8.1951>
- Lidell, M., Betz, M., & Enerbäck, S. (2014). Brown adipose tissue and its therapeutic potential. *J Intern Med*, 276(4), 364-377. <http://dx.doi.org/10.1111/joim.12255>

- Lim, S., Honek, J., Xue, Y., Seki, T., Cao, Z., & Andersson, P. et al. (2012). Cold-induced activation of brown adipose tissue and adipose angiogenesis in mice. *Nat Protoc*, 7(3), 606-615. <http://dx.doi.org/10.1038/nprot.2012.013>
- Lowell, B., S-Susulic, V., Hamann, A., Lawitts, J., Himms-Hagen, J., & Boyer, B. et al. (1993). Development of obesity in transgenic mice after genetic ablation of brown adipose tissue. *Nature*, 366(6457), 740-742. <http://dx.doi.org/10.1038/366740a0>
- Miyata, A., Arimura, A., Dahl, R., Minamino, N., Uehara, A., & Jiang, L. et al. (1989). Isolation of a novel 38 residue-hypothalamic polypeptide which stimulates adenylate cyclase in pituitary cells. *Biochemical And Biophysical Research Communications*, 164(1), 567-574. [http://dx.doi.org/10.1016/0006-291x\(89\)91757-9](http://dx.doi.org/10.1016/0006-291x(89)91757-9)
- Moitra, J., Mason, M., Olive, M., Krylov, D., Gavrilova, O., & Marcus-Samuels, B. et al. (1998). Life without white fat: a transgenic mouse. *Genes & Development*, 12(20), 3168-3181. <http://dx.doi.org/10.1101/gad.12.20.3168>
- Morrison, S. (2016). Central control of body temperature. *F1000research*, 5, 880. <http://dx.doi.org/10.12688/f1000research.7958.1>
- Mizuno, T., Kelley, K., Pasinetti, G., Roberts, J., & Mobbs, C. (2003). Transgenic Neuronal Expression of Proopiomelanocortin Attenuates Hyperphagic Response to Fasting and Reverses Metabolic Impairments in Leptin-Deficient Obese Mice. *Diabetes*, 52(11), 2675-2683. <http://dx.doi.org/10.2337/diabetes.52.11.2675>
- Mueller, W., Gregoire, F., Stanhope, K., Mobbs, C., Mizuno, T., & Warden, C. et al. (1998). Evidence That Glucose Metabolism Regulates Leptin Secretion from Cultured Rat Adipocytes 1. *Endocrinology*, 139(2), 551-558. <http://dx.doi.org/10.1210/endo.139.2.5716>
- Nakata, M., Kohno, D., Shintani, N., Nemoto, Y., Hashimoto, H., Baba, A., & Yada, T. (2004). PACAP deficient mice display reduced carbohydrate intake and PACAP activates NPY-containing neurons in the rat hypothalamic arcuate nucleus. *Neuroscience Letters*, 370(2-3), 252-256. <http://dx.doi.org/10.1016/j.neulet.2004.08.034>
- Nakata, M., Shioda, S., Oka, Y., Maruyama, I., & Yada, T. (1999). Insulinotropin PACAP potentiates insulin-stimulated glucose uptake in 3T3 L1 cells*. *Peptides*, 20(8), 943-948. [http://dx.doi.org/10.1016/s0196-9781\(99\)00085-6](http://dx.doi.org/10.1016/s0196-9781(99)00085-6)
- Nakata, M. & Yada, T. (2007). PACAP in the Glucose and Energy Homeostasis: Physiological Role and Therapeutic Potential. *CPD*, 13(11), 1105-1112. <http://dx.doi.org/10.2174/138161207780618948>
- Nedergaard, J., Bengtsson, T., & Cannon, B. (2007). Unexpected evidence for active brown adipose tissue in adult humans. *AJP: Endocrinology And Metabolism*, 293(2), E444-E452. <http://dx.doi.org/10.1152/ajpendo.00691.2006>
- Obesity and overweight*. (2016). *World Health Organization*. Retrieved 2 June 2016, from <http://www.who.int/mediacentre/factsheets/fs311/en/>

- Peirce, V., Carobbio, S., & Vidal-Puig, A. (2014). The different shades of fat. *Nature*, *510*(7503), 76-83. <http://dx.doi.org/10.1038/nature13477>
- Pfannenberger, C., Werner, M., Ripkens, S., Stef, I., Deckert, A., & Schmadl, M. et al. (2010). Impact of Age on the Relationships of Brown Adipose Tissue With Sex and Adiposity in Humans. *Diabetes*, *59*(7), 1789-1793. <http://dx.doi.org/10.2337/db10-0004>
- Resch, J., Boisvert, J., Hourigan, A., Mueller, C., Yi, S., & Choi, S. (2011). Stimulation of the hypothalamic ventromedial nuclei by pituitary adenylate cyclase-activating polypeptide induces hypophagia and thermogenesis. *AJP: Regulatory, Integrative And Comparative Physiology*, *301*(6), R1625-R1634. <http://dx.doi.org/10.1152/ajpregu.00334.2011>
- Resch, J., Maunze, B., Gerhardt, A., Magnuson, S., Phillips, K., & Choi, S. (2013). Intrahypothalamic pituitary adenylate cyclase-activating polypeptide regulates energy balance via site-specific actions on feeding and metabolism. *AJP: Endocrinology And Metabolism*, *305*(12), E1452-E1463. <http://dx.doi.org/10.1152/ajpendo.00293.2013>
- Rudecki, A. & Gray, S. (2016). PACAP in the Defense of Energy Homeostasis. *Trends In Endocrinology & Metabolism*. <http://dx.doi.org/10.1016/j.tem.2016.04.008>
- Saito, M. (2013). Brown adipose tissue as a therapeutic target for human obesity. *Obesity Research & Clinical Practice*, *7*(6), e432-e438. <http://dx.doi.org/10.1016/j.orcp.2013.09.001>
- Saito, M., Yoneshiro, T., & Matsushita, M. (2016). Activation and recruitment of brown adipose tissue by cold exposure and food ingredients in humans. *Best Practice & Research Clinical Endocrinology & Metabolism*, *30*(4), 537-547. <http://dx.doi.org/10.1016/j.beem.2016.08.003>
- Sakurai, T., Ogasawara, J., Kizaki, T., Sato, S., Ishibashi, Y., & Takahashi, M. et al. (2013). The Effects of Exercise Training on Obesity-Induced Dysregulated Expression of Adipokines in White Adipose Tissue. *International Journal Of Endocrinology*, *2013*, 1-28. <http://dx.doi.org/10.1155/2013/801743>
- Satoh, N., Ogawa, Y., Katsuura, G., Numata, Y., Tsuji, T., & Hayase, M. et al. (1999). Sympathetic activation of leptin via the ventromedial hypothalamus: leptin-induced increase in catecholamine secretion. *Diabetes*, *48*(9), 1787-1793. <http://dx.doi.org/10.2337/diabetes.48.9.1787>
- Scarpace, P., Matheny, M., Pollock, B., & Tumer, N. (1997). Leptin increases uncoupling protein expression and energy expenditure. *American Journal Of Physiology - Endocrinology And Metabolism*, *273*(1), E226-E230.
- Stern, J., Rutkowski, J., & Scherer, P. (2016). Adiponectin, Leptin, and Fatty Acids in the Maintenance of Metabolic Homeostasis through Adipose Tissue Crosstalk. *Cell Metabolism*, *23*(5), 770-784. <http://dx.doi.org/10.1016/j.cmet.2016.04.011>

- Tabeta, K., & Beutler, B. (2012). *Mutagenetix - LabArchives, Your Electronic Lab Notebook*. Mynotebook.labarchives.com. Retrieved 26 April 2017, from <https://mynotebook.labarchives.com/share/Mutagenetix/MjMyLjd8MzA4My8xNzkvVHJlZU5vZGUvMTV8NTkwLjc=>
- Tanida, M., Shintani, N., & Hashimoto, H. (2011). The melanocortin system is involved in regulating autonomic nerve activity through central pituitary adenylate cyclase-activating polypeptide. *Neuroscience Research*, 70(1), 55-61. <http://dx.doi.org/10.1016/j.neures.2011.01.014>
- Thermogenesis*. (2016). *En.wikipedia.org*. Retrieved 20 November 2016, from <https://en.wikipedia.org/wiki/Thermogenesis>
- Trayhurn, P. (2005). Endocrine and signalling role of adipose tissue: new perspectives on fat. *Acta Physiologica Scandinavica*, 184(4), 285-293. <http://dx.doi.org/10.1111/j.1365-201x.2005.01468.x>
- Trayhurn, P. & Beattie, J. (2001). Physiological role of adipose tissue: white adipose tissue as an endocrine and secretory organ. *Proceedings Of The Nutrition Society*, 60(03), 329-339. <http://dx.doi.org/10.1079/pns200194>
- van Marken Lichtenbelt, W., Vanhommerig, J., Smulders, N., Drossaerts, J., Kemerink, G., & Bouvy, N. et al. (2009). Cold-Activated Brown Adipose Tissue in Healthy Men. *New England Journal Of Medicine*, 360(15), 1500-1508. <http://dx.doi.org/10.1056/nejmoa0808718>
- Vaudry, D., Falluel-Morel, A., Bourgault, S., Basille, M., Burel, D., & Wurtz, O. et al. (2009). Pituitary Adenylate Cyclase-Activating Polypeptide and Its Receptors: 20 Years after the Discovery. *Pharmacological Reviews*, 61(3), 283-357. <http://dx.doi.org/10.1124/pr.109.001370>
- Vaughan, C., Shrestha, Y., & Bartness, T. (2011). Characterization of a novel melanocortin receptor-containing node in the SNS outflow circuitry to brown adipose tissue involved in thermogenesis. *Brain Research*, 1411, 17-27. <http://dx.doi.org/10.1016/j.brainres.2011.07.003>
- Vázquez-Vela, M., Torres, N., & Tovar, A. (2008). White Adipose Tissue as Endocrine Organ and Its Role in Obesity. *Archives Of Medical Research*, 39(8), 715-728. <http://dx.doi.org/10.1016/j.arcmed.2008.09.005>
- Vijgen, G., Bouvy, N., Teule, G., Brans, B., Schrauwen, P., & van Marken Lichtenbelt, W. (2011). Brown Adipose Tissue in Morbidly Obese Subjects. *Plos ONE*, 6(2), e17247. <http://dx.doi.org/10.1371/journal.pone.0017247>
- Voss-Andreae, A., Murphy, J., Ellacott, K., Stuart, R., Nillni, E., Cone, R., & Fan, W. (2007). Role of the Central Melanocortin Circuitry in Adaptive Thermogenesis of

- Brown Adipose Tissue. *Endocrinology*, 148(4), 1550-1560.
<http://dx.doi.org/10.1210/en.2006-1389>
- Walley, A. (2006). Genetics of obesity and the prediction of risk for health. *Human Molecular Genetics*, 15(Review Issue 2), R124-R130.
<http://dx.doi.org/10.1093/hmg/ddl215>
- Wang, Q., Zhang, M., Xu, M., Gu, W., Xi, Y., & Qi, L. et al. (2015). Brown Adipose Tissue Activation Is Inversely Related to Central Obesity and Metabolic Parameters in Adult Human. *PLOS ONE*, 10(4), e0123795. <http://dx.doi.org/10.1371/journal.pone.0123795>
- Westerterp-Plantenga, M., Saris, W., Huckshorn, C., & Campfield, L. (2001). Effects of weekly administration of pegylated recombinant human OB protein on appetite profile and energy metabolism in obese men. *Am J Clin Nutr*, 74(4), 426-34.
- WHO | *Controlling the global obesity epidemic*. (2016). *Who.int*. Retrieved 2 June 2016, from <http://www.who.int/nutrition/topics/obesity/en/>
- WHO | *Obesity*. (2016). *Who.int*. Retrieved 2 June 2016, from http://www.who.int/gho/ncd/risk_factors/obesity_text/en/
- Xu, Z., Ohtaki, H., Watanabe, J., Miyamoto, K., Murai, N., & Sasaki, S. et al. (2016). Pituitary adenylate cyclase-activating polypeptide (PACAP) contributes to the proliferation of hematopoietic progenitor cells in murine bone marrow via PACAP-specific receptor. *Sci. Rep.*, 6, 22373. <http://dx.doi.org/10.1038/srep22373>
- Yaswen, L., Diehl, N., Brennan, M., & Hochgeschwender, U. (1999). Obesity in the mouse model of pro-opiomelanocortin deficiency responds to peripheral melanocortin. *Nat Med*, 5(9), 1066-70.
- Yeo, G. & Heisler, L. (2012). Unraveling the brain regulation of appetite: lessons from genetics. *Nature Neuroscience*, 15(10), 1343-1349. <http://dx.doi.org/10.1038/nn.3211>
- Yoneshiro, T., Aita, S., Matsushita, M., Okamatsu-Ogura, Y., Kameya, T., & Kawai, Y. et al. (2011). Age-Related Decrease in Cold-Activated Brown Adipose Tissue and Accumulation of Body Fat in Healthy Humans. *Obesity*, 19(9), 1755-1760.
<http://dx.doi.org/10.1038/oby.2011.125>
- Yoo, H., Qiao, L., Bosco, C., Leong, L., Lytle, N., & Feng, G. et al. (2014). Intermittent Cold Exposure Enhances Fat Accumulation in Mice. *Plos ONE*, 9(5), e96432.
<http://dx.doi.org/10.1371/journal.pone.0096432>
- Zhang, Y., Proenca, R., Maffei, M., Barone, M., Leopold, L., & Friedman, J. (1994). Positional cloning of the mouse obese gene and its human homologue. *Nature*, 372(6505), 425-432. <http://dx.doi.org/10.1038/372425a>

CHAPTER 2

Pharmacological Intervention with Melanotan II Partially Rescues the Impaired

Thermogenic Capacity of PACAP $-/-$ Mice

2.1 INTRODUCTION

Owing to the thermogenic capabilities of brown and beige adipocytes, the recent discovery that BAT is present and functional in adult humans has attracted increasing attention to this tissue, particularly due to its energy dissipating activity and potential protective function against body fat accumulation (Chen et al., 2013; Chondronikolina et al., 2016; Saito, Yoneshiro, & Matsushita, 2016). While several endocrine regulators are involved in the activation of BAT such as thyroid hormones, heart natriuretic peptides and liver bile acids, the greatest physiological stimulus is via sympathetic activation, which is induced in response to both feeding and cold exposure (Figure 2.1) (Chechi, Carpentier, & Richard, 2013; Labbé et al., 2015; Saito, Yoneshiro, & Matsushita, 2016). The focus of this chapter will be to further understand the mechanisms by which sympathetic nerve activity is activated in response to cold exposure.

Cold stress is initially identified by sensory neurons on the body surface that transmit neurochemical signals to the brain, resulting in increased sympathetic activity (Figure 2.1) (Morrison, & Nakamura, 2011). Norepinephrine (NE) is released from abundantly distributed sympathetic nerve endings that innervate BAT and stimulate brown adipocytes via binding primarily to β 3-adrenergic receptors (β 3-ARs) (Inokuma et al., 2005; Saito, Yoneshiro, & Matsushita, 2016). This triggers cAMP-activated cellular events including hydrolysis of triglycerides via hormone sensitive lipase (HSL), oxidation of resulting FAs, and activation of uncoupling protein 1 (UCP1); the key mitochondrial protein involved in adaptive thermogenesis, resulting in heat production (Figure 1.8) (Inokuma et al., 2005; Saito, Yoneshiro, & Matsushita, 2016). Sympathetic activation also results in increased fat mobilization in WAT, releasing FAs that are used by peripheral tissues, such as BAT

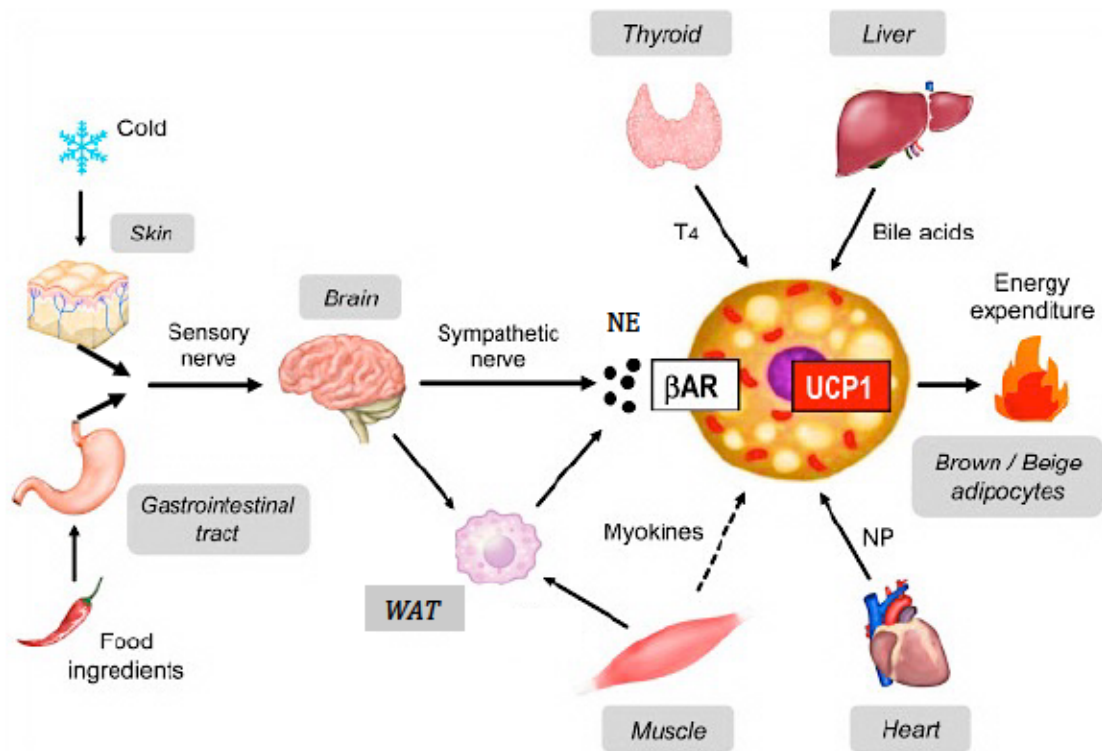


Figure 2.1. Sympathetic and endocrine control of BAT thermogenesis. β AR; beta-adrenergic receptor, NE; norepinephrine, NP; natriuretic peptide, T4; thyroxine, UCP1; uncoupling protein 1, WAT; white adipose tissue. Adapted from “Activation and recruitment of brown adipose tissue by cold exposure and food ingredients in humans”, by M. Saito, T. Yoneshiro, & M. Matsushita, 2016, *Best Practice & Research Clinical Endocrinology & Metabolism*, 30(4), 537-547. Copyright © 2017 Elsevier B.V. Adapted with permission from publisher.

where they are used as a substrate for oxidative metabolism (Chondronikola et al., 2016; Saito, Yoneshiro, & Matsushita, 2016). Changes in adaptive thermogenesis can be measured along the pathways indicated in Figure 2.1 through the following: measurements of SNA and NE turnover at the level of BAT, thermogenic gene and protein expression of β 3-ARs, HSL and UCP1 in BAT, measurements of oxygen consumption (energy expenditure) using indirect calorimetry, core body temperature and BAT temperature, as well as examination of histological changes of BAT morphology indicative of thermogenic activity (Cannon, & Nedergaard, 2010; Crane et al., 2014; Rothwell, 2001; Virtue, & Vidal-Puig, 2013). For example, mice housed at thermoneutrality (30°C) exhibit inactive adaptive thermogenesis, resulting in the *accumulation* of lipids in both WAT and BAT (Goldgof et al., 2014; Heldmaier, 1975; Virtue, & Vidal-Puig, 2013). Histologically, WAT in animals housed at thermoneutrality presents with large, lipid-filled adipocytes, while BAT in animals housed at thermoneutrality presents with large, multilocular lipid droplets within brown adipocytes (Goldgof et al., 2014; Heldmaier, 1975; Virtue, & Vidal-Puig, 2013). In contrast, adaptive thermogenesis is maximally active in BAT during cold exposure (4°C), resulting in the *breakdown* of triglycerides in both WAT and BAT, to release FAs that fuel thermogenesis (Chondronikola et al., 2016; Ngyuen et al., 2011; Saito, Yoneshiro, & Matsushita, 2016). Therefore, the resulting histological appearance of WAT in cold-exposed animals consists of smaller white adipocytes and increased numbers of thermogenically active, beige adipocytes, while BAT in cold-exposed animals contains brown adipocytes with smaller, multilocular lipid droplets (Heldmaier, 1975; Nguyen et al., 2011; Virtue, & Vidal-Puig, 2013).

Activation of BAT by cold exposure has been repeatedly demonstrated in humans, as visualized with (18)F-fluorodeoxyglucose (FDG)-positron emission tomography (PET). In response to short-term mild cold exposure (15-19°C), both blood flow and glucose uptake in

human BAT increases, as well as whole body energy expenditure (Chen et al., 2013; Orava et al., 2011; Muzik et al., 2013; Ouellet et al., 2012; Yoneshiro et al., 2010). Notably, these results are observed only in individuals that possess significant amounts of BAT. Studies have shown that BAT activity is inversely related to BMI and body fat percentage such that activity is lower in obese subjects as compared to lean individuals (van Marken Lichtenbelt et al., 2009; van Marken Lichtenbelt, 2011; Vijgen et al., 2011; Wang et al., 2015). To determine if low levels of BAT activity could be increased, Yoneshiro et al. (2013) exposed subjects with low or undetectable levels of BAT to repeated cold exposure over 6 weeks. Results indicated both an increase in BAT activity and a decrease in body fat mass (Yoneshiro et al., 2013). Importantly, the change in body fat mass was inversely correlated with BAT activity, suggesting an important interaction between BAT recruitment and body fat reduction (Yoneshiro et al., 2013). Taking the literature into consideration, it is therefore conceivable that BAT may be a promising target for combatting obesity and related metabolic disorders in humans, by restoring BAT activity to the upper range of physiologically normal levels. In order to determine effective therapeutic targets, however, physiological mechanisms and pathways regulating BAT activation through SNA must be further elucidated.

As discussed in Chapter 1, the mechanism of interest and focus of this chapter is the potential connection between PACAP and the melanocortin system in the activation of SNA in BAT thermogenesis. The evidence demonstrating both PACAP and the melanocortin system's involvement in BAT activation introduced in Chapter 1 will be further discussed here.

As a result of PACAP's pleiotropic biological actions as a neuropeptide and its role as a master stress regulator, PACAP $-/-$ mice have been shown to have several sympathetically

controlled abnormalities including respiratory control defects, impaired counter-regulatory response to hypoglycaemia, and impaired thermogenesis (Adams et al., 2008; Cummings, Pendlebury, Sherwood, & Wilson, 2004; Diané et al., 2014; Gray, Cummings, Jirik, & Sherwood, 2001; Gray, Yamaguchi, Vencova, & Sherwood, 2002). Consequently, PACAP^{-/-} mice displayed high rates of mortality, particularly in early post-natal life (Gray et al., 2001; Gray et al., 2002). Notably, mice that did not survive exhibited severely depleted adipose tissue and additional dysfunctions in lipid and carbohydrate metabolism, absent in those that did survive, indicating the complexity of the PACAP^{-/-} phenotype (Gray et al., 2011). Interestingly, the mortality rate of PACAP^{-/-} pups decreased significantly when mice were raised at 24°C rather than 21°C, indicating a temperature-sensitive phenotype (Gray et al., 2002). This temperature-sensitive phenotype was further supported by the reduced thermogenic capacity displayed in adult PACAP^{-/-} mice as compared to PACAP^{+/+} mice during a 4°C cold challenge, as indicated by reduced levels of NE and expression of β 3-ARs, impaired upregulation of UCP1 protein, and reduced oxygen consumption during NE-induced thermogenesis (Diané et al., 2014; Gray et al., 2002). Further evidence for PACAP's role in adaptive thermogenesis originate from pharmacological studies that include the injection of PACAP into the third cerebral ventricle of PACAP^{-/-} mice, intrathecal administrations of PACAP in healthy rats, and VMN injections of PACAP in wildtype mice; all of which resulted in increased BAT thermogenesis, indicated by increased SNA to BAT and NE-secreting neuroendocrine cells, increased core body temperature, and upregulated UCP1 mRNA expression (Inglott, Farnham, & Pilowsky, 2011; Resch et al., 2011; Resch et al., 2013; Tanida et al., 2010). Conclusively, PACAP is deemed essential for the thermogenic response in BAT.

Similarly to PACAP, the central melanocortin system also plays a critical role in energy homeostasis in both animals and humans. In particular, the melanocortin 4 receptor (MC4R) signaling pathway influences both energy intake and energy expenditure (discussed in Chapter 1), including thermogenesis with binding of the melanocortin peptide, α -MSH (Berglund et al., 2014; Fan, Voss-Andreae, Cao, & Morrison, 2005). As a result, MC4R $-/-$ mice exhibit increased adiposity and weight gain due to both increased food intake and decreased energy expenditure via reduced physical activity and thermogenesis (Berglund et al., 2014; Butler & Cone, 2003; Butler et al., 2001; Cone, 1999). Additionally, MC4R $-/-$ mice exhibit a defect in BAT UCP1 upregulation in response to cold exposure, as compared to MC4R $+/+$ mice (Berglund et al., 2014; Voss-Andreae et al., 2007). To mimic the biological action of α -MSH, Melanotan II (MTII), a synthetic MC3/4R agonist, was designed and synthesized in 1989 by Al-Obeidi et al. Because the activity of MC3Rs in energy homeostasis is much more subtle than MC4Rs, the focus here will be on MC4Rs (Girardet & Butler, 2014; Tao, 2010). Upon both peripheral and central (intracerebroventricular (ICV)) delivery of MTII, thermogenesis was increased in MC4R $-/-$ and $+/+$ mice, wildtype rats and wildtype hamsters, as observed by increased oxygen consumption and SNA to BAT through NE turnover, increased BAT temperatures and UCP1 mRNA expression, and decreased weight and adiposity through WAT lipolysis in diet-induced obese phenotypes (Brito et al., 2007; Enriori et al., 2011; Fan, Morrison, Cao, & Yu, 2007; Gavini, Jones, & Novak, 2016; Glavas et al., 2007; Haynes et al., 1999; Li, Zheng, Wilsey, & Scarpace, 2004; Skibicka & Grill, 2009; Song et al., 2008; Strader et al., 2007; Williams et al., 2003; Yasuda, Masaki, Sakata, & Yoshimatsu, 2004). Convincingly, and similarly to PACAP, the melanocortin system is also deemed essential for the thermogenic response in BAT.

Both PACAP and MCRs are colocalized in the VMN; one of the key hypothalamic nuclei thought to be involved in activation of BAT thermogenesis (introduced in Chapter 1 and discussed in detail in Chapter 3) (Bartness, Vaughan, & Song, 2010; Hawke et al., 2009; Nakata et al., 1999). Upon stereotaxic MTII injections into the VMN, similar results were observed to those with pharmacological injections of PACAP into the VMN: an increase in energy expenditure and thermogenesis (Gavini, Jones, & Novak, 2016). These results suggest that PACAP and the melanocortin system share a common pathway in activating BAT thermogenesis, however; while considerable amounts of literature exist for the crucial role of PACAP and the melanocortin system in BAT thermogenesis individually, very little evidence exists connecting the two. Of the limited existing evidence for the connection between PACAP and the melanocortin system in energy *intake*, available literature suggests that PACAP acts upstream from the melanocortin-dependent pathway to inhibit food intake (Dürr et al., 2007; Iemolo, Ferragud, Cottone, & Sabino, 2015; Mounien et al., 2008). Similarly, the sole piece of literature that exists for the connection between PACAP and the melanocortin system in energy *expenditure* also suggests that PACAP acts upstream from the melanocortin system in activating BAT thermogenesis (Tanida, Shintani, & Hashimoto, 2011). As described in Chapter 1, researchers illustrated this connection by performing ICV injections of a MC4R antagonist followed by PACAP, and compared the neural response in BAT to those without the antagonist injection (Tanida, Shintani, & Hashimoto, 2011). Without the antagonist, PACAP injections showed increased neural activity to BAT. However, when the MC4R antagonist was injected prior to PACAP, negligible sympathetic nerve activity was observed at the level of BAT, suggesting that PACAP acts upstream of the melanocortin system in activating BAT (Tanida, Shintani, & Hashimoto 2011). Further research is

necessary to support (or refute) these results, which has been conducted here in the Gray lab and described in this chapter.

Hypothesis and Aims

We hypothesize that PACAP acts upstream from the melanocortin system to regulate SNA to stimulate adaptive thermogenesis in BAT (Figure 2.2).

The objectives of this chapter are:

- To determine if the impaired thermogenesis in PACAP *-/-* mice can be rescued pharmacologically with a melanocortin agonist, Melanotan II (MTII), and thus provide evidence using a genetic model of PACAP deficiency for the connection between PACAP and the melanocortin system in regulating thermogenesis in BAT

To address the hypothesis and aims, thermogenic capacity was evaluated through physiological (body weight and composition, metabolic rate (open circuit calorimetry), and respiratory exchange ratio (RER)), molecular (thermogenic gene expression), and histological (lipid area and cell count) analyses. Complete materials and methods are described in detail below.

2.2 MATERIALS AND METHODS

Animals

Adult, female mice (aged 2-5 months) were generated from a breeding colony of PACAP null mice at the University of Northern British Columbia. Mice used in this study were derived from the PACAP null line generated by Gray et al. (2001) and were of mixed genetic background (C57BL/6-129/SvJ). Genotypes were determined prior to experiments via an established polymerase chain reaction (PCR) genotyping reaction, described below (Gray et al., 2002). Briefly, pups were ear-clipped in order to provide a tissue sample for

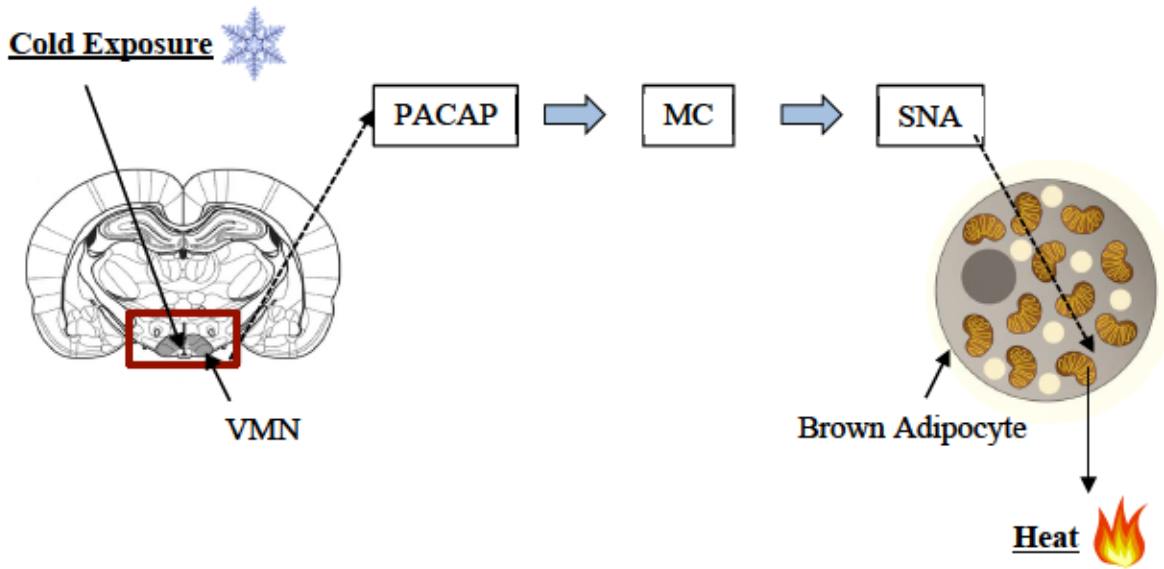


Figure 2.2. Proposed pathways of interaction for adaptive thermogenesis in BAT in response to cold exposure. VMN; ventromedial nucleus, PACAP; pituitary adenylate cyclase-activating polypeptide, MC; melanocortin system, SNA; sympathetic nerve activity, BAT; brown adipose tissue. Images adapted from “Revisiting the Ventral Medial Nucleus of the Hypothalamus: The Roles of SF-1 Neurons in Energy Homeostasis”, by Y. Choi, T. Fujikawa, J. Lee, A. Reuter, & K. Kim, 2013, *Frontiers In Neuroscience*, 7. Copyright © 2013 Choi, Fujikawa, Lee, Reuter and Kim. Adapted with permission from author.

DNA extraction as well as for animal identification. Genomic DNA was extracted from the ear clip tissue sample using a solution of 10% Chelex (Bio-Rad Laboratories, Inc., Hercules, CA) with proteinase K and 10% Tween 20. The reaction was incubated at 50°C for 45 minutes, followed by 15 minutes at 95°C to inactivate the proteinase K. The solution was mixed and the Chelex was allowed to settle to the bottom of the tube. Genomic DNA (2 µl) was then added to a 20-µl PCR reaction containing 0.25 µl Taq polymerase (Thermo Fisher Scientific, Waltham, Mass.), 10 × New England Biolabs PCR buffer, 10 µM deoxynucleoside triphosphates (dNTPs), and 10 µM of three primers: 5'MP1 (5' ATG TGT AGC GGA GCA AGG CTG G 3'), 5'MP2 (5' GAA CAC GAG TGA TGA CTG GTC AGT C 3'), and PA1 (5' CAC TCG CAC GGC ATC TTC ACA GAT AG 3'). The reaction conditions were: denaturation at 94°C for 5 min followed by 94°C for 30 sec; annealing at 67°C for 30 sec; extension at 72°C for 30 sec for 32 cycles and a long extension at 72°C for 7 min. PCR reaction products were run on an ethidium bromide stained 1.5% agarose gel and visualized under ultraviolet (UV) light. The genotypes of the mice were classified by visualized bands: the wild-type allele produced a band of approximately 550 base pair (bp), whereas the knockout allele produced a band of approximately 950 bp (Appendix Figure S2.1). Water, rather than genomic DNA, served as a negative control for PCR reactions.

Using four cohorts, a total of 32 mice were generated for this study. PACAP *+/+* (n=16) and PACAP *-/-* (n=16) littermate mice were housed in pairs, with one PACAP *+/+* and one PACAP *-/-* per cage with a standardized amount of nesting material (1 square/cage) and corn cob bedding to control for the amount of bedding material that could be used as a thermogenic substrate. Throughout the experiment, the mice were exposed to a normal 12 h light:12 h dark cycle (lights on 0700–1900 h) and had free access to water and standard rodent chow diet (LabDiet 5001, LabDiet, Inc., Brentwood, Leduc, AB, Canada;

metabolizable energy 3.02 kcal/g). Mice were weighed twice weekly and cages changed twice weekly. The care and treatment of the mice was in accordance with the guidelines of the Canadian Council on Animal Care, and protocols were approved by the University of Northern British Columbia's Animal Care and Use Committee.

Cold Acclimation and Melanotan II treatment

Female mice (PACAP $+/+$ (n=16), PACAP $-/-$ (n=16)) were acclimated to 4°C by initially being moved in their home cages from 24°C to 18°C for 7 days and then to 4°C for 30 days (Figure 2.3). This timeframe was selected as full acclimation to cold and maximal induction of adaptive thermogenesis requires 3-4 weeks at 4°C (Cannon & Nedergaard, 2010; Meyer et al., 2010; Ukropec et al., 2006).

After 7 days of acclimation in 4°C, the mice were given daily intraperitoneal (IP) injections (alternating injection site on left and right sides every 3 days) of either phosphate-buffered saline (PBS) as the vehicle (1xPBS, 0.12ml) or Melanotan II (MTII, 0.4mg/kg in 0.12ml 1xPBS) for 23 days. PACAP $+/+$ (n=9) and PACAP $-/-$ mice (n=9) received PBS, and PACAP $+/+$ (n=7) and PACAP $-/-$ mice (n=7) received MTII. During the day of calorimetry, injections were not given. Throughout this paper, PACAP $+/+$ mice will be referred to as wildtype (WT) and PACAP $-/-$ as knockout (KO). Thus, four treatment groups exist and will be referred to as the following: PBS WT, PBS KO, MTII WT and MTII KO.

Body Composition

Body composition was measured pre- and post-treatment using time-domain nuclear magnetic resonance (TD-NMR). Unanaesthetised mice were individually placed in a restrainer with access to oxygen and then placed in the minispec mq TD-NMR machine for two minutes while measurements of total body fat, fluid, and lean mass were obtained (minispec mq, TD-NMR, Bruker, CA). The fat and lean masses were calculated as a

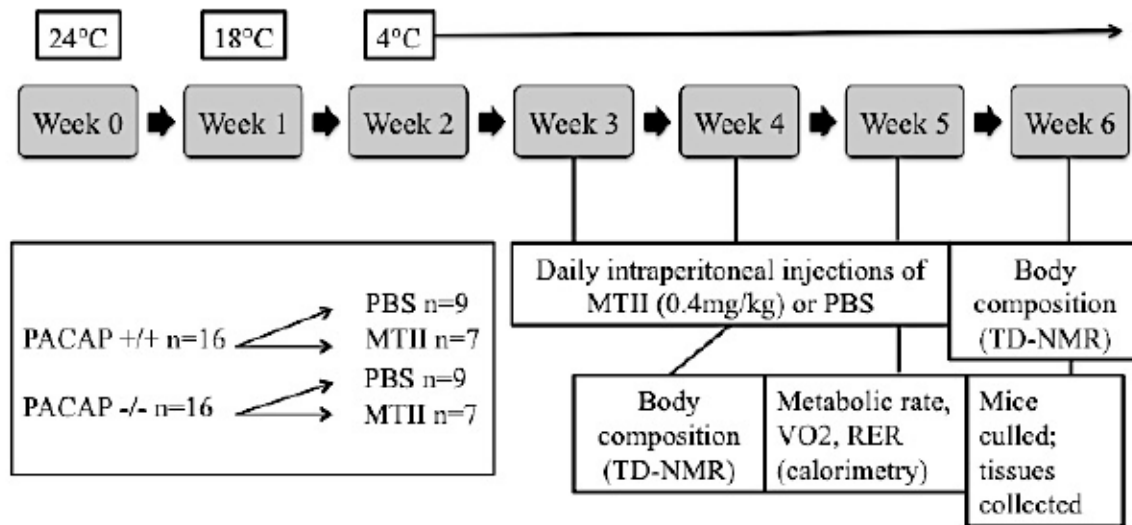


Figure 2.3. Schematic of methodology over the course of the 6-week experiment.

percentage of total body mass, and the pre- and post-treatment fat and lean mass percentages were calculated.

Thermogenic Capacity through Oxygen Consumption

On day 21 of treatment, oxygen consumption of the mice was individually measured by open circuit calorimetry (Oxymax machine, Columbus Instruments, Columbus, OH, USA). The single-mouse Oxymax housing chamber was equilibrated for two hours before basal oxygen consumption was measured in the animals. Animals were anesthetised with sodium pentobarbital (50-60mg/kg, ip). Once a plane of anesthesia was reached, the interscapular region was shaved and disinfected with 90% isopropyl alcohol. A cannula was inserted subcutaneously over the interscapular BAT to allow for the administration of NE later in the experiment while avoiding opening the chamber. The mice were then placed into the Oxymax chamber for 10 minutes to allow for equilibration of the machine. The animals then spent approximately 15 minutes in the chamber to allow for basal metabolic rate (BMR) (defined below) to be recorded. After oxygen consumption readings were stable, NE (1mg/kg, sc) was injected over the BAT of the mice via the cannula and oxygen consumption was measured for approximately one hour until the maximal metabolic rate (MMR) occurred, as determined by a peak in oxygen consumption followed by a steady decline in oxygen consumption. BMR was defined as the mean of the five lowest oxygen consumption values prior to the NE injection. MMR was defined as the mean of the five highest oxygen consumption values after NE administration. Oxygen consumption values were recorded every 10 seconds and were then calculated and reported as an average reading over 2 minutes, beginning 10 minutes prior to NE injection and ending approximately 34 minutes post NE injection. Oxygen consumption values from the Oxymax software were normalized to each animal's pre-treatment lean mass (ml/min/kg lean mass). Respiratory exchange ratio

(RER) is a calculated ratio between the volume of carbon dioxide (VCO_2) produced and oxygen (VO_2) used (VCO_2/VO_2) and represents a measure of which macronutrient (fat or carbohydrate) is oxidized for fuel utilization (Gavini, Jones, & Novak, 2016). As with oxygen consumption value, RER values were recorded every 10 seconds and were then calculated and reported as an average reading over 2 minutes, beginning 10 minutes prior to NE injection and ending approximately 34 minutes post NE injection.

Post-mortem Analysis

Upon completion of the 23-day treatment, the non-fasted mice were weighed and deeply anesthetized with isoflurane. Blood was collected into heparinized tubes by cardiac puncture (approx. 0.7-1.0 ml/mouse) and spun down at 3,000 rpm for 10 minutes and plasma collected. The mice were then euthanized with isoflurane and cervical dislocation. Tissues weighed and collected included BAT, inguinal and gonadal white adipose tissue (ingWAT, gWAT), liver and pancreas. These tissues, in addition to skeletal muscle, small intestine, kidney, heart and lungs were flash frozen in liquid nitrogen and stored in -80°C . Tissues fixed in 10% formalin included BAT, ingWAT, gWAT, skeletal muscle, kidney, pancreas, and adrenal glands. The brain was collected, frozen and stored at -80°C .

RNA Extraction and cDNA generation

RNA extractions were performed on frozen samples of BAT, ingWAT and gWAT. Tissues (0.05-1g) were homogenized in TRIzol (Life Technologies) and RNA was extracted according to the manufacturer's protocol, using the additional optional process for samples with high fat content provided. TURBO DNase (Life Technologies) was used in accordance with the manufacturer's protocol to remove DNA contamination. RNA concentration and purity were evaluated through UV light absorbance measurements using spectrophotometry (Nanodrop ND-1000; Thermo Scientific, Rockford, IL, USA). Absorbance levels of the

sample at 260nm were used as a surrogate measure of RNA concentration (the wavelength at which nucleotides absorb UV light). The ratio of absorbance at 260nm and 280nm (the wavelength at which protein absorbs UV light) was used to assess the purity of RNA, where a ratio of ~2.0 is generally accepted as “pure” for RNA. As a secondary measure of nucleic acid purity, the ratio of absorbance at 260nm and 230nm was used to identify the presence of contaminants that absorb at 230nm, such as phenol present in the TRIzol reagent used during RNA extractions. 260/230 values commonly range between 2.0-2.2 for “pure” nucleic acid. RNA integrity was assessed by observing intact, bright and distinct 18S and 28S rRNA bands on ethidium bromide stained 1.5% agarose gels (Appendix Figure S2.2). RNA (500ng) was reverse transcribed into cDNA (Superscript III, Invitrogen) with a blend of oligo(dT) and random hexamer primers according to the manufacturer’s protocol.

Gene Expression

BAT thermogenic gene expression (β 3-AR, HSL, and UCP1), one control gene (β 1-AR), and six reference genes (18S, TBP, GAPDH, PGK1, RPL19, and PPIA) were assessed using quantitative real-time polymerase chain reaction (qPCR). 15 μ l reactions were carried out using an iQ5 thermocycler (Bio-Rad Laboratories) and contained forward and reverse primers (1 μ M; Sigma), nuclease-free H₂O, 1/10 cDNA (1.5 μ l), and SYBR Green Supermix (1X). Primers used in this experiment had been previously optimized in the Gray lab (by Daemon Cline) and conformed to the Minimum Information for Publication of Quantitative Real-time PCR Experiments (MIQEs) guidelines (Bustin et al., 2009). A measure of reference gene stability (*M*) across genotypes and treatments was determined with Biogazelle (Biogazelle qBasePlus 2.4, Zwijnaarde, Belgium) where reference genes with *M* < 0.5 were accepted. Two reference genes (RPL19 and PPIA) were selected for each gene expression

analysis ($M = 0.26$). Fold change in gene expression was calculated for each gene, in each group, as compared to expression from PBS WT animals.

Histology

Formalin-fixed tissues were sent for histological sectioning (Wax-It Histological Services, UBC, Vancouver, Canada): BAT, ingWAT, and gWAT (PBS WT (n=4), PBS KO (n=4), MTII WT (n=4), MTII KO (n=4)). Tissues were paraffin embedded, sectioned (5 μ m thick), and stained with hematoxylin and eosin for viewing on a light microscope (Olympus BX61). Analyses were completed for BAT and gWAT in conjunction with an undergraduate honours thesis (in collaboration with Maeghan Forster).

Histological Micrographs

Histological analyses performed in this study were recently developed by UNBC Gray lab members and have not been previously documented in our research. Therefore, control animals with well-documented differences in the histological presentation of BAT were initially analyzed (thermoneutral (30°C) versus cold stressed (4°C) animals; results not shown or discussed). Results using this newly developed protocol were consistent with those documented in the literature, thus ensuring the validity of the protocol for experimental analyses.

Ten micrographs of BAT were taken (Olympus BX61) per mouse (n = 4 mice per treatment) at 60x magnification using an oil immersion objective within three tissue sections (3 tissue sections/slide). Tissue sections used for the micrographs were selected randomly, however, care was taken to avoid field of views that contained large blood vessels, damaged cells, or heterogeneity among cell types to ensure proper representation of adipocytes.

Three micrographs of gWAT were taken (Olympus BX61) per mouse (n = 4 mice per treatment) at 20x magnification. In cold-acclimated PBS WT and MTII WT mice,

micrographs were taken using the same methodology for BAT with respect to random selection described above. In contrast, homogenous gWAT areas were selectively chosen in cold-acclimated PBS KO and MTII KO mice due to a high degree of unexpected beige adipocytes within the gWAT sections, which left very few areas with large enough regions of white adipocytes.

BAT Lipid Area

CellSens Software (Olympus) was used in all preparation and analysis of lipid area measurements of BAT. Images were converted from bright field to grayscale (Figure 2.4A), and contrast was maximized before analyses to distinguish black from white (Figure 2.4B). In grayscale adipocyte histology, lipid area and intracellular spaces appeared “white,” while cell membranes, nuclei, and blood cells appeared as different shades of “grey.” Micrographs were further edited by selectively deleting areas that were not homogeneous representatives of brown adipose cells, such as large intracellular spaces, blood vessels, or erythrocytes (Figure 2.4C). Deleting an object from the region of interest (ROI) also removed that area from the total ROI for future area percentage calculations. A manual intensity threshold was set that best represented the “grey” regions, which represented non-lipid areas of each of the cross section (gray channel: min = 0, max = 172). These “grey” areas were quantified after segmenting the micrographs into binary photos (Figure 2.4D), and then measuring area for each colour (white or grey). Results were normalized to their respective ROI area per photo (excluding deleted regions) by converting to percentages, and subtracted from 100 to give total lipid (“white”) area per micrograph.

BAT Cell Count

Cell count per field of view in BAT was performed by individually counting the number of nuclei in each image, providing a surrogate measure of overall cell size between

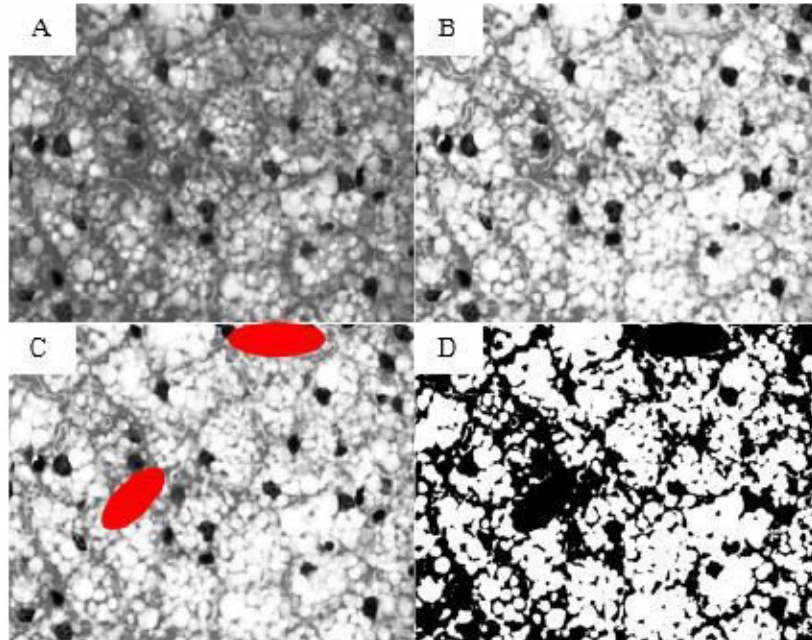


Figure 2.4. Methodological steps used to analyze BAT sections for lipid area at 60x oil immersion. A. Images were converted to grayscale. B. Contrast was maximized. C. Segments that were not brown adipocytes were selectively deleted (indicated as red). D. Image was binarized and “white” area counted as lipid.

treatment groups. To increase counting accuracy, a 4-segment grid was laid over each image (Microsoft Powerpoint). Nuclei counts of each quarter segment of a photo were added together to give one count per image. Average number of cells in a field of view was then calculated.

gWAT Cell Area Binning

To determine the distribution of different white adipocyte sizes in gWAT, CellSens Software (Olympus) was used to measure the area of white adipocytes in images taken using a 20x objective. Images were prepared for analysis by converting them to grayscale (Figure 2.5A) followed by maximizing contrast using a differential contrast enhancement filter (Band Width = 35, Enhancement = 100, Overflow = 0.05%) (Figure 2.5B). Subsequently, images were binarized to separate lipid (white) from non-lipid areas (grey) (Figure 2.5C) (Grey channel: min = 0, max = 213). Cell boundaries were then split automatically by the CellSens software, followed by manual splitting for cells that contained very thin cell membrane staining and were thus missed by automated splitting. Cells along the outer micrograph edges that did not display the entire cell circumference were deleted (Figure 2.5D). An average of the largest and smallest cell areas across micrographs was calculated to determine a range for adipose cell size binning analysis (Min: $80\mu\text{m}^2$, Max: $2000\mu\text{m}^2$). Object sizes too large or too small to represent adipocytes were excluded as they likely represent artifacts of graininess or large intracellular spaces within a micrograph. Area data was exported to Excel and sorted from largest to smallest. Cell areas were sorted into bins based on cell area (in μm^2 : 80-499, 500-999, 1000-1499, 1500-2000). Only the gWAT of cold-acclimated PBS and MTII treated PACAP WT mice were statistically analyzed due to the unexpected observation of an immense amount of beige adipocytes in gWAT of cold-acclimated PBS and MTII treated PACAP KO mice.

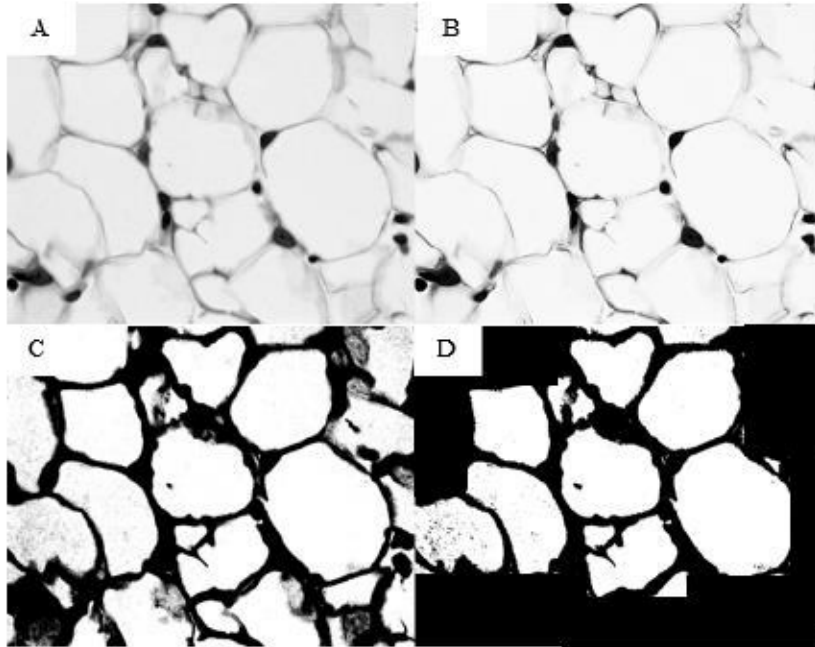


Figure 2.5. Methodological steps used to determine cell area counts in histological sections of gWAT imaged at 20x. A. Images were converted to grayscale. B. Differential contrast was maximized. C. Images were binarized. D. Adipocytes not entirely displayed within the field of view were excluded from analyses.

Statistical Analyses

Results were expressed as group mean \pm standard error mean (SEM). Two-way ANOVA was used to determine mean differences between treatment groups (cold-acclimated PBS WT, PBS KO, MTII WT, and MTII KO mice), where interactions between two independent variables may influence the dependent variable. The independent variables were time and treatment group, and the dependent variable was one of the following: body mass, body composition, oxygen consumption, or RER. One-way ANOVA with Tukey's test for pairwise comparisons was used for comparisons between all four treatment group means and were performed for gene expression, BAT lipid area, and BAT cell count. Unpaired t-tests were used to analyze mean differences between tissue masses for cold-acclimated PBS WT and cold-acclimated PBS KO mice, as well as cold-acclimated PBS WT and cold-acclimated MTII KO mice. Unpaired t-tests were also used for the number of ingWAT cells within each cell size bin between cold-acclimated PBS WT and cold-acclimated MTII WT mice. The detection of outliers was determined using Grubb's test. Results were considered statistically significant using an alpha of 0.05. Statistical analyses were performed using GraphPad Prism Software, version 6.0b.

2.3 RESULTS

Analyses Between Different Genotypes and Treatments

This study examined the effect and interaction of both PACAP genotype and melanocortin agonist treatment on thermogenic capacity in mice and thus, as described above, we present here results for 4 groups of cold-acclimated animals: PBS WT, PBS KO, MTII WT and MTII KO. Comparisons between cold-acclimated MTII WT and PBS KO are not reported, as they are not physiologically relevant; cold-acclimated MTII WT animals were used to determine the effects of MTII on WT animals (if any) to ensure proper analysis

of MTII KO animals. Although no significance was observed in *any* result between cold-acclimated PBS WT and MTII WT, the trends that did exist will be discussed and suggest that, as expected MTII may have had some physiological effect on cold-acclimated WT animals, and thus allowed us to confidently assess the cold-acclimated MTII KO animals.

Comparisons between cold-acclimated PBS KO and MTII KO mice (or between cold-acclimated MTII WT and MTII KO mice) were also not the focus of these analyses (but will be discussed where appropriate) as we aimed to determine if MTII KO mice were rescued back to physiological normal levels (as compared to cold-acclimated PBS WT animals). Therefore, *changes in the differences* between cold-acclimated PBS WT and PBS KO mice versus cold-acclimated PBS WT and MTII KO mice will be the focus of the analyses.

MTII Treatment Caused No Significant Effect on Body Weight or Body Composition

No significant difference in body weight or body composition was observed between cold-acclimated PBS WT, PBS KO, MTII WT or MTII KO animals (two-way ANOVA, $p > 0.05$) (Figure 2.6, Figure 2.7).

MTII Partially Rescues Diminished gWAT Depot in Cold-Acclimated PACAP KO Mice

As expected from previously published results, there was a significant decrease in gWAT mass in cold-acclimated PBS KO mice compared to cold-acclimated control mice, PBS WT (unpaired t-test, $p < 0.05$) (Figure 2.8) (Adams et al., 2008; Diané et al., 2014). This significance was not observed between cold-acclimated PBS WT and MTII KO (unpaired t-test, $p > 0.05$). Similar trends were observed in both ingWAT and BAT, but no significance was identified (Figure 2.8).

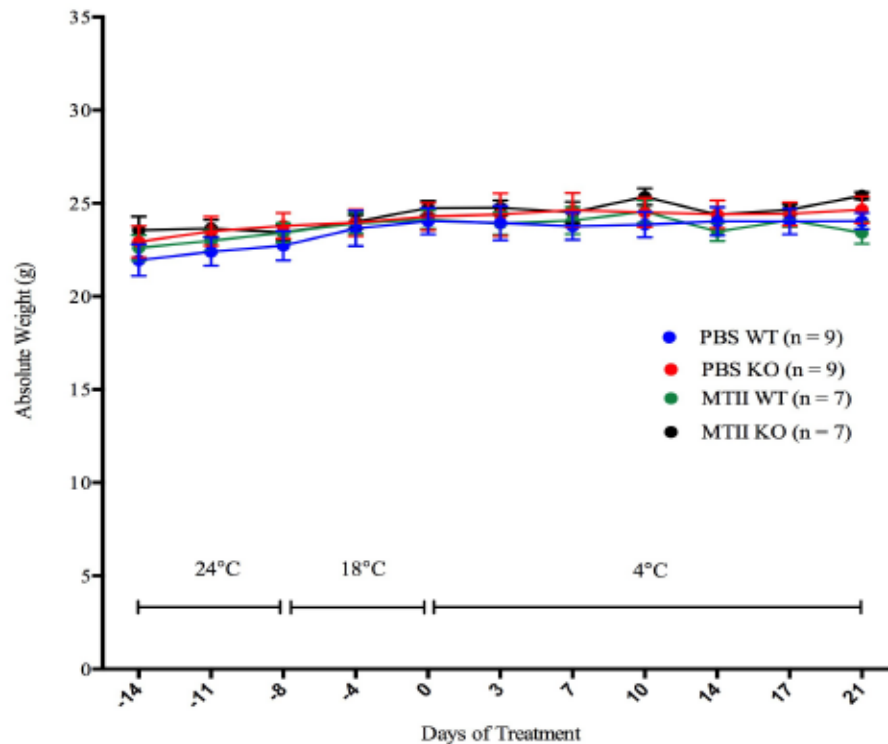


Figure 2.6. Body mass of PBS WT, PBS KO, MTII WT, and MTII KO mice over the course of the experiment. Treatment with vehicle (PBS) or MTII began on Day 7. Data are mean \pm SEM. Two-way ANOVA, $p > 0.05$.

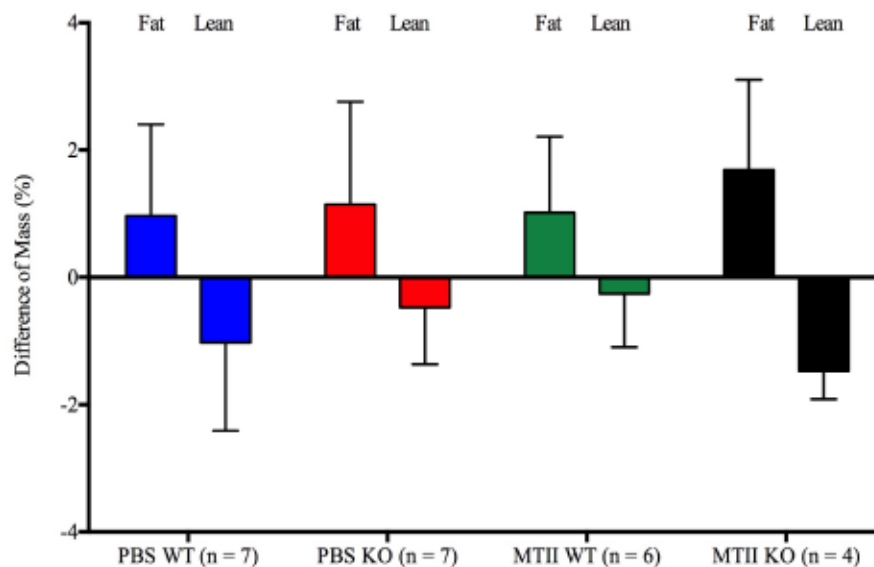


Figure 2.7. Difference of fat and lean mass as a percentage of total mass in PBS WT, PBS KO, MTII WT, and MTII KO mice pre and post 4°C cold challenge. Data are mean \pm SEM. Two-way ANOVA, $p > 0.05$.

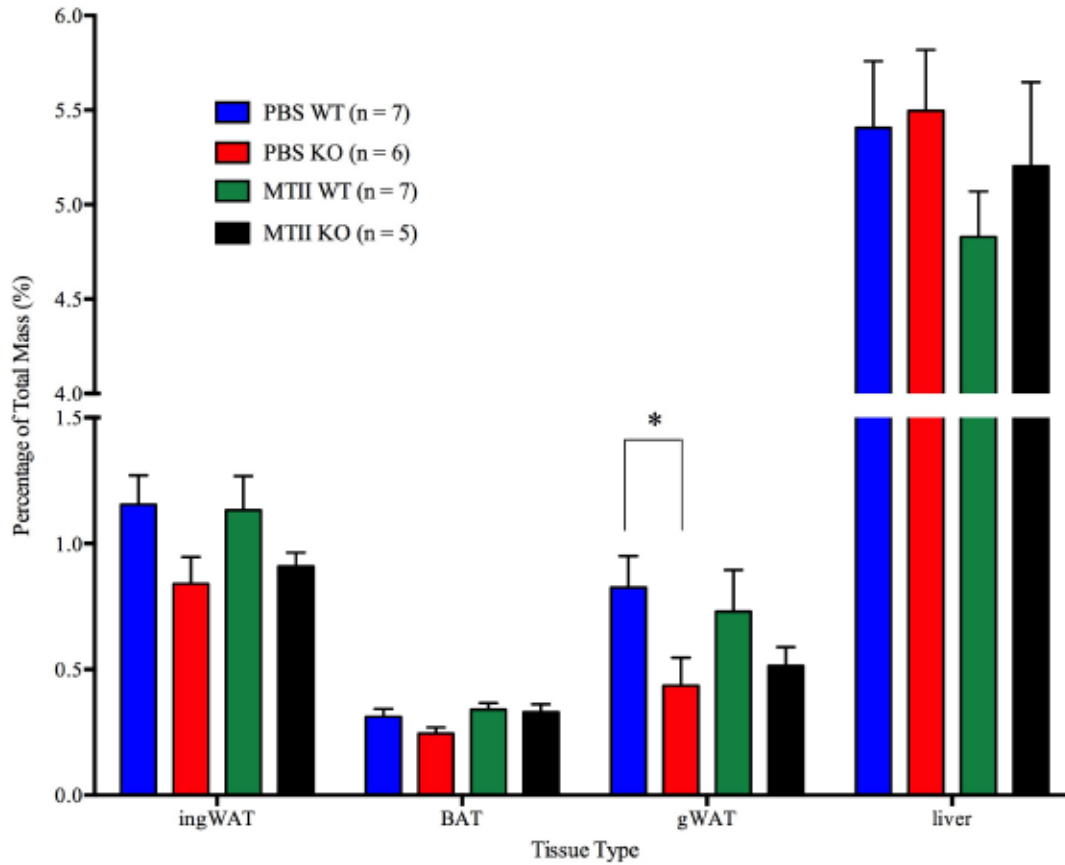


Figure 2.8. Percent tissue mass per total body mass of different tissue types in PBS WT, PBS KO, MTII WT, and MTII KO mice after 4-week 4°C cold challenge. Data are mean ± SEM. Unpaired t-tests. *p < 0.05 indicates a genotype effect within the same treatment.

MTII Partially Rescues Impaired Thermogenic Capacity of Cold-Acclimated PACAP KO Mice

To test the hypothesis that PACAP acts upstream of the melanocortin system, the effect of the melanocortin agonist, MTII (0.4mg/kg, 23 days) on thermogenesis in cold-acclimated PACAP WT and PACAP KO mice was evaluated first through oxygen consumption as a measurement of thermogenic capacity. Although no significance was observed between cold-acclimated PBS WT and PBS KO or cold-acclimated PBS WT and MTII KO, a trend showed cold-acclimated PBS WT achieving higher oxygen consumption values than cold-acclimated PBS KO, while cold-acclimated MTII KO values trended higher than cold-acclimated PBS KO (two-way ANOVA, $p > 0.05$) (Figure 2.9A). Additionally, while no difference was observed in BMR between all four groups (two-way ANOVA, $p > 0.05$), as previously reported by the Gray lab, there was a significant difference in MMR between cold-acclimated PBS WT and PBS KO mice (two-way ANOVA, $p < 0.05$) (Figure 2.9B) (Diané et al., 2014). This significance was lost between cold-acclimated PBS WT and MTII KO mice (two-way ANOVA, $p > 0.05$) (Figure 2.9B).

MTII Partially Rescues Impaired Fuel Usage in Cold-Acclimated PACAP KO Mice

Respiratory exchange ratio (RER), a measure of which macronutrient (fat or carbohydrate) is metabolized for fuel utilization, was calculated from Oxymax data as a ratio of VCO_2 to VO_2 and showed that, as expected, the administration of NE induced a decrease in RER in both cold-acclimated PBS WT and MTII WT mice, indicating preferential oxidation of lipids over carbohydrates following adrenergic stimulation (Figure 2.10). Previously, the Gray lab has shown that cold-acclimated PACAP KO mice do not experience this shift in RER with adrenergic stimulation: a finding that was repeated in this study, where RER in cold-acclimated PBS KO mice remained steady at ~ 0.85 after the NE injection.

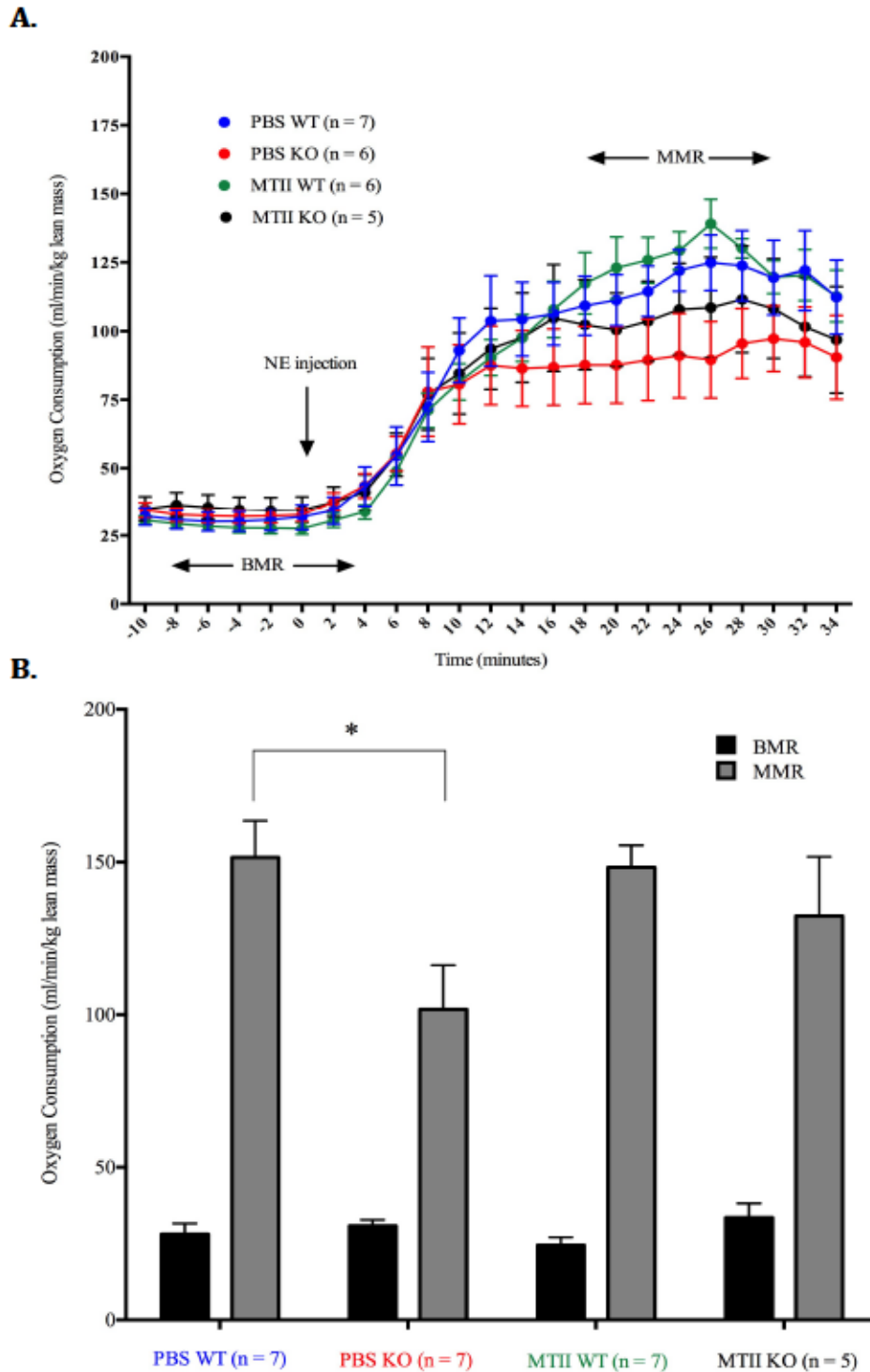


Figure 2.9. A. Norepinephrine induced thermogenesis in cold-acclimated PBS WT, PBS KO, MTII WT, and MTII KO mice. B. Mean basal metabolic rate (BMR) and maximal metabolic rate (MMR) of cold-acclimated PBS WT, PBS KO, MTII WT, and MTII KO mice. Data are expressed as mean \pm SEM. Two-way ANOVA. * $p < 0.05$ indicates a genotype effect within the same treatment.

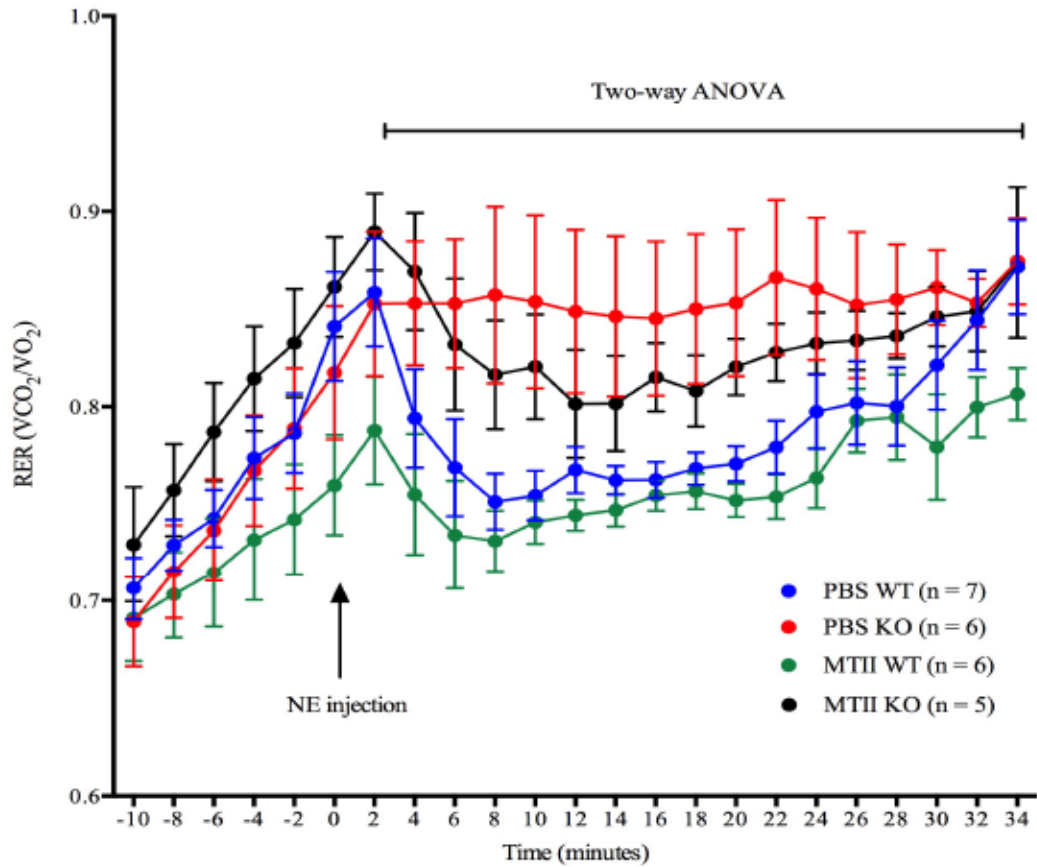


Figure 2.10. Respiratory exchange ratio (RER) of cold-acclimated PBS WT, PBS KO, MTII WT, and MTII KO mice. Statistical significance ($p < 0.05$) between PBS WT and PBS KO at 8 and 10 minutes and between MTII WT and MTII KO at 2, 4 and 6 minutes. Two-way ANOVA.

Interestingly, cold-acclimated MTII KO mice showed a decrease in RER representing a preference toward lipid utilization following adrenergic stimulation, as observed in cold-acclimated PBS WT mice (Figure 2.10). Statistical significance was exhibited between cold-acclimated PBS WT and PBS KO at 8 and 10 minutes and between cold-acclimated MTII WT and MTII KO at 2, 4 and 6 minutes (two-way ANOVA, $p < 0.05$).

No Difference in Thermogenic Gene Expression was Observed in BAT Between Cold-Acclimated PBS or MTII Treated PACAP WT or PACAP KO Mice

No significant difference was observed between cold-acclimated PBS WT, PBS KO, MTII WT, or MTII KO mice for thermogenic gene expression of β 3-ARs, HSL and UCP1 (one-way ANOVA, $p > 0.05$) (Figure 2.11). β 1-AR expression, used as a control to ensure MTII effects were localized to pathways involved in thermogenesis, was also not significantly different between groups (one-way ANOVA, $p > 0.05$) (Figure 2.11).

No Significant Difference Between Lipid Area or Cell Size in BAT of Cold-Acclimated MTII WT and MTII KO Mice

Although no significant difference in lipid area between cold-acclimated PACAP WT or PACAP KO mice treated with either PBS or MTII was observed (one-way ANOVA, Tukey's Test, $p > 0.05$) (Figure 2.12A), a trend indicated that both cold-acclimated MTII WT and MTII KO animals displayed greater lipid area per ROI compared to cold-acclimated PBS WT and PBS KO mice.

In agreement with these results, no significant difference in the number of cells per field of view between cold-acclimated PACAP WT or PACAP KO mice treated with either PBS or MTII was observed (one-way ANOVA, Tukey's Test, $p > 0.05$) (Figure 2.12B). However, a trend indicated that both cold-acclimated MTII WT and MTII KO animals displayed fewer numbers of cells per ROI compared to cold-acclimated PBS WT and PBS

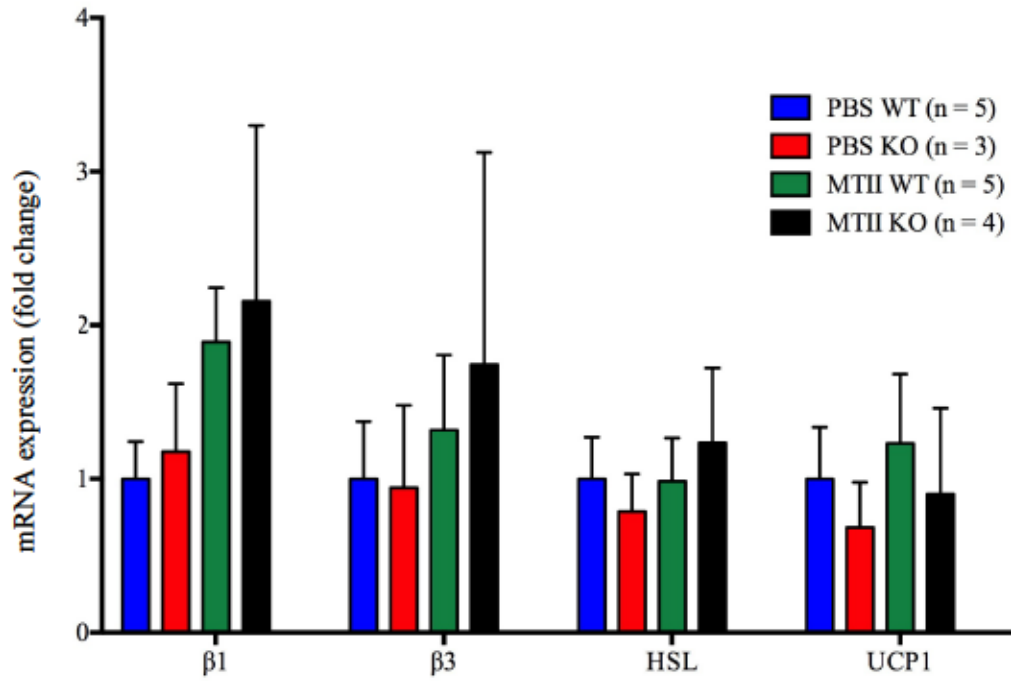
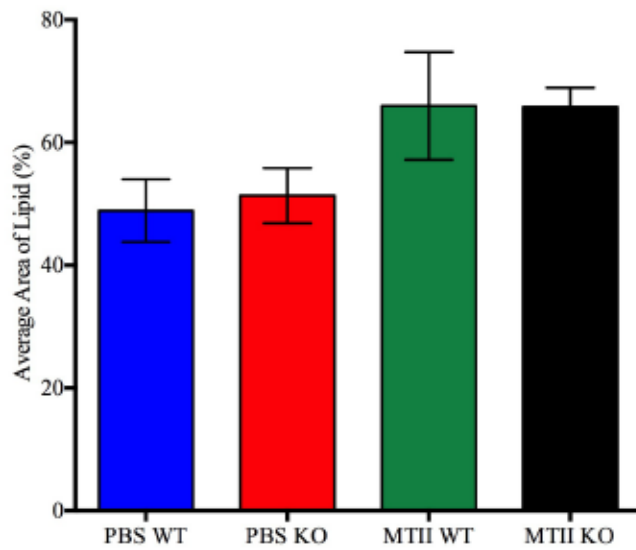


Figure 2.11. Gene expression in BAT of cold-acclimated PBS WT, PBS KO, MTII WT, and MTII KO mice. Target gene expression was normalized to two reference genes: RPL19 and PPIA. Data are expressed as \pm SEM. One-way ANOVA for each gene, $p > 0.05$.

A.



B.

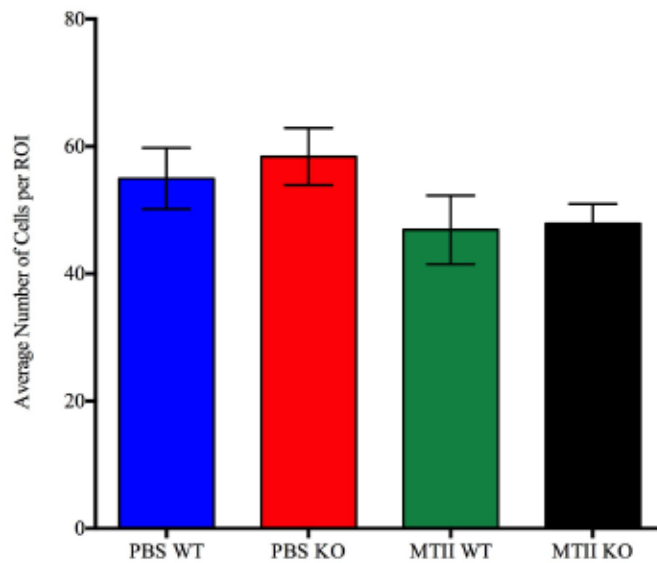


Figure 2.12. A. Average percent lipid area/field of view in cold-acclimated PBS WT, PBS KO, MTII WT, and MTII KO mice. B. Average numbers of nuclei per ROI in cold-acclimated PBS WT, PBS KO, MTII WT, and MTII KO mice. Data are expressed as \pm SEM. One-way ANOVA, $p > 0.05$.

KO mice.

MTII WT Mice Display Increased Number of Small White Adipocytes Compared to PBS WT Mice

There was no significant difference between the number of white adipocytes within each cell size bin between cold-acclimated PACAP WT animals treated with PBS or MTII (unpaired t-test, $p > 0.05$) (Figure 2.13). However, a trend showed cold-acclimated MTII WT mice had higher numbers of small cells (80-900 μ m) than those in cold-acclimated PBS WT mice. The analyses were not completed for cold-acclimated PBS KO or MTII KO animals due to unexpected heterogeneity of adipocyte types (brown or beige adipocytes) within the gWAT of cold-acclimated PACAP KO animals (discussed below).

Cold-Acclimated PACAP KO Mice Have Extensive Browning Within Their gWAT Depot

Cold-acclimated PBS WT and MTII WT displayed homogeneous gWAT composed of characteristic unilocular white adipocytes with isolated, small regions of mild browning (Figure 2.14A, C). In contrast, histological sections of gWAT in cold-acclimated PBS KO and MTII KO revealed extensive multilocular adipocytes (beige or brown) within the WAT sections (Figure 2.14B, D). Browning was so extensive in gWAT samples of all cold-acclimated PACAP KO mice examined ($n = 7$), that it was not possible to obtain three images comprised predominantly of unilocular, white adipocytes.

2.4 DISCUSSION

In response to cold exposure, literature shows PACAP KO mice exhibit impaired thermogenic capacity compared to PACAP WT mice, indicated by both physiological and molecular detriments (Adams et al., 2008; Diané et al., 2014; Gray et al., 2001; Gray et al., 2002). Physiological impairments previously observed in cold-acclimated PACAP KO mice

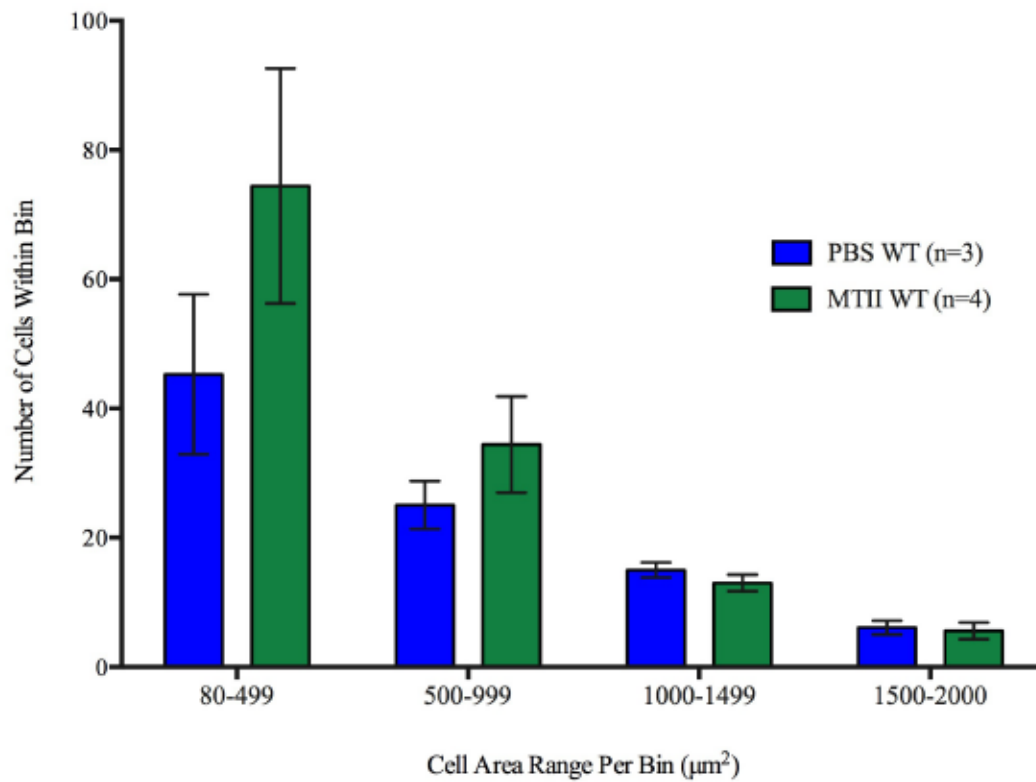


Figure 2.13. Number of cells within each cell area bin (μm^2) in cold-acclimated PBS WT or MTH WT mice. Data are expressed as \pm SEM. Unpaired t-tests, $p > 0.05$.

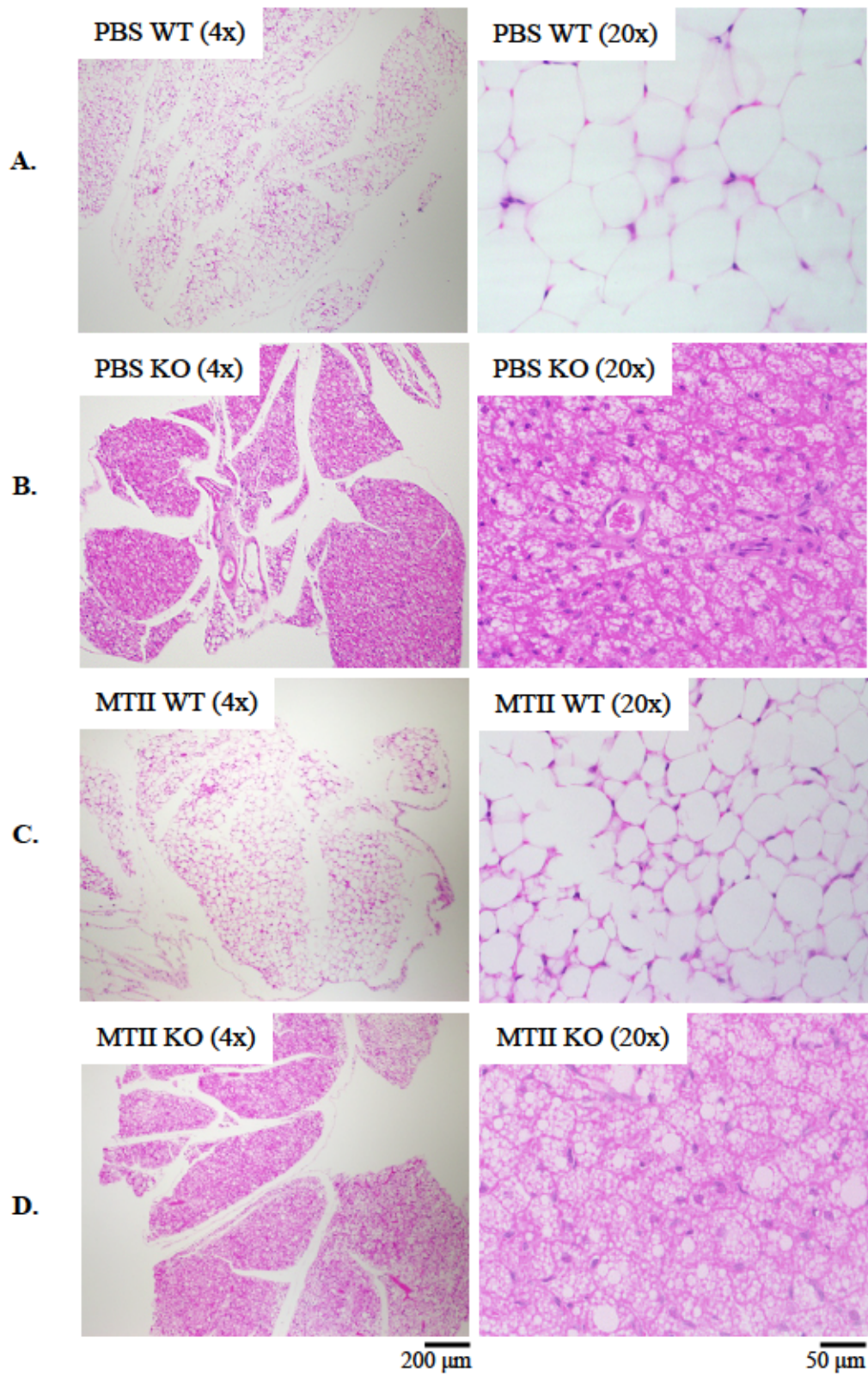


Figure 2.14. Representative images of hematoxylin and eosin-stained gWAT observed at 4x and 20x in cold-acclimated PBS WT (A), PBS KO (B), MTII WT (C), and MTII KO mice (D).

and documented in the published literature include: decreased adaptive thermogenesis in response to cold stress as measured by decreased NE-induced oxygen consumption, an inability to utilize lipid as the primary fuel source in response to sympathetic stimulation, and decreased white adipose tissue mass compared to PACAP WT mice (Diané et al., 2014; Gray et al., 2002). Notably, these results have been replicated here in cold-acclimated PACAP KO mice (PBS KO mice), although not to the same degree as indicated in previously published studies, possibly due to the different genetic background of the PACAP null mouse line used between studies (discussed below) (Figure 2.9, 2.10, and 2.8, respectively). Furthermore, in this study, all three observed physiological impairments were partially rescued in cold-acclimated PACAP KO mice treated with MTII (MTII KO mice), as indicated by intermediate phenotypes in this group compared to cold-acclimated PBS-treated PACAP WT (PBS WT mice) (Figure 2.8, 2.9, and 2.10). Each of these findings will be discussed here in detail.

Importantly, NE-induced oxygen consumption is a measure of adaptive thermogenesis in BAT, a process that is imperative in maintaining homeostasis of body temperature in response to cold exposure or feeding (Cannon & Nedergaard, 2004; Nedergaard & Lindberg, 1979). When BAT is absent or functionally deficient, one mechanism by which the body attempts to control body temperature is via skeletal muscle oxidation through shivering or increased physical activity (Grubb & Folk, 1976; Schaeffer, Villarin, & Lindstedt, 2003; Shiota & Masumi, 1988). Therefore, in order to ensure the measurements of NE-induced oxygen consumption reflected the thermogenic capacity of BAT to perform adaptive thermogenesis, rather than increased muscle activity, oxygen consumption measurements were performed on anesthetized animals. The lower oxygen consumption values observed in cold-acclimated PBS KO mice as compared to cold-

acclimated PBS WT mice (Figure 2.9) therefore confirms impaired BAT activity in PACAP KO mice: a result previously observed (Diane et al., 2014). Interestingly, NE-induced oxygen consumption measurements increased in cold-acclimated MTII KO mice as they displayed oxygen consumption levels higher than those of cold-acclimated PBS KO mice. Although, cold-acclimated MTII KO mice did not exhibit improvements in adaptive thermogenesis to levels observed in genetically unaltered cold-acclimated PBS WT mice, an intermediate phenotype was observed (Figure 2.9). This intermediate phenotype was observed over time, as indicated in the oxygen consumption curve (Figure 2.9A), and was further supported with the calculated MMR (Figure 2.9B), suggesting a partial rescue of the impaired BAT activity in cold-acclimated PACAP KO mice with MTII treatment.

A previously published study showed increased spontaneous locomotor activity in PACAP KO mice compared to control WT mice, while other studies showed increased skeletal muscle activity and oxidative consumption capacity in cold-acclimated animals with absent BAT (Grubb & Folk, 1976; Hashimoto et al., 2001; Mollica et al., 2005; Schaeffer, Villarin, & Lindstedt, 2003; Shiota & Masumi, 1988; Simonyan et al., 2001). Increased skeletal muscle activity was observed by increased muscle temperature where calories were presumably dissipated as heat energy, and increased NE turnover to skeletal muscle indicating increased sympathetic nerve activity to skeletal muscle (Nogueiras et al., 2007). Therefore, increased skeletal muscle activity may be a mechanism by which PACAP KO mice adapt to survive cold exposure when confronted with impaired adaptive thermogenesis (Grubb & Folk, 1976; Hashimoto et al., 2001; Mollica et al., 2005; Schaeffer, Villarin, & Lindstedt, 2003; Shiota & Masumi, 1988; Simonyan et al., 2001).

Altering fuel usage is another method of adaptation that is required for a response to environmental stressors such as cold exposure (Haman et al., 2002). Fuel sources include

carbohydrates, protein, and lipids (Haman et al., 2002). During prolonged cold exposure, muscle contractions receive the majority of their fuel from carbohydrates with a minor contribution from protein, whereas adaptive thermogenesis in BAT is fueled by FFAs derived from the breakdown of intracellular or circulating triglycerides (Figure 1.8) (Baba et al., 2012; Haman et al., 2002; Ouellet et al., 2012). Because the oxidation of these macronutrients produce different quantities of CO₂, calculating the ratio between the volume of CO₂ and the volume of O₂ (RER) as measured by indirect calorimetry is an indicator of which substrate is preferentially oxidized for fuel utilization (Virtue & Vidal-Puig, 2013). RERs range from 0.7 (pure lipid oxidation) to 1.0 (pure carbohydrate oxidation) (Gavini, Jones, & Novak, 2016; Virtue & Vidal-Puig, 2013). Normally, as observed in cold-acclimated PBS WT control mice, RER drops towards lipid utilization (0.7) upon NE stimulation, as adrenergic stimulation promotes lipolysis of triglycerides to FFAs in WAT and BAT, providing substrate for adaptive thermogenesis in BAT (Figure 2.10) (Diane et al., 2014). As previously published and shown here in these results, cold-acclimated PBS KO mice failed to display a drop in RER in response to NE and instead displayed a consistent RER over time with values closer to those indicative of carbohydrate use (Figure 2.10) (Diane et al., 2014; Nedergaard & Lindberg, 1979; Ouellet et al., 2012). This altered RER displayed in cold-acclimated PBS KO mice could indicate a dysfunction in lipid mobilization from adipose tissue, possibly due to a decreased ability to respond to NE, which is known to induce lipolysis in WAT and BAT (Chondronikola et al., 2016; Saito, Yoneshiro, & Matsushita, 2016).

Interestingly, RER of cold-acclimated MTII KO mice followed a similar trend to that of cold-acclimated PBS WT mice, suggesting a partial rescue of the altered fuel usage observed in PACAP KO mice with MTII treatment (Figure 2.10). Furthermore, cold-

acclimated MTII WT mice displayed a trend in RER that decreased beyond values observed in cold-acclimated PBS WT mice (Figure 2.10); a result observed previously in the literature in rats treated with MTII at the level of the VMN (during both steady and increased physical activity) and consistent with the melanocortin system's role in increasing lipid mobilization (Gavini, Jones, & Novak, 2016; Nogueiras et al., 2007). This observation was further supported in the histological examination of gWAT where a trend indicated cold-acclimated MTII WT mice displayed higher numbers of small cells (80-900 μ m) than those in cold-acclimated PBS WT mice (Figure 2.13), suggesting increased lipid mobilization with MTII treatment.

PBS KO mice have been shown previously to display decreased WAT mass; a trend observed here in ingWAT (non-significant) and gWAT (significant) (Figure 2.8) (Diané et al., 2014). The reduced WAT depots in cold-acclimated PACAP KO mice may be related to the impaired NE-induced oxygen consumption observed in cold-acclimated PACAP KO mice. In a mouse model with severely reduced WAT mass (lipoatrophic A-ZIP/F-1, discussed in Chapter 1), mice treated with a β 3 agonist did not display an increase in oxygen consumption, suggesting a key driver for NE-induced thermogenesis in the availability of fuel stores from adipocytes (Gavrilova, Marcus-Samuels, & Reitman, 2000). Therefore, impairments in WAT may lead to impairment of adaptive thermogenesis in BAT of PACAP KO mice, as FFAs released from triglyceride stores in WAT are a key substrate for lipid oxidation in adaptive thermogenesis (Chondronikola et al., 2016; Saito, Yoneshiro, & Matsushita, 2016). Supporting the intermediate phenotype of cold-acclimated MTII KO mice discussed above, treatment of cold-acclimated PACAP KO mice with MTII partially rescued the decreased adipose tissue mass of cold-acclimated PACAP KO mice compared to cold-acclimated PACAP WT mice (Figure 2.8).

Collectively, these physiological results show an intermediate phenotype displayed in cold-acclimated PACAP KO mice upon activation of the melanocortin system with MTII. Activation of the melanocortin system using this approach did not fully restore the impaired physiological responses of the cold-acclimated PACAP KO mice to normal (as measured in control, cold-acclimated PBS WT mice) but provides preliminary evidence that supports the hypothesis that PACAP acts upstream of the melanocortin system in regulating SNA to stimulate BAT thermogenesis in response to cold exposure. Furthermore, these observations provide *genetic* support for the study described above and in Chapter 1 where Tanida, Shintani, & Hashimoto (2011) used a *pharmacological* intervention showing that PACAP signaling to BAT does not occur when a MC4R antagonist is used, thus suggesting PACAP acts upstream from the melanocortin system in activating SNA to stimulate thermogenesis.

Molecular analyses of thermogenic gene expression were performed in order to refute or support the preliminary physiological improvements in thermogenesis observed in cold-acclimated PACAP KO mice with MTII treatment. However, of the 28 mice that underwent Oxymax experiments, 13 died either during or shortly after the experiment, possibly due to the inability to effectively regulate body temperature after prolonged anesthesia. As a consequence of the acute effects of NE stimulation on BAT, particularly on the genes involved in the mechanism of adaptive thermogenesis, only tissues from animals that lived until the day of dissection were used for qPCR thermogenic gene expression analysis (Cannon & Nedergaard, 2004). Due to the low sample sizes (particularly in cold-acclimated PBS KO (n = 3) and MTII KO (n = 4) mice), large standard error (particularly in cold-acclimated MTII KO mice), and inconsistent results compared to previously published literature, it was concluded that additional samples were necessary in order to confidently compare results of gene expression analysis between groups (Figure 2.11).

Histological analyses of BAT and gWAT were also performed to provide further evidence in support or opposition of the intermediate phenotype displayed in cold-acclimated PACAP KO mice upon activation of the melanocortin system with MTII. Although no significance was observed, histological analyses of BAT revealed a trend where both cold-acclimated MTII WT and MTII KO exhibited greater lipid area and decreased number of cells compared to cold-acclimated PBS WT and PBS KO mice (Figure 2.12). Initially, this result appeared to be contradictory to predicted results, where stimulating adaptive thermogenesis with MTII treatment would be expected to decrease lipid stores in BAT. However, upon further investigation as described above, this observation may be explained for cold-acclimated MTII WT mice by the alternative use of lipids from WAT to fuel adaptive thermogenesis in response to MTII treatment. This explanation was supported by the increased number of small cells (80-900 μ m) in gWAT of cold-acclimated MTII WT mice compared to cold-acclimated PBS WT mice, consistent with previous literature (Figure 2.13) (Qian et al., 2013). The white adipocytes areas in gWAT of cold-acclimated MTII KO mice, however, were not analyzed due the extensive browning that was observed (Figure 2.14).

Classically, gWAT contains homogeneous white adipocytes and functions as a major lipid storage depot and as insulation for organs (Giralt, & Villarroya, 2013; van Beek et al., 2015). Alternatively, the heterogeneity in ingWAT (not analyzed here) has been well documented, where beige adipocytes appear within the WAT depot in response to cold exposure (Bartelt, & Heeren, 2013; Shabalina et al., 2013). This selective browning in WAT is thought to occur within subcutaneous WAT depots (such as ingWAT), as they are closer to the surface of the body and therefore expected to lose heat faster than internal WAT depots (such as gWAT) (Bartelt, & Heeren, 2013). Interestingly, gWAT in both cold-acclimated PBS KO and MTII KO mice displayed extensive browning, suggesting that in response to

impaired thermogenesis during cold exposure, yet another method of adaption may exist, in addition to increased skeletal muscle activity and altered fuel usage discussed above.

Notably, the extent of the observed browning in gWAT in cold-acclimated PACAP KO mice has not been previously documented in the literature. Browning in gWAT has, however, been observed upon central administrations of thyroid hormones in the VMN, IP injections of a $\beta 3$ agonist, and stimulation of natriuretic peptides receptors (Kim et al., 2016; Martinez-Sanchez et al., 2016; Neinast et al., 2015; Weiner et al., 2016). Interestingly, these are known regulators of BAT thermogenesis described in Figure 2.1.

Although not quantified, gWAT in cold-acclimated MTII KO mice appeared to contain fewer beige adipocytes compared to cold-acclimated PBS KO mice, suggesting less compensation by browning WAT in cold-acclimated PACAP KO mice with MTII treatment (Figure 2.13). Although this finding on its own does not provide enough evidence to support the partial rescue of impaired thermogenesis in cold-acclimated PACAP KO mice with MTII treatment, it does provide another piece of evidence to contribute to the physiological results discussed above that suggest PACAP acts upstream from the melanocortin system in regulating SNA to stimulate adaptive thermogenesis in response to cold exposure. Future quantifications of the amount of “browning” through molecular analyses could further support or refute the partial rescue of the impaired adaptive thermogenesis in cold-acclimated PACAP KO mice treated with MTII discussed above.

Importantly, the genetic background of the mice should be considered when referencing previous literature to enable appropriate interpretation of the phenotypic expression of the specific genes (as mentioned above). The mice used in these experiments were of mixed genetic background (C57BL/6 and 129/SvJ), whereas mice used previously in the Gray lab were of pure genetic background (backcrossed onto a C57BL/6 background)

(Diané et al., 2014; Gray et al., 2002). As a result of extensive inbreeding, pure genetic backgrounds are genetically uniform, which allows for a more accurate evaluation of the observed phenotype (resulting from genetic manipulation) by eliminating phenotypic variations caused by mixed genetic backgrounds (Yoshiki & Moriwaki, 2006). As such, mice from pure genetic backgrounds are typically the gold standard used in transgenic research, which is why they were initially used in the Gray lab. However, due to the complexity of the PACAP KO phenotype that resulted in high mortality rates, animal care and financial concerns were considered: because a large number of animals were required to provide sufficient animal numbers for robust experiments and analyses, the decision to use mice with a mixed genetic background in order to improve PACAP KO pup survival and reduce colony numbers was made.

Animals on a pure genetic background often display a more severe phenotype compared to those of mixed genetic background that display greater variability in the phenotype: a result that was observed here when comparing results derived in C57BL/6-129/SvJ PACAP KO mice to previous literature, that used pure C57BL/6 PACAP KO mice (Doetschman, 2009; Yoshiki & Moriwaki, 2006). This phenomenon is particularly prevalent in mice with targeted mutations (KO animals) and may be due to modifier genes that influence gene expression through suppression or enhancement, alteration of DNA transcription, and epigenetic effects such as DNA methylation (Doetschman, 2009; Jackson Laboratory, 2006; Yoshiki & Moriwaki, 2006). Therefore, PACAP KO mice of mixed genetic background used here may have compensatory physiological mechanisms in response to cold exposure when compared to genetically pure PACAP KO mice, leading to a less severe phenotype.

Furthermore, controversy exists as to whether MTII is capable of crossing the blood brain barrier (BBB), and it is imperative to take this into consideration as we suggest PACAP interacts with the melanocortin system *centrally* in the VMN of the hypothalamus (where both PACAP and melanocortins are expressed) when our methodological approach consisted of *peripheral* MTII injections (Glavas et al., 2007; Kim et al., 2000; Modi et al., 2015; Piggins et al., 1996; Trivedi et al., 2003). Notably, in addition to receptors located in the brain, MC4R mRNAs have been detected in peripheral tissues including skeletal muscle and adipose tissue, suggesting both central and peripheral action of the melanocortin system (Boston & Cone, 1996; Chagnon et al., 1997; Hoggard et al., 2004; Mountjoy et al., 2003). Interestingly, whether administered centrally or peripherally, MTII elicits inhibitory effects on food intake and excitatory effects on energy expenditure, suggesting that either brain penetration is not required for MC4R agonists such as MTII to suppress food intake and increase energy expenditure, or, more likely, that the BBB is leaky, allowing MC4R agonists to cross at certain areas and act on central systems (Gavini, Jones, & Novak, 2016; Glavas et al., 2007; Hagan, Bolon, & Keene, 2012; Kievit et al., 2012; Trivedi et al., 2003). To further elucidate hypothalamic pathways between PACAP and the melanocortin system in activating BAT thermogenesis, therefore, central administration of MTII in cold-acclimated PACAP KO mice could be performed. This, however, first relies on the knowledge of which hypothalamic brain region PACAP acts to regulate thermogenesis. This is the major focus of Chapter 3 and will be discussed in detail.

In conclusion, activation of the melanocortin system with peripheral injections of MTII partially rescues the impaired thermogenesis of cold-acclimated PACAP KO mice, providing preliminary evidence to support the hypothesis that PACAP acts upstream from the melanocortin system in regulating SNA to BAT to induce adaptive thermogenesis during

cold exposure. Future directions of this project include increasing sample size to more robustly measure gene and protein expression of thermogenic proteins in BAT, ingWAT, and gWAT depots. Additionally, further histological analyses of adipose tissues to identify characteristics of thermogenically active adipose tissue, such as measuring lipid content and browning in ingWAT and gWAT depots will be performed. These analyses will help support or refute the partial physiological rescue of adaptive thermogenesis with MTII treatment of cold-acclimated PACAP KO mice described here.

2.5 REFERENCES

- Adams, B., Gray, S., Isaac, E., Bianco, A., Vidal-Puig, A., & Sherwood, N. (2008). Feeding and Metabolism in Mice Lacking Pituitary Adenylate Cyclase-Activating Polypeptide. *Endocrinology*, *149*(4), 1571-1580. <http://dx.doi.org/10.1210/en.2007-0515>
- Al-Obeidi, F., Castrucci, A., Hadley, M., & Hruby, V. (1989). Potent and prolonged-acting cyclic lactam analogs of α -melanotropin: design based on molecular dynamics. *Journal Of Medicinal Chemistry*, *32*(12), 2555-2561. <http://dx.doi.org/10.1021/jm00132a010>
- Baba, S., Jacene, H., Engles, J., Honda, H., & Wahl, R. (2010). CT Hounsfield Units of Brown Adipose Tissue Increase with Activation: Preclinical and Clinical Studies. *Journal Of Nuclear Medicine*, *51*(2), 246-250. <http://dx.doi.org/10.2967/jnumed.109.068775>
- Bartness, T., Vaughan, C., & Song, C. (2010). Sympathetic and sensory innervation of brown adipose tissue. *Int J Obes Relat Metab Disord*, *34*, S36-S42. <http://dx.doi.org/10.1038/ijo.2010.182>
- Berglund, E., Liu, T., Kong, X., Sohn, J., Vong, L., & Deng, Z. et al. (2014). Melanocortin 4 receptors in autonomic neurons regulate thermogenesis and glycemia. *Nature Neuroscience*, *17*(7), 911-913. <http://dx.doi.org/10.1038/nn.3737>
- Boston, B., & Cone, R. (1996). Characterization of melanocortin receptor subtype expression in murine adipose tissues and in the 3T3-L1 cell line. *Endocrinology*, *137*(5), 2043-2050. <http://dx.doi.org/10.1210/endo.137.5.8612546>
- Brito, M., Brito, N., Baro, D., Song, C., & Bartness, T. (2007). Differential Activation of the Sympathetic Innervation of Adipose Tissues by Melanocortin Receptor Stimulation. *Endocrinology*, *148*(11), 5339-5347. <http://dx.doi.org/10.1210/en.2007-0621>
- Bustin, S., Benes, V., Garson, J., Helleman, J., Huggett, J., & Kubista, M. et al. (2009). The MIQE Guidelines: Minimum Information for Publication of Quantitative Real-Time PCR Experiments. *Clinical Chemistry*, *55*(4), 611-622. <http://dx.doi.org/10.1373/clinchem.2008.112797>
- Butler, A. & Cone, R. (2003). Knockout Studies Defining Different Roles for Melanocortin Receptors in Energy Homeostasis. *Annals Of The New York Academy Of Sciences*, *994*(1), 240-245. <http://dx.doi.org/10.1111/j.1749-6632.2003.tb03186.x>
- Butler, A., Marks, D., Fan, W., Kuhn, C., Bartolome, M., & Cone, R. (2001). Melanocortin-4 receptor is required for acute homeostatic responses to increased dietary fat. *Nature Neuroscience*, *4*(6), 605-611. <http://dx.doi.org/10.1038/88423>
- Cannon, B., & Nedergaard, J. (2004). Brown Adipose Tissue: Function and Physiological Significance. *Physiological Reviews*, *84*(1), 277-359. <http://dx.doi.org/10.1152/physrev.00015.2003>

- Cannon, B. & Nedergaard, J. (2010). Nonshivering thermogenesis and its adequate measurement in metabolic studies. *Journal Of Experimental Biology*, 214(2), 242-253. <http://dx.doi.org/10.1242/jeb.050989>
- Chagnon, Y., Chen, W., Perusse, L., Chagnon, M., Nadeau, A., Wilkison, W., & Bouchard, C. (1997). Linkage and association studies between the melanocortin receptors 4 and 5 genes and obesity-related phenotypes in the Québec Family Study. *Mol Med*, 3(10), 663-673.
- Chechi, K., Carpentier, A., & Richard, D. (2013). Understanding the brown adipocyte as a contributor to energy homeostasis. *Trends In Endocrinology & Metabolism*, 24(8), 408-420. <http://dx.doi.org/10.1016/j.tem.2013.04.002>
- Choi, Y., Fujikawa, T., Lee, J., Reuter, A., & Kim, K. (2013). Revisiting the Ventral Medial Nucleus of the Hypothalamus: The Roles of SF-1 Neurons in Energy Homeostasis. *Frontiers In Neuroscience*, 7. <http://dx.doi.org/10.3389/fnins.2013.00071>
- Chondronikola, M., Volpi, E., Børsheim, E., Porter, C., Saraf, M., & Annamalai, P. et al. (2016). Brown Adipose Tissue Activation Is Linked to Distinct Systemic Effects on Lipid Metabolism in Humans. *Cell Metabolism*, 23(6), 1200-1206. <http://dx.doi.org/10.1016/j.cmet.2016.04.029>
- Cone, R. (1999). The Central Melanocortin System and Energy Homeostasis. *Trends In Endocrinology & Metabolism*, 10(6), 211-216. [http://dx.doi.org/10.1016/s1043-2760\(99\)00153-8](http://dx.doi.org/10.1016/s1043-2760(99)00153-8)
- Crane, J., Mottillo, E., Farncombe, T., Morrison, K., & Steinberg, G. (2014). A standardized infrared imaging technique that specifically detects UCP1-mediated thermogenesis in vivo. *Molecular Metabolism*, 3(4), 490-494. <http://dx.doi.org/10.1016/j.molmet.2014.04.007>
- Cummings, K., Pendlebury, J., Sherwood, N., & Wilson, R. (2004). Sudden neonatal death in PACAP-deficient mice is associated with reduced respiratory chemoresponse and susceptibility to apnoea. *The Journal Of Physiology*, 555(1), 15-26. <http://dx.doi.org/10.1113/jphysiol.2003.052514>
- Diané, A., Nikolic, N., Rudecki, A., King, S., Bowie, D., & Gray, S. (2014). PACAP is essential for the adaptive thermogenic response of brown adipose tissue to cold exposure. *Journal Of Endocrinology*, 222(3), 327-339. <http://dx.doi.org/10.1530/joe-14-0316>
- Doetschman, T. (2009). Influence of Genetic Background on Genetically Engineered Mouse Phenotypes. *Methods In Molecular Biology*, 423-433. http://dx.doi.org/10.1007/978-1-59745-471-1_23
- Dürr, K., Norsted, E., Gömüç, B., Suarez, E., Hannibal, J., & Meister, B. (2007). Presence of pituitary adenylate cyclase-activating polypeptide (PACAP) defines a subpopulation of hypothalamic POMC neurons. *Brain Research*, 1186, 203-211. <http://dx.doi.org/10.1016/j.brainres.2007.10.015>

- Enriori, P., Sinnayah, P., Simonds, S., Garcia Rudaz, C., & Cowley, M. (2011). Leptin Action in the Dorsomedial Hypothalamus Increases Sympathetic Tone to Brown Adipose Tissue in Spite of Systemic Leptin Resistance. *Journal Of Neuroscience*, 31(34), 12189-12197. <http://dx.doi.org/10.1523/jneurosci.2336-11.2011>
- Fan, W., Morrison, S., Cao, W., & Yu, P. (2007). Thermogenesis activated by central melanocortin signaling is dependent on neurons in the rostral raphe pallidus (rRPa) area. *Brain Research*, 1179, 61-69. <http://dx.doi.org/10.1016/j.brainres.2007.04.006>
- Fan, W., Voss-Andreae, A., Cao, W., & Morrison, S. (2005). Regulation of thermogenesis by the central melanocortin system. *Peptides*, 26(10), 1800-1813. <http://dx.doi.org/10.1016/j.peptides.2004.11.033>
- Gavini, C., Jones, W., & Novak, C. (2016). Ventromedial hypothalamic melanocortin receptor activation: regulation of activity energy expenditure and skeletal muscle thermogenesis. *The Journal Of Physiology*, 594(18), 5285-5301. <http://dx.doi.org/10.1113/jp272352>
- Gavrilova, O., Marcus-Samuels, B., & Reitman, M. (2000). Lack of responses to a β 3-adrenergic agonist in lipoatrophic A-ZIP/F-1 mice. *Diabetes*, 49(11), 1910-1916. <http://dx.doi.org/10.2337/diabetes.49.11.1910>
- Girardet, C. & Butler, A. (2014). Neural melanocortin receptors in obesity and related metabolic disorders. *Biochimica Et Biophysica Acta (BBA) - Molecular Basis Of Disease*, 1842(3), 482-494. <http://dx.doi.org/10.1016/j.bbadis.2013.05.004>
- Glavas, M., Joachim, S., Draper, S., Smith, M., & Grove, K. (2007). Melanocortinerigic Activation by Melanotan II Inhibits Feeding and Increases Uncoupling Protein 1 Messenger Ribonucleic Acid in the Developing Rat. *Endocrinology*, 148(7), 3279-3287. <http://dx.doi.org/10.1210/en.2007-0184>
- Goldgof, M., Xiao, C., Chanturiya, T., Jou, W., Gavrilova, O., & Reitman, M. (2014). The Chemical Uncoupler 2,4-Dinitrophenol (DNP) Protects against Diet-induced Obesity and Improves Energy Homeostasis in Mice at Thermoneutrality. *Journal Of Biological Chemistry*, 289(28), 19341-19350. <http://dx.doi.org/10.1074/jbc.m114.568204>
- Gray, S., Cummings, K., Jirik, F., & Sherwood, N. (2001). Targeted Disruption of the Pituitary Adenylate Cyclase-Activating Polypeptide Gene Results in Early Postnatal Death Associated with Dysfunction of Lipid and Carbohydrate Metabolism. *Molecular Endocrinology*, 15(10), 1739-1747. <http://dx.doi.org/10.1210/mend.15.10.0705>
- Gray, S., Yamaguchi, N., Vencova, P., & Sherwood, N. (2002). Temperature-Sensitive Phenotype in Mice Lacking Pituitary Adenylate Cyclase-Activating Polypeptide. *Endocrinology*, 143(10), 3946-3954. <http://dx.doi.org/10.1210/en.2002-220401>
- Grubb, B., & Folk, G. (1976). Effect of cold acclimation on norepinephrine stimulated oxygen consumption in muscle. *Journal Of Comparative Physiology ? B*, 110(2), 217-226. <http://dx.doi.org/10.1007/bf00689310>

- Hagan, C., Bolon, B., & Keene, C. (2012). Nervous System. *Comparative Anatomy And Histology*, 339-394. <http://dx.doi.org/10.1016/b978-0-12-381361-9.00020-2>
- Haman, F., Péronnet, F., Kenny, G., Massicotte, D., Lavoie, C., Scott, C., & Weber, J. (2002). Effect of cold exposure on fuel utilization in humans: plasma glucose, muscle glycogen, and lipids. *Journal Of Applied Physiology*, 93(1), 77-84. <http://dx.doi.org/10.1152/jappphysiol.00773.2001>
- Hashimoto, H., Shintani, N., Tanaka, K., Mori, W., Hirose, M., & Matsuda, T. et al. (2001). Altered psychomotor behaviors in mice lacking pituitary adenylate cyclase-activating polypeptide (PACAP). *Proceedings Of The National Academy Of Sciences*, 98(23), 13355-13360. <http://dx.doi.org/10.1073/pnas.231094498>
- Hawke, Z., Ivanov, T., Bechtold, D., Dhillon, H., Lowell, B., & Luckman, S. (2009). PACAP Neurons in the Hypothalamic Ventromedial Nucleus Are Targets of Central Leptin Signaling. *Journal Of Neuroscience*, 29(47), 14828-14835. <http://dx.doi.org/10.1523/jneurosci.1526-09.2009>
- Haynes, W., Morgan, D., Djalali, A., Sivitz, W., & Mark, A. (1999). Interactions Between the Melanocortin System and Leptin in Control of Sympathetic Nerve Traffic. *Hypertension*, 33(1), 542-547. <http://dx.doi.org/10.1161/01.hyp.33.1.542>
- Heldmaier, G. (1975). The effect of short daily cold exposures on development of brown adipose tissue in mice. *Journal Of Comparative Physiology ? B*, 98(2), 161-168. <http://dx.doi.org/10.1007/bf00706127>
- Hoggard, N., Hunter, L., Duncan, J., & Rayner, D. (2004). Regulation of adipose tissue leptin secretion by alpha-melanocyte-stimulating hormone and agouti-related protein: further evidence of an interaction between leptin and the melanocortin signalling system. *Journal Of Molecular Endocrinology*, 32(1), 145-153. <http://dx.doi.org/10.1677/jme.0.0320145>
- Iemolo, A., Ferragud, A., Cottone, P., & Sabino, V. (2015). Pituitary Adenylate Cyclase-Activating Peptide in the Central Amygdala Causes Anorexia and Body Weight Loss via the Melanocortin and the TrkB Systems. *Neuropsychopharmacology*, 40(8), 1846-1855. <http://dx.doi.org/10.1038/npp.2015.34>
- Inglott, M., Farnham, M., & Pilowsky, P. (2011). Intrathecal PACAP-38 causes prolonged widespread sympathoexcitation via a spinally mediated mechanism and increases in basal metabolic rate in anesthetized rat. *AJP: Heart And Circulatory Physiology*, 300(6), H2300-H2307. <http://dx.doi.org/10.1152/ajpheart.01052.2010>
- Inokuma, K., Ogura-Okamatsu, Y., Toda, C., Kimura, K., Yamashita, H., & Saito, M. (2005). Uncoupling Protein 1 Is Necessary for Norepinephrine-Induced Glucose Utilization in Brown Adipose Tissue. *Diabetes*, 54(5), 1385-1391. <http://dx.doi.org/10.2337/diabetes.54.5.1385>
- Kievit, P., Halem, H., Marks, D., Dong, J., Glavas, M., & Sinnayah, P. et al. (2012). Chronic Treatment With a Melanocortin-4 Receptor Agonist Causes Weight Loss, Reduces

- Insulin Resistance, and Improves Cardiovascular Function in Diet-Induced Obese Rhesus Macaques. *Diabetes*, 62(2), 490-497. <http://dx.doi.org/10.2337/db12-0598>
- Kim, M., Rossi, M., Abusnana, S., Sunter, D., Morgan, D., & Small, C. et al. (2000). Hypothalamic localization of the feeding effect of agouti-related peptide and alpha-melanocyte-stimulating hormone. *Diabetes*, 49(2), 177-182. <http://dx.doi.org/10.2337/diabetes.49.2.177>
- Kim, S., Jung, Y., Kwon, H., Seong, J., Granneman, J., & Lee, Y. (2016). Sex differences in sympathetic innervation and browning of white adipose tissue of mice. *Biology Of Sex Differences*, 7(1). <http://dx.doi.org/10.1186/s13293-016-0121-7>
- Labbé, S., Caron, A., Lanfray, D., Monge-Rofarello, B., Bartness, T., & Richard, D. (2015). Hypothalamic control of brown adipose tissue thermogenesis. *Front. Syst. Neurosci.*, 9. <http://dx.doi.org/10.3389/fnsys.2015.00150>
- Li, G., Zhang, Y., Wilsey, J., & Scarpace, P. (2004). Unabated anorexic and enhanced thermogenic responses to melanotan II in diet-induced obese rats despite reduced melanocortin 3 and 4 receptor expression. *Journal Of Endocrinology*, 182(1), 123-132. <http://dx.doi.org/10.1677/joe.0.1820123>
- Martínez-Sánchez, N., Moreno-Navarrete, J., Contreras, C., Rial-Pensado, E., Fernø, J., & Nogueiras, R. et al. (2016). Thyroid hormones induce browning of white fat. *Journal Of Endocrinology*, 232(2), 351-362. <http://dx.doi.org/10.1530/joe-16-0425>
- Meyer, C., Willershauser, M., Jastroch, M., Rourke, B., Fromme, T., & Oelkrug, R. et al. (2010). Adaptive thermogenesis and thermal conductance in wild-type and UCP1-KO mice. *AJP: Regulatory, Integrative And Comparative Physiology*, 299(5), R1396-R1406. <http://dx.doi.org/10.1152/ajpregu.00021.2009>
- Modi, M., Inoue, K., Barrett, C., Kittelberger, K., Smith, D., Landgraf, R., & Young, L. (2015). Melanocortin Receptor Agonists Facilitate Oxytocin-Dependent Partner Preference Formation in the Prairie Vole. *Neuropsychopharmacology*, 40(8), 1856-1865. <http://dx.doi.org/10.1038/npp.2015.35>
- Mollica, M., Lionetti, L., Crescenzo, R., Tasso, R., Barletta, A., Liverini, G., & Iossa, S. (2005). Cold exposure differently influences mitochondrial energy efficiency in rat liver and skeletal muscle. *FEBS Letters*, 579(9), 1978-1982. <http://dx.doi.org/10.1016/j.febslet.2005.02.044>
- Morrison, S. & Nakamura, K. (2011). Central neural pathways for thermoregulation. *Frontiers In Bioscience*, 16(1), 74. <http://dx.doi.org/10.2741/3677>
- Mounien, L., Do Rego, J., Bizet, P., Boutelet, I., Gourcerol, G., & Fournier, A. et al. (2008). Pituitary Adenylate Cyclase-Activating Polypeptide Inhibits Food Intake in Mice Through Activation of the Hypothalamic Melanocortin System. *Neuropsychopharmacology*, 34(2), 424-435. <http://dx.doi.org/10.1038/npp.2008.73>

- Mountjoy, K., Jenny Wu, C., Dumont, L., & Wild, J. (2003). Melanocortin-4 Receptor Messenger Ribonucleic Acid Expression in Rat Cardiorespiratory, Musculoskeletal, and Integumentary Systems. *Endocrinology*, *144*(12), 5488-5496. <http://dx.doi.org/10.1210/en.2003-0570>
- Muzik, O., Mangner, T., Leonard, W., Kumar, A., Janisse, J., & Granneman, J. (2013). 15O PET Measurement of Blood Flow and Oxygen Consumption in Cold-Activated Human Brown Fat. *Journal Of Nuclear Medicine*, *54*(4), 523-531. <http://dx.doi.org/10.2967/jnumed.112.111336>
- Nakata, M., Shioda, S., Oka, Y., Maruyama, I., & Yada, T. (1999). Insulinotropin PACAP potentiates insulin-stimulated glucose uptake in 3T3 L1 cells*. *Peptides*, *20*(8), 943-948. [http://dx.doi.org/10.1016/s0196-9781\(99\)00085-6](http://dx.doi.org/10.1016/s0196-9781(99)00085-6)
- Nedergaard, J., & Lindberg, O. (1979). Norepinephrine-Stimulated Fatty-Acid Release and Oxygen Consumption in Isolated Hamster Brown-Fat Cells. Influence of Buffers, Albumin, Insulin and Mitochondrial Inhibitors. *European Journal Of Biochemistry*, *95*(1), 139-145. <http://dx.doi.org/10.1111/j.1432-1033.1979.tb12948.x>
- Neinast, M., Frank, A., Zechner, J., Li, Q., Vishvanath, L., & Palmer, B. et al. (2015). Activation of natriuretic peptides and the sympathetic nervous system following Roux-en-Y gastric bypass is associated with gonadal adipose tissues browning. *Molecular Metabolism*, *4*(5), 427-436. <http://dx.doi.org/10.1016/j.molmet.2015.02.006>
- Nogueiras, R., Wiedmer, P., Perez-Tilve, D., Veyrat-Durebex, C., Keogh, J., & Sutton, G. et al. (2007). The central melanocortin system directly controls peripheral lipid metabolism. *Journal Of Clinical Investigation*, *117*(11), 3475-3488. <http://dx.doi.org/10.1172/jci31743>
- Nguyen, K., Qiu, Y., Cui, X., Goh, Y., Mwangi, J., & David, T. et al. (2011). Alternatively activated macrophages produce catecholamines to sustain adaptive thermogenesis. *Nature*, *480*(7375), 104-108. <http://dx.doi.org/10.1038/nature10653>
- Orava, J., Nuutila, P., Lidell, M., Oikonen, V., Nojonen, T., & Viljanen, T. et al. (2011). Different Metabolic Responses of Human Brown Adipose Tissue to Activation by Cold and Insulin. *Cell Metabolism*, *14*(2), 272-279. <http://dx.doi.org/10.1016/j.cmet.2011.06.012>
- Ouellet, V., Labbé, S., Blondin, D., Phoenix, S., Guérin, B., & Haman, F. et al. (2012). Brown adipose tissue oxidative metabolism contributes to energy expenditure during acute cold exposure in humans. *Journal Of Clinical Investigation*, *122*(2), 545-552. <http://dx.doi.org/10.1172/jci60433>
- Piggins, H., Stamp, J., Burns, J., Rusak, B., & Semba, K. (1996). Distribution of pituitary adenylate cyclase activating polypeptide (PACAP) immunoreactivity in the hypothalamus and extended amygdala of the rat. *The Journal Of Comparative Neurology*, *376*(2), 278-294. [http://dx.doi.org/10.1002/\(sici\)1096-9861\(19961209\)376:2<278::aid-cne9>3.3.co;2-e](http://dx.doi.org/10.1002/(sici)1096-9861(19961209)376:2<278::aid-cne9>3.3.co;2-e)

- Qian, S., Tang, Y., Li, X., Liu, Y., Zhang, Y., & Huang, H. et al. (2013). BMP4-mediated brown fat-like changes in white adipose tissue alter glucose and energy homeostasis. *Proceedings Of The National Academy Of Sciences*, 110(9), E798-E807. <http://dx.doi.org/10.1073/pnas.1215236110>
- Resch, J., Boisvert, J., Hourigan, A., Mueller, C., Yi, S., & Choi, S. (2011). Stimulation of the hypothalamic ventromedial nuclei by pituitary adenylate cyclase-activating polypeptide induces hypophagia and thermogenesis. *AJP: Regulatory, Integrative And Comparative Physiology*, 301(6), R1625-R1634. <http://dx.doi.org/10.1152/ajpregu.00334.2011>
- Resch, J., Maunze, B., Gerhardt, A., Magnuson, S., Phillips, K., & Choi, S. (2013). Intrahypothalamic pituitary adenylate cyclase-activating polypeptide regulates energy balance via site-specific actions on feeding and metabolism. *AJP: Endocrinology And Metabolism*, 305(12), E1452-E1463. <http://dx.doi.org/10.1152/ajpendo.00293.2013>
- Rothwell, N. (2001). Thermogenesis: where are we and where are we going?. *International Journal Of Obesity*, 25(9), 1272-1274.
- Saito, M., Yoneshiro, T., & Matsushita, M. (2016). Activation and recruitment of brown adipose tissue by cold exposure and food ingredients in humans. *Best Practice & Research Clinical Endocrinology & Metabolism*, 30(4), 537-547. <http://dx.doi.org/10.1016/j.beem.2016.08.003>
- Schaeffer, P., Villarin, J., & Lindstedt, S. (2003). Chronic Cold Exposure Increases Skeletal Muscle Oxidative Structure and Function in *Monodelphis domestica*, a Marsupial Lacking Brown Adipose Tissue. *Physiological And Biochemical Zoology*, 76(6), 877-887. <http://dx.doi.org/10.1086/378916>
- Shabalina, I., Petrovic, N., de Jong, J., Kalinovich, A., Cannon, B., & Nedergaard, J. (2013). UCP1 in Brite/Beige Adipose Tissue Mitochondria Is Functionally Thermogenic. *Cell Reports*, 5(5), 1196-1203. <http://dx.doi.org/10.1016/j.celrep.2013.10.044>
- Shiota, M., & Masumi, S. (1988). Effect of norepinephrine on consumption of oxygen in perfused skeletal muscle from cold-exposed rats. *American Journal Of Physiology - Endocrinology And Metabolism*, 254(4), E482-E489.
- Simonyan, R., Jimenez, M., Ceddia, R., Giacobino, J., Muzzin, P., & Skulachev, V. (2001). Cold-induced changes in the energy coupling and the UCP3 level in rodent skeletal muscles. *Biochimica Et Biophysica Acta (BBA) - Bioenergetics*, 1505(2-3), 271-279. [http://dx.doi.org/10.1016/s0005-2728\(01\)00168-2](http://dx.doi.org/10.1016/s0005-2728(01)00168-2)
- Skibicka, K. & Grill, H. (2009). Hypothalamic and Hindbrain Melanocortin Receptors Contribute to the Feeding, Thermogenic, and Cardiovascular Action of Melanocortins. *Endocrinology*, 150(12), 5351-5361. <http://dx.doi.org/10.1210/en.2009-0804>
- Song, C., Vaughan, C., Keen-Rhinehart, E., Harris, R., Richard, D., & Bartness, T. (2008). Melanocortin-4 receptor mRNA expressed in sympathetic outflow neurons to brown adipose tissue: neuroanatomical and functional evidence. *AJP: Regulatory, Integrative*

And Comparative Physiology, 295(2), R417-R428.
<http://dx.doi.org/10.1152/ajpregu.00174.2008>

- Strader, A., Shi, H., Ogawa, R., Seeley, R., & Reizes, O. (2007). The Effects of the Melanocortin Agonist (MT-II) on Subcutaneous and Visceral Adipose Tissue in Rodents. *Journal Of Pharmacology And Experimental Therapeutics*, 322(3), 1153-1161.
<http://dx.doi.org/10.1124/jpet.107.123091>
- Tanida, M., Shintani, N., & Hashimoto, H. (2011). The melanocortin system is involved in regulating autonomic nerve activity through central pituitary adenylate cyclase-activating polypeptide. *Neuroscience Research*, 70(1), 55-61.
<http://dx.doi.org/10.1016/j.neures.2011.01.014>
- Tanida, M., Shintani, N., Morita, Y., Tsukiyama, N., Hatanaka, M., & Hashimoto, H. et al. (2010). Regulation of autonomic nerve activities by central pituitary adenylate cyclase-activating polypeptide. *Regulatory Peptides*, 161(1-3), 73-80.
<http://dx.doi.org/10.1016/j.regpep.2010.02.002>
- Tao, Y. (2010). The Melanocortin-4 Receptor: Physiology, Pharmacology, and Pathophysiology. *Endocrine Reviews*, 31(4), 506-543. <http://dx.doi.org/10.1210/er.2009-0037>
- The Importance of Genetic Background in Mouse-Based Biomedical Research*. (2006). *The Jackson Laboratory*. Retrieved 27 March 2017, from <https://www.jax.org/news-and-insights/2006/june/the-importance-of-genetic-background-in-mouse-based-biomedical-research>
- Trivedi, P., Jiang, M., Tamvakopoulos, C., Shen, X., Yu, H., & Mock, S. et al. (2003). Exploring the site of anorectic action of peripherally administered synthetic melanocortin peptide MT-II in rats. *Brain Research*, 977(2), 221-230.
[http://dx.doi.org/10.1016/s0006-8993\(03\)02683-0](http://dx.doi.org/10.1016/s0006-8993(03)02683-0)
- Ukropec, J., Anunciado, R., Ravussin, Y., Hulver, M., & Kozak, L. (2006). UCP1-independent Thermogenesis in White Adipose Tissue of Cold-acclimated Ucp1^{-/-} Mice. *Journal Of Biological Chemistry*, 281(42), 31894-31908.
<http://dx.doi.org/10.1074/jbc.m606114200>
- van Beek, L., van Klinken, J., Pronk, A., van Dam, A., Dirven, E., & Rensen, P. et al. (2015). The limited storage capacity of gonadal adipose tissue directs the development of metabolic disorders in male C57Bl/6J mice. *Diabetologia*, 58(7), 1601-1609.
<http://dx.doi.org/10.1007/s00125-015-3594-8>
- van Marken Lichtenbelt, W. (2011). Human Brown Fat and Obesity: Methodological Aspects. *Frontiers In Endocrinology*, 2. <http://dx.doi.org/10.3389/fendo.2011.00052>
- van Marken Lichtenbelt, W., Vanhommerig, J., Smulders, N., Drossaerts, J., Kemerink, G., & Bouvy, N. et al. (2009). Cold-Activated Brown Adipose Tissue in Healthy Men. *New England Journal Of Medicine*, 360(15), 1500-1508.
<http://dx.doi.org/10.1056/nejmoa0808718>

- Vijgen, G., Bouvy, N., Teule, G., Brans, B., Schrauwen, P., & van Marken Lichtenbelt, W. (2011). Brown Adipose Tissue in Morbidly Obese Subjects. *Plos ONE*, *6*(2), e17247. <http://dx.doi.org/10.1371/journal.pone.0017247>
- Virtue, S., & Vidal-Puig, A. (2013). Assessment of brown adipose tissue function. *Frontiers In Physiology*, *4*. <http://dx.doi.org/10.3389/fphys.2013.00128>
- Voss-Andreae, A., Murphy, J., Ellacott, K., Stuart, R., Nillni, E., Cone, R., & Fan, W. (2007). Role of the Central Melanocortin Circuitry in Adaptive Thermogenesis of Brown Adipose Tissue. *Endocrinology*, *148*(4), 1550-1560. <http://dx.doi.org/10.1210/en.2006-1389>
- Wang, Q., Zhang, M., Xu, M., Gu, W., Xi, Y., & Qi, L. et al. (2015). Brown Adipose Tissue Activation Is Inversely Related to Central Obesity and Metabolic Parameters in Adult Human. *PLOS ONE*, *10*(4), e0123795. <http://dx.doi.org/10.1371/journal.pone.0123795>
- Weiner, J., Kranz, M., Klötting, N., Kunath, A., Steinhoff, K., & Rijntjes, E. et al. (2016). Thyroid hormone status defines brown adipose tissue activity and browning of white adipose tissues in mice. *Scientific Reports*, *6*(1). <http://dx.doi.org/10.1038/srep38124>
- Williams, D., Bowers, R., Bartness, T., Kaplan, J., & Grill, H. (2003). Brainstem Melanocortin 3/4 Receptor Stimulation Increases Uncoupling Protein Gene Expression in Brown Fat. *Endocrinology*, *144*(11), 4692-4697. <http://dx.doi.org/10.1210/en.2003-0440>
- Yasuda, T., Masaki, T., Sakata, T., & Yoshimatsu, H. (2004). Hypothalamic neuronal histamine regulates sympathetic nerve activity and expression of uncoupling protein 1 mRNA in brown adipose tissue in rats. *Neuroscience*, *125*(3), 535-540. <http://dx.doi.org/10.1016/j.neuroscience.2003.11.039>
- Yoneshiro, T., Aita, S., Matsushita, M., Kameya, T., Nakada, K., Kawai, Y., & Saito, M. (2010). Brown Adipose Tissue, Whole-Body Energy Expenditure, and Thermogenesis in Healthy Adult Men. *Obesity*, *19*(1), 13-16. <http://dx.doi.org/10.1038/oby.2010.105>
- Yoneshiro, T., Aita, S., Matsushita, M., Kayahara, T., Kameya, T., & Kawai, Y. et al. (2013). Recruited brown adipose tissue as an antiobesity agent in humans. *Journal Of Clinical Investigation*, *123*(8), 3404-3408. <http://dx.doi.org/10.1172/jci67803>
- Yoshiki, A., & Moriwaki, K. (2006). Mouse Phenome Research: Implications of Genetic Background. *ILAR Journal*, *47*(2), 94-102. <http://dx.doi.org/10.1093/ilar.47.2.94>

2.6 APPENDIX

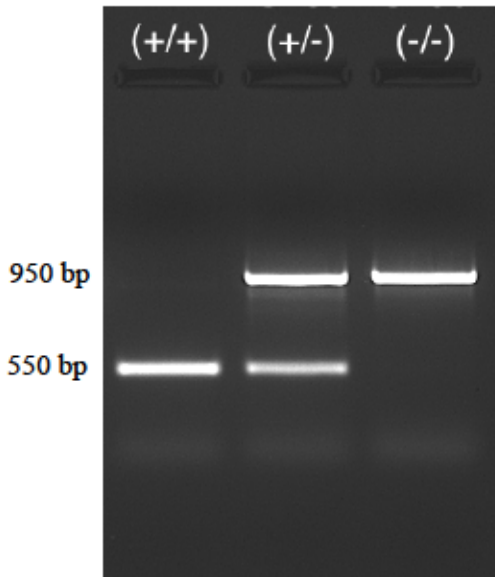


Figure S2.1. PCR assessment of PACAP genotype in *Mus musculus*. Electrophoresis performed on ethidium bromide stained 1.5% agarose gel at 100V for 20 minutes. Each well represents a different animal. (+/+) denotes PACAP wildtype, (+/-) PACAP heterozygote, and (-/-) PACAP knockout.

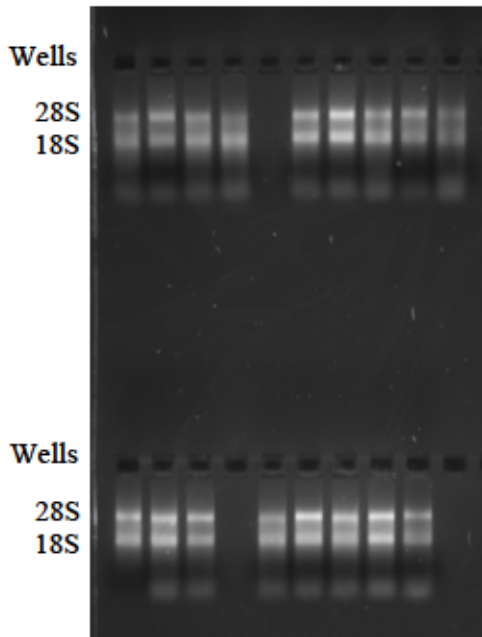


Figure S2.2. Assessment of RNA integrity of isolated *Mus musculus* brown adipose tissue (BAT) with electrophoresis on an ethidium bromide stained 1.5% agarose gel at 100V for 30 minutes. Each well represents a different BAT sample. The top band indicates intact 28S rRNA and the bottom band indicates intact 18S rRNA.

CHAPTER 3

Creating a Viral Construct and Delivery Method for Genetic Intervention Aimed at Restoring Impaired Thermogenesis of PACAP $-/-$ Mice

3.1 INTRODUCTION

As discussed in detail in Chapter 2, PACAP is essential for the normal thermogenic response of BAT as indicated by loss and gain of function experiments using both genetic and pharmacological interventions (Adams et al., 2008; Cummings, Pendlebury, Sherwood, & Wilson, 2004; Diané et al., 2014; Gray et al., 2001; Gray et al., 2002; Inglott, Farnham, & Pilowsky, 2011; Resch et al., 2011; Resch et al., 2013; Tanida et al., 2010). The mechanisms by which PACAP regulates body temperature and thus energy metabolism, however, remain unknown. Because the greatest physiological stimulus of adaptive thermogenesis in BAT is sympathetic nerve activation initiated at the level of the hypothalamus (discussed below), the evidence for PACAP's central role in the brain will be reviewed here, with the future aim of elucidating the specific hypothalamic mechanisms by which PACAP acts to regulate thermogenesis (Bamshad, Song, & Bartness, 1999; Bartness, Vaughn, & Song, 2010; Chechi, Carpentier, & Richard, 2013; Labbé et al., 2015; Saito, Yoneshiro, & Matsushita, 2016).

Briefly introduced in Chapter 1, the hypothalamus is composed of several distinct nuclei, including the ARC (discussed in Chapter 1), DMN, VMN, LHA and PVN (Figure 1.5), and collectively integrates both central and peripheral signals of body energy status to regulate food intake and energy expenditure to appropriately maintain body weight and energy homeostasis (Rea, 2015). While PACAP and PACAP receptors are expressed in each of the nuclei named above, significantly higher expression levels occur in the VMN and the PVN (Arimura et al., 1991; Das, Vihlen, & Legradi, 2006; Hannibal et al., 2002; Hashimoto et al., 1996; Jolivel et al., 2009; Masuo et al., 1993; Segal et al., 2005; Sheward, Lutz, Copp, & Harmar, 1998). Although the functional role of certain hypothalamic nuclei are well known (such as appetite regulation in the ARC), others have overlapping and even opposing functions, making it challenging to discern the pathways regulating energy homeostasis. For

example, disinhibiting neurons of the DMN or the LHA with a GABA receptor antagonist resulted in increased thermogenesis as measured by increased core and BAT temperature, suggesting that activation of these nuclei results in increased energy expenditure (Cao, Fan, & Morrison, 2004; Cerri, & Morrison, 2005; DiMicco, & Zaretsky, 2006; Morrison, & Nakamura, 2011; Zaretskaia, Zaretsky, Shekhar, & DiMicco, 2000). Additionally, disruption of leptin receptors in the DMN blocked thermogenic responses to peripheral leptin, resulting in obesity (Dodd et al., 2014; Enriori et al., 2011). Conversely, however, lesions to the DMN or LHA resulted in hypophagia and *reduced* body weight, suggesting that the role of these nuclei in energy expenditure may be inhibitory rather than excitatory, and that multiple pathways are involved in regulating energy homeostasis; a phenomenon that will be further discussed below (Bellinger, & Bernardis, 2002; Yoshida, Kemnitz, & Bray, 1983).

Other hypothalamic nuclei are also implicated in regulating energy homeostasis. Activation of the melanocortin system via injections of the synthetic agonist MTII into both the PVN and the VMN resulted in increased BAT temperatures via thermogenesis (Gavini, Jones, & Novak, 2016; Song et al., 2008). Additionally, both hormonal and electrical stimulation of the PVN and the VMN resulted in decreased food intake, while loss of function of either in these nuclei (via functional disruptions by toxins, or electrolytic or chemical lesions) resulted in hyperphagia and increased body weight, leading to obesity (Choi, & Dallman, 1999; Leibowitz, Hammer, & Chang, 1981; Perkins et al., 1981; Resch et al., 2011; Resch et al., 2013; Sabatier, Leng, & Menzies, 2013). Both nuclei are, therefore, commonly associated with satiety and are known to be important nuclei for the regulation of energy metabolism (Perkins et al., 1981; Sabatier, Leng, & Menzies, 2013; Segal et al., 2005).

In support of the literature that indicates PACAP is involved in the regulation of energy metabolism (detailed in Chapter 2), site-specific PACAP injections into the PVN and the VMN significantly decreased food intake, which was reversed with a PACAP receptor antagonist (Resch et al., 2013). Notably, however, PACAP injections into the VMN resulted in significantly increased core body temperature and spontaneous locomotor activity, whereas PVN injections of PACAP had no effect on energy expenditure (Resch et al., 2013). This suggests that despite similar regulation of energy intake upon PACAP stimulation in the PVN and VMN, these nuclei are differentially responsive to PACAP in terms of energy expenditure (Resch et al., 2013). Furthermore, in contrast to increased BAT temperatures observed in animals receiving injections of an MC4R agonist (MTII) in the PVN, the reintroduction of MC4R expression in the PVN of MC4R KO mice did *not* result in increased thermogenesis (Balthasar et al., 2005; Song et al., 2008). Notably, MC4R KO mice display a morbidly obese phenotype, resulting from increased appetite and decreased energy expenditure (Balthasar et al., 2005). The restoration of MC4R expression in the PVN of MC4R KO mice prevented 60% of the obesity, where the increased food intake was completely rescued, while the reduced energy expenditure was not (Balthasar et al., 2005; Madden, & Morrison, 2008). This suggests that, similar to the differential response to PACAP in the PVN and VMN discussed above, MC4Rs in the PVN control food intake while MC4Rs elsewhere control energy expenditure (Balthasar et al., 2005). Potentially, this regulation of energy expenditure by MC4Rs may occur in the VMN, possibly under the regulation of PACAP (the focus of Chapter 2).

While the VMN exhibits a major role in appetite regulation, it is also recognized for its role in energy expenditure, including thermogenesis, and continues to be a site of interest for body weight regulation (Choi et al., 2013; Lopez, & Tena-Sempere, 2017; Martinez de

Morentin et al., 2014; Perkins et al., 1981; Whittle et al., 2012). It contains numerous receptor types known to regulate energy metabolism, including high expression of leptin and PACAP receptors (Bingham et al., 2008; Dhillon et al., 2006; Hawke et al., 2009; Segal et al., 2005). As discussed in Chapter 1, leptin's function in energy metabolism is not solely in appetite regulation in the ARC: leptin also regulates energy expenditure mainly via the VMN (Bingham et al., 2008). As such, when leptin receptors were knocked out in the VMN only, mice exhibited significantly increased adipose mass on a low-fat diet, and obesity on a high-fat diet (Bingham et al., 2008). Leptin function is also connected to that of PACAP, whereby leptin-deficient mice exhibited significantly reduced PACAP mRNA levels that were restored with exogenous leptin treatments (Hawke et al., 2009). Additionally, leptin acts by means of steroidogenic factor 1 (SF1), where leptin depolarization results in increased firing rate of SF1 neurons in the VMN (Dhillon et al., 2006; Hawke et al., 2009). The importance of SF1 in regulating gene expression in the VMN will be discussed here.

SF1 is a transcriptional factor required both for terminal differentiation of the VMN as well as energy metabolism processes (Choi et al., 2013). Notably, of all the genes expressed in the VMN, SF1 is the only gene that is specifically and exclusively expressed in the VMN (Choi et al., 2013). SF1 expression also occurs in the pituitary gland, adrenal glands and the testes, but in no other brain region (Ikeda et al., 1995; Ingraham et al., 1994; Parker, & Schimmer, 1997). In SF1 KO animals, impaired development of the VMN ensued while other hypothalamic nuclei remained intact, ultimately resulting in high death rates likely attributable to adrenal insufficiency (Dellovade et al., 2000; Ikeda et al., 1995; Luo, Ikeda, & Parker, 1994). To circumvent these deaths, healthy adrenal glands were transplanted into SF1 KO mice, resulting in a complete rescue of the adrenal phenotype while allowing for the analysis of predominantly VMN SF1 KO effects (Majdic et al., 2002). Interestingly,

adrenal-transplanted SF1 KO mice exhibited massive obesity compared to WTs, suggesting that the expression of SF1 in the VMN is critical in regulating body weight (Majdic et al., 2002). However, the obese phenotype may have resulted as a consequence of the grossly impaired VMN structure, the inherent secondary effects from the transplantation or a combination of both, rather than the absence of SF1 signaling in the VMN. Therefore, mouse models were developed using the Cre transgene where SF1 was deleted postnatally to allow for proper development of the VMN and thus avoid confounding development side effects (Bingham, Verma-Kurvari, Parada, & Parker, 2006; Kim et al., 2011). Interestingly, these VMN specific SF1 KO animals continued to exhibit an obese phenotype, with impaired thermogenesis and decreased leptin receptor expression in the VMN (Kim et al., 2011). Collectively, these results provide compelling evidence that SF1 expression in the VMN is imperative for regulating energy homeostasis, including thermogenesis.

Altogether, a considerable amount of evidence connects PACAP and the VMN in their essential roles in activating thermogenesis. The final piece of evidence to consider is the hypothalamic innervation to BAT, as this is the site of adaptive thermogenesis (Cannon, & Nedergaard, 2004).

Neuronal pathways mediating hypothalamic regulation of adaptive thermogenesis in BAT have been elucidated with the use of retrograde viral tracers. When such viruses are injected into BAT, they infect and simultaneously label neurons (through expression of a molecular label) in a retrograde fashion, such that the entire efferent chain is labeled from the peripheral tissue to the brain regions from which the signal originated. Interestingly, retrograde viral tracing studies in BAT have shown connections to the PVN, LHA, DMN, and ARC, but not the VMN (Bamshad, Song, & Bartness, 1999; Bartness, Vaughn, & Song, 2010; Oldfield et al., 2002; Ryu et al., 2015). Similarly, during short-term cold exposure

(four hours), virally-infected neurons were observed in the PVN, LHA and DMN, but again, not the VMN (Cano et al., 2003). The conspicuous absence of viral tracing in the VMN is at odds with functional evidence discussed above that clearly demonstrates a role for the VMN in energy expenditure. This may be due to the limitations of viral tracing studies, which are generally limited to three synaptic relays (Stefanidis, Wiedmann, Adler, & Oldfield, 2014). Therefore, if the VMN is the initial nuclei in which thermogenesis is activated, from which neurons project to other nuclei, the VMN may be beyond the extent of penetration of the retrograde viral tracers in the CNS. Alternatively, functional studies that implicate the VMN may actually be involving nearby regions, resulting in compromised analysis. For example, chemical lesions of the VMN likely damages surrounding regions, while microinjections into the VMN may result in leakage outside the targeted area (Choi et al., 2013). However, because SF1 is exclusively expressed in the VMN, the evidence discussed above for SF1's, and thus the VMN's, role in energy metabolism is indubitable (Bingham et al., 2008). Nevertheless, although complex and potentially contrasting evidence exists for the hypothalamic regions regulating energy expenditure, the key players remain consistent and include leptin and the melanocortin system. Additionally, we propose PACAP to be a key neurochemical regulator of energy metabolism in the VMN.

Because maintenance of energy homeostasis is fundamental for life, it is likely that hypothalamic neurons overlap, communicating both directly and indirectly with each other and thus providing redundant processes to maintain energy homeostasis (Choi et al., 2013). As such, both PACAP and leptin innervation to nerve terminals in the PVN have been shown to originate in other hypothalamic nuclei, with major projections initiated in the VMN (Das, Vihlen, & Legradi, 2007; Elmquist et al., 1998). With immense research evidence considered, it is reasonable to suggest that hypothalamic signaling regulating BAT

thermogenesis likely includes multiple hypothalamic nuclei and that the complete networks of neural pathways involved remain to be elucidated. Given the functional evidence of the VMN's role in thermogenesis, the high expression of PACAP in the VMN, the data from the PACAP KO mouse model that shows impaired thermogenesis in the absence of PACAP, and the evidence from pharmacological studies that show injections of PACAP in the VMN increases SNA to BAT, we conclude that the VMN is a logical and valid target to further elucidate PACAP's role in thermogenesis.

In order to target the VMN, limitations in the current literature need to be overcome. Although intracerebroventricular and intrathecal injections of PACAP have resulted in increased BAT activity, these injections do not differentiate between the hypothalamic regions specifically involved in BAT activation, as injected PACAP likely spreads to various surrounding brain regions (Inglott, Farnham, & Pilowsky, 2011; Tanida et al., 2010). Additionally, in differentiating PACAP's role in the PVN and VMN, Resch et al. (2013) provided results that were only collected over a 24-hour period. Therefore, in addition to replicating results to ensure accuracy, assessing the long-term function of PACAP in the VMN would expand the literature, particularly in elucidating PACAP's role in activating adaptive thermogenesis during cold challenges, as full acclimation to cold and maximal induction of adaptive thermogenesis requires 3-4 weeks at 4°C (Cannon & Nedergaard, 2010; Meyer et al., 2010; Ukropec et al., 2006). As such, in future, an SF1-driven expression vector housing PACAP will be introduced by viral delivery using stereotaxic injections directly into the VMN of PACAP KO mice to assess the effect of genetic reintroduction of PACAP specifically in the VMN of animals lacking PACAP. The use of an adeno-associated virus serotype 9 (AAV9) will allow for rapid onset of transduction of the brain tissues in the absence of immune responses, as well as long term expression, and the use of a construct

where PACAP expression is driven by the SF1 promoter will ensure PACAP is only expressed in VMN infected neurons that specifically express SF1 (Daya, & Berns, 2008; Zincarelli et al., 2008). Complete methodology will be discussed below.

Hypothesis and Aims

I hypothesize that the cold sensitivity of PACAP $-/-$ mice may be due to the absence of PACAP signaling within the VMN specifically.

Due to the complexity and long-term nature of this project, my involvement and thus the objectives of this chapter are:

- To create an adenoviral construct that expresses GFP under the regulation of the SF1 promoter to act as a control vector, thus ensuring VMN-specific expression of the vector
- Develop a protocol for stereotaxic injection of the vector which reaches the VMN in live animals

Future directions will be discussed in detail below (see 3.4 Discussion); however, to provide further understanding they are stated here:

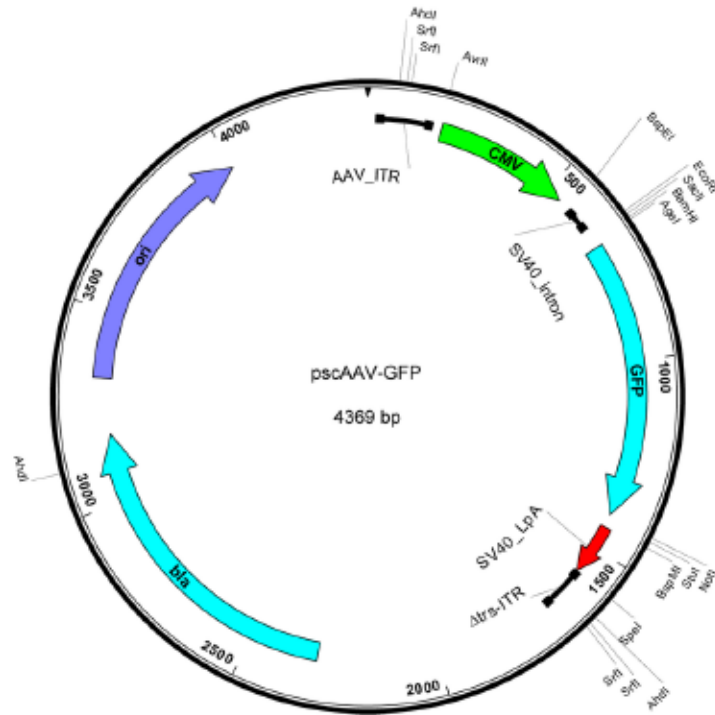
- To create an adenoviral construct for VMN-specific expression of PACAP to determine if the impaired thermogenesis in PACAP $-/-$ mice can be genetically rescued by transgenic expression of PACAP in the VMN only, thus determining the importance of VMN PACAP in regulating thermogenesis

3.2 MATERIALS AND METHODS

AAV Plasmid Vector Backbone

The self-complementary (sc) pscAAV-GFP plasmid (Figure 3.1A) (created by John T. Gray, Addgene Plasmid #32396) was chosen as the expression vector backbone for large-

A.



B.

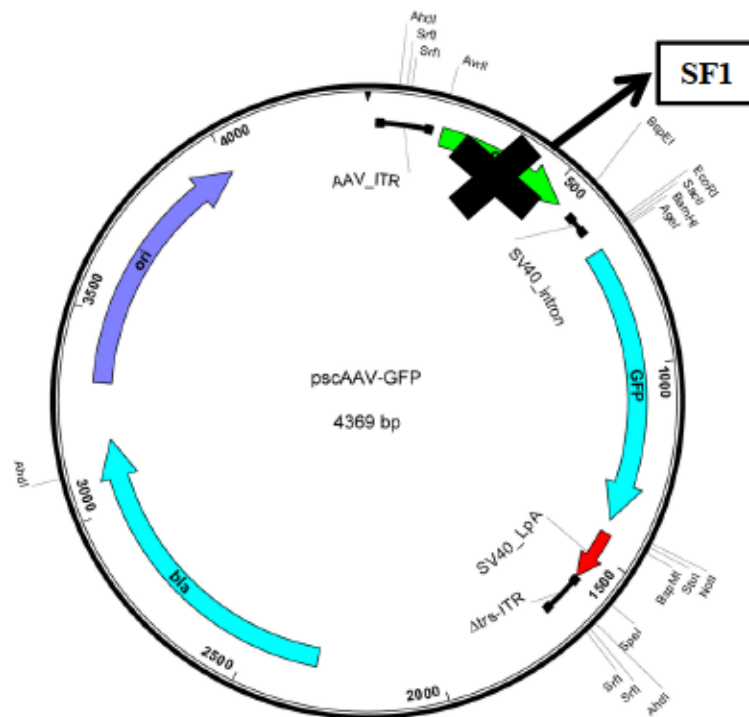


Figure 3.1. A. Plasmid map for pscAAV-GFP (Addgene Plasmid #32396). Image courtesy of John T. Gray. B. The CMV promoter within pscAAV-GFP was replaced with the SF1 promoter (pscAAV-SF1-GFP) with the goal of expressing GFP specifically in the VMN of the hypothalamus, a region of the brain known to specifically express SF1. Virus will be delivered to the brain via stereotaxic injection into the VMN. Adapted with permission from the author. Source: <https://www.addgene.org/32396/>. Accessed May 4, 2017.

scale packaging and production of AAV9 aimed at transfecting cells in the VMN. To ensure specific VMN transfection, the ubiquitous promoter in pscAAV-GFP, cytomegalovirus (CMV), was replaced with the VMN-specific SF1 promoter (Figure 3.1B) from isolated mouse DNA prior to AAV9 packaging. To ensure adenoviral expression of GFP under the SF1 promoter upon stereotaxic injections in the VMN, the region of the SF1 gene chosen for isolation and amplification was 400 bp long with the inclusion of upstream transcription factor binding sites necessary for SF1 promoter function (Woodson, Crawford, Sadovsky, & Milbrandt, 1997). Detailed methodology is discussed below.

Isolating the pscAAV-GFP Plasmid

The pscAAV-GFP plasmid was purchased from Addgene and received packaged within *Escherichia coli* (*E. coli*) bacteria (transformed in Stbl2 competent cells) in an agar stab. Bacteria within the agar stab were streaked onto Luria broth (LB) agar plates containing ampicillin (Amp) (100µg/ml) (prepared according to Addgene protocol) and incubated overnight (18 hours) at 30°C, in accordance with the bacterial growth conditions. Three isolated single bacteria colonies were picked from the plates and each grown in 2ml of LB-Amp liquid culture (prepared according to Addgene protocol) in a shaking incubator (300 rpm) for 12 hours at 30°C, which served as starter cultures for scaled production of this low copy plasmid. A negative control that contained LB media and Amp without any bacteria was included in the above steps as an indicator of non-specific bacterial growth. Cells from each starter culture were pelleted by centrifugation, resuspended in 1ml of fresh LB-Amp media and added to 100ml LB-Amp media, which served as a secondary culture. Only one starter culture resulted in pelleted cells and was therefore used, while the other two were discarded. The secondary culture was placed in a shaking incubator (300 rpm) for 12 hours at 30°C to allow for growth. Cells were pelleted 6 x 1ml in 4 separate eppendorf tubes (1.5ml)

according to the manufacturer's protocol for the QIAprep Spin Miniprep Kit (Qiagen, Hilden, Germany). Resuspension and lysis buffer (P1 and P2) volumes used were 1.6x those directed to ensure complete rinsing of the cells from the remaining LB media as well as complete cell lysis. Neutralizing buffer (N3) was used at a volume 1.6x that directed by the manufacturer's protocol and upon addition, tubes were inverted for 3 minutes to allow for complete DNA renaturation and precipitation of proteins and lipids. The optional wash step was used to remove endonucleases present in the bacteria strain (Stbl2). To increase yield, the eluted DNA from one eppendorf tube was used subsequently to elute the next in a sequential manner. All other steps were followed according to QIAprep Spin Miniprep Kit protocols (Qiagen, Hilden, Germany). DNA concentration and purity was assessed through UV light absorbance measurements using spectrophotometry (Nanodrop ND-1000; Thermo Scientific, Rockford, IL). As nucleotides absorb UV light at a wavelength of 260nm, absorbance levels of the sample at 260nm were used as a surrogate measure of DNA concentration. The ratio of absorbance at 260nm and 280nm (the wavelength at which protein absorbs UV light) was used to assess the purity of DNA, where a ratio of ~1.8 is generally accepted as "pure" for DNA. As a secondary measure of nucleic acid purity, the ratio of absorbance at 260nm and 230nm was used to identify the presence of contaminants that absorb at 230nm. 260/230 values commonly range between 2.0-2.2 for "pure" nucleic acid. To confirm integrity of the vector's sequence (i.e. the absence of mutations or deletions), a diagnostic restriction digest was performed according to manufacturer's protocols (New England BioLabs, Ipswich, Massachusetts). The reaction included plasmid DNA (0.5µg), HindIII and EcoRI (10 units of enzyme each), and New England BioLabs (NEB) Buffer 2.1. Digestion products were run on an ethidium bromide stained 1.5% agarose gel for 30 minutes at 100V and visualized under UV light. Expected band sizes were 3714 bp

and 655 bp. To further confirm the plasmid DNA was free of transcriptional errors sequencing, sequencing was performed using M13 Forward and Reverse primers (Applied Biosystems 3130x, UNBC Genetics Lab).

Isolating the SF1 Promoter

Methodology described in this section was completed in conjunction with an undergraduate honours thesis student (in collaboration with Aaron Germuth).

SF1 DNA Extraction

C57BL/6 WT mice were euthanized (110mg/kg euthanyl) and brains were collected and immediately placed in -80°C, ensuring rapid freezing. The hypothalamus was dissected from the frozen brain (~40mg), homogenized in TRIzol (Life Technologies), and DNA was isolated according to the manufacturer's protocol. DNA concentration and purity were assessed by spectrophotometry as detailed above (Nanodrop ND-1000; Thermo Scientific, Rockford, IL).

SF1 Primer Design and Amplification with PCR

Primers were designed for PCR amplification of the 400 bp region of SF1 with at least 20 complimentary nucleotides. To facilitate future cloning, RE sites, matching those on either ends of the CMV promoter region within pscAAV-GFP, were added to each side end of the SF1 promoter region, with a 5 bp overhang to facilitate RE digestion. RE sites added were specific to AvrII (5' CCT AAG 3') and BspEI (5' TCC GGA 3'). Care was taken to ensure similar GC content and melting points of the primers. PCR conditions were as follows: initial denaturation at 98°C (30 seconds), followed by 35 cycles of denaturation (98°C for 10 seconds), annealing (67°C for 30 seconds), and extension (72°C for 30 seconds). A final extension was performed at 72°C for 5 minutes. PCR products were run on

an ethidium bromide stained 1.5% agarose gel for 40 minutes at 100V and visualized under UV light with an expected band size of 400 bp.

TA Cloning

PCR-amplified SF1 was ligated into pGEM®-T Vector (Figure 3.2) using 2X Rapid Ligation Buffer and T4 DNA Ligase according to manufacturer's protocol (Promega, Madison, WI), which allowed for blue-white screening selection. An aliquot of the ligation reaction (2.5µl) was added to 50µl of MAX Efficiency Stbl2 Competent Cells (Invitrogen, Carlsbad, CA) and plated on LB-Amp plates according to Addgene's "Bacterial Transformation" protocols, and incubated overnight at 37°C. Resulting white colonies were picked into 10ml of LB-Amp media and incubated overnight at 37°C in a shaking incubator (225 rpm). Colony PCR for the SF1 promoter was performed on multiple colonies and successfully cloned plasmids (as determined by bright 400 bp bands on the resulting PCR gel) were isolated using Wizard® Plus SV Minipreps DNA Purification System (Promega, Madison, WI). Glycerol stocks of the ligated SF1 fragment and pGEM®-T Vector (further referred to here as the SF1-pGEM®-T Vector) were created using overnight culture and glycerol according to Addgene protocols. Extracted plasmids were screened for correct placement of the SF1 promoter fragment by performing a double RE digest according to manufacturers protocols (Thermo Scientific, Rockford, IL). The reaction contained: plasmid DNA (1µg), AvrII and BspEI (10 units of enzyme each) and 1X Thermo Scientific Tango Buffer. Products were run on an ethidium bromide stained 1.5% agarose gel for 30 minutes at 100V and visualized under UV light. Expected band sizes were 2600 bp and 400 bp. To further confirm the SF1-pGEM®-T plasmid was free of transcriptional errors, it was sequenced using T7 and SP6 primers (Applied Biosystems 3130x, UNBC Genetics Lab).

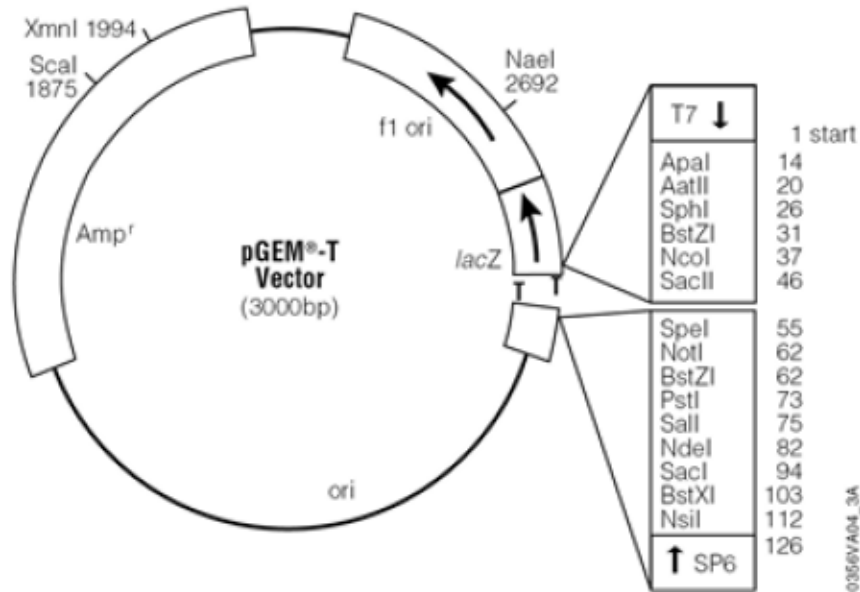


Figure 3.2. Plasmid map for pGEM®-T Vector (Promega). SF1 insert is ligated into the lacZ gene by attaching to overhanging thymine nucleotides, disrupting the lacZ gene. Accessed from <https://www.promega.ca/products/pcr/pcr-cloning/pgem-t-vector-systems/>. Copyright © 2017 Promega Corporation. Image reproduced with permission from the corporation.

Replacing the CMV Promoter with the SF1 Promoter in the pscAAV-GFP Vector

The isolated pscAAV-GFP plasmid (15µg) and isolated SF1-pGEM®-T plasmid (5µg) were sent to Vigene Biosciences Inc. (Rockville, MD) where SF1 was cloned into the pscAAV-GFP vector to replace the CMV promoter (Figure 3.1B) using AvrII and BspEI RE digestion and ligation reactions. The new plasmid was named pscAAV-SF1-GFP.

Production of AAV9 Expressing pscAAV-SF1-GFP

AAV9 packaging of the expression vector (pscAAV-SF1-GFP) and large-scale production of the virus AAV9-SF1-GFP was performed (concentration 2.24×10^{14} genome copy/ml) (Vigene Biosciences, Inc., Rockville, MD). This virus will be used as a control virus for this project, expressing GFP under the control of the SF1 promoter in specific brain regions infected with the virus through stereotaxic injections (described below).

Devising a Stereotaxic Protocol for Injections into the VMN

Stereotaxic surgery is a new procedure in the Gray lab and therefore required training and development of experimental procedures. Stereotaxic workshops were held under the direction of Shelley McErlane (DVM), Senior Clinical Veterinarian and Head of Training for Animal Care Services at the University of British Columbia, and Lydia Troc (RVT and RLAT) from the University of Northern British Columbia, before performing surgeries independently.

Positioning the Mouse in the Stereotaxic Frame

Mice were weighed, anesthetized with sodium pentobarbital (90mg/kg, IP), and placed in a separate cage until a plane of anesthesia was reached, as observed by deep, regular breathing and no withdrawal upon a toe pinch. Fur was shaved from the surgical site, with care taken not to shave the whiskers, and disinfected with 70% alcohol. Eye lubricant was placed over the corneas of both eyes. Ear bars of the stereotaxic frame (Stoetling, Wood

Dale, Illinois) were gently placed in the external auditory canal within the bulla in both ears and tightened into place. Correct positioning was determined by smooth rotational movement of the snout up and down, with little or no lateral movement. Ear bar measurements were consistent on each side such that the mouse was centered. Incisors were then placed over the incisor bar and the anesthetic cone was fitted snugly over the nose. Oxygen flow rate was kept at 0.8L/min while isoflurane was adjusted throughout to maintain a surgical level of anesthetic (normally maintained at 2%). Throughout the procedure, the animal was placed on a heating pad controlled by a thermometer placed in the rectum, measuring body temperature continuously and adjusting the heating pad temperature accordingly (Rodent Warmer, Stoetling, Wood Dale, Illinois). A local anesthetic (bupivacaine, 2.5mg/ml; not exceeding 8mg/kg) was injected subcutaneously along the planned incision site as a line block.

Stereotaxic Surgery

Stereotaxic coordinates published for the VMN and used in this experiment were: - 1.46mm posterior from bregma, \pm 0.39mm laterally from midline and -5.50mm below the surface of the brain (Allen Institute for Brain Science, 2016). A stable plane of anesthesia was ensured prior to commencing surgery. An incision was then made such that lambda and bregma were exposed on the skull (Figure 3.3). The skin was gently pulled back and the skull was cleaned using cotton tipped applicators. A drill with a 1mm drill bit was attached to the stereotaxic arm. The tip of the drill bit was positioned on lambda and the height was recorded. The tip of the drill bit was then positioned on bregma (Figure 3.4A) where the height was recorded again. The incisor bar was raised or lowered to level the skull such that the height of lambda and bregma were the same. The drill was moved in the posterior direction away from bregma 1.46mm, and to the right of the midline 0.39mm until the appropriate readings were aligned on the Vernier scale of the stereotaxic frame. At the

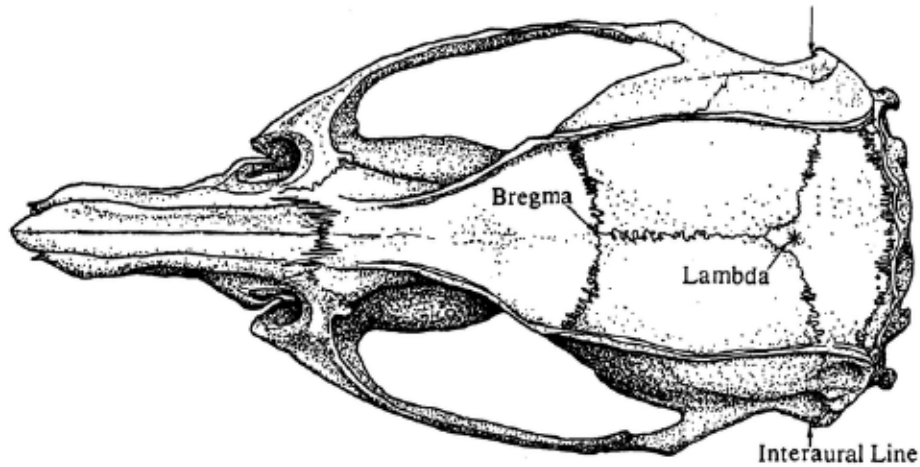


Figure 3.3. Location of lambda and bregma as defined by Dr. George Paxinos. Interaural line corresponds with the placement of the ear bars. Reproduced from “The rat brain in stereotaxic coordination”, by G. Paxinos, & C. Watson, 1998, 1st Edition, p. 11. Copyright © 2017 Academic Press/Elsevier. Reproduced with permission from publisher.

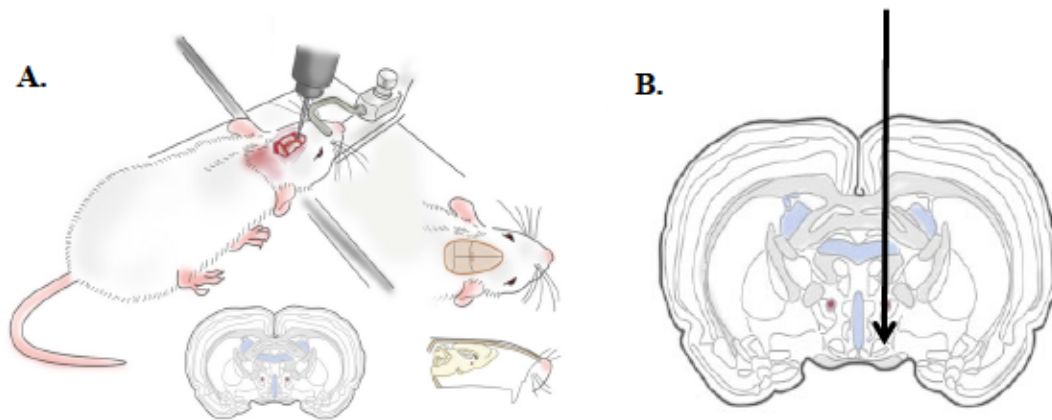


Figure 3.4. A. Stereotaxic administrations are given using x, y, and z coordinates to a specific location and depth. B. Location of injection into the VMN of the hypothalamus. Illustrations by Encapsula NanoSciences LLC, Brentwood, TN. Copyright © 2014 Encapsula NanoSciences LLC. Obtained from <https://www.clodrosome.com/animal-injection/>. Adapted with permission from Encapsula NanoSciences.

intersection of these coordinates, in the X and Y plane, a hole in the skull was made by drilling in small increments such that the underlying brain was not damaged. The height of the top of the brain was then measured on the Vernier scale. The drill was replaced with a Hamilton syringe (70001KH, Hamilton Robotics, Switzerland) with a 25-gauge needle loaded with 1 μ l of 5x loading dye. From the surface of the brain, the needle was lowered 5.50mm in the Z plane at a rate of 1mm/minute (Figure 3.4B). Dye was injected very slowly at a rate of 200nl/minute, and then the needle was left in place for 5 minutes to allow the fluid to be adsorbed before removing the needle it at a rate of 1mm/min.

Post-Operative Procedure

Mice were euthanized with isoflurane and cervical dislocation. The brain was removed immediately and placed in 10% formalin for 24 hours. The fixed brain was dissected and the hypothalamus viewed under a stereo microscope (Olympus SXZ7) to visualize the location and to determine accuracy of the injection. Images were taken with an Infinity1 camera and Infinity Capture Software (Lumenera, Ottawa, ON).

3.3 RESULTS

pscAAV-GFP Plasmid was Successfully Isolated, Free of Transcription Errors

To confirm that the bacteria containing the low-copy pscAAV-GFP plasmid had been grown up successfully with no transcriptional errors, the plasmid DNA was sequenced using M13 Forward and Reverse primers. Using the National Center for Biotechnology Information's (NCBI) Basic Local Alignment Search Tool (BLAST), sequencing results of the isolated pscAAV-GFP plasmid indicated matching nucleotide sequences to that of the purchased plasmid (Addgene Plasmid #32396), indicating no transcription errors (Figure 3.5).

Score	Expect	Identities	Gaps	Strand
1330 bits(1474)	0.0	776/809(96%)	2/809(0%)	Plus/Plus
Query 395	CTCCATCACTAGGGGTTCCCTGGAGGGTGGAGTCGTGACCTAGGCATATGCCAAGTACGC	454		
Sbjct 38	CTCCCTCACTAGGGGTTCCCTGGAGGGTGNNTNNNACTAGGCATATGCCAAGTACGC	97		
Query 455	CCCCTATTGACGTC AATGACGGTAAATGGCCCGCTGGCATTATGCCCAGTACATGACCT	514		
Sbjct 98	CCCCTATTGACGTC AATGACGGTAAATGGCCCGCTGGCATTATGCCCAGTACATGACCT	157		
Query 515	TATGGGACTTTCC TACTTGGCAGTACATCTACGTATTAGTCATCGCTATTACCATGGTGA	574		
Sbjct 158	TATGGGACTTTCC TACTTGGCAGTACATCTACGTATTAGTCATCGCTATTACCATGGTGA	217		
Query 575	TGCGGTTTGGCAGTACATCAATGGCGCTGGATAGCGGTTTGACTCACGGGATTCCAA	634		
Sbjct 218	TGCGGTTTGGCAGTACATCAATGGCGCTGGATAGCGGTTTGACTCACGGGATTCCAA	277		
Query 635	GTCTCCACCCCA TTGACGTC AATGGGAGTTTGT TTTGGCACCAAATCAACGGGACTTTC	694		
Sbjct 278	GTCTCCACCCCA TTGACGTC AATGGGAGTTTGT TTTGGCACCAAATCAACGGGACTTTC	337		
Query 695	CAAAATGTCGTAACA AACTCCGCCCCATTGACGCAAATGGGCGGTAGGCGGTACGGTGGG	754		
Sbjct 338	CAAAATGTCGTAACA AACTCCGCCCCATTGACGCAAATGGGCGGTAGGCGGTACGGTGGG	397		
Query 755	AGGTCTATATAAGCAGAGCTCGTTTAGTGAACCGTCAGATCGCCTGGAGACGCCATCCGG	814		
Sbjct 398	AGGTCTATATAAGCAGAGCTCGTTTAGTGAACCGTCAGATCGCCTGGAGACGCCATCCGG	457		
Query 815	ACTCTAAGGTAAATATAAAATTTTAAAGTGTATAATGTGTAAACTACTGATTCTAATTG	874		
Sbjct 458	ACTCTAAGGTAAATATAAAATTTTAAAGTGTATAATGTGTAAACTACTGATTCTAATTG	517		

Figure 3.5. A section of nucleotides matching from NCBI's BLAST between the pscAAV-GFP plasmid sequence provided from Addgene (Query) and the isolated plasmid (Sbjct) sequenced using M13 Reverse primer. Yellow indicates AvrII RE site (5' CCT AGG 3') and red indicates BspEI RE site (5' TCC GGA 3'). A small section of the isolated plasmid DNA was unreadable (indicated by "N") using M13 Reverse primer. A matching sequence was confirmed using M13 Forward primer (results not shown).

SF1 was Successfully Ligated with the pGEM®-T Vector

To confirm that SF1 was successfully ligated into the pGEM®-T Vector with no transcriptional errors, bacterial plasmid DNA was sequenced using T7 and SP6 primers. Using NCBI's BLAST, the DNA sequence of the ligated SF1-pGEM®-T Vector matched nucleotide sequences to that of *Mus musculus* strain C57BL/6J, chromosome 2, Genome Reference Consortium Mouse Reference 38 patch 4 (GRCm38.p4), which corresponds to the sequence of SF1 in the mouse genome (Figure 3.6).

Stereotactic Injected-Dye was Localized in the Hypothalamus

To confirm the stereotaxic injection of the dye successfully targeted the VMN of the hypothalamus, the brain was crudely cross-sectioned and visualized under a stereo microscope (Olympus SXZ7). Images showed blue dye visible in the third ventricle (3V) of the hypothalamus and surrounding areas, including the VMN (Figure 3.7). However, dye appeared further dorsal in the hypothalamus than anticipated (Figure 3.7). The dye was not observed in any regions outside of the hypothalamus such as the basal forebrain (results not shown).

3.4 DISCUSSION

Central and vital to this project was ensuring that the constructs for the VMN-specific adeno-associated viruses were properly designed and created such that future viral injections into the VMN via stereotaxic surgery will prove safe and effective. The cloning strategy developed for this project utilized an expression vector called pscAAV-GFP as a backbone. This vector can be packaged in an adeno-associated virus serotype 9, such that infected cells express GFP under control of the CMV promoter. Because the CMV promoter would drive gene expression in all brain tissues, CMV was replaced with SF1, which when injected into the brain will drive gene expression in cells of the VMN only. Using the SF1 gene region that

Score	Expect	Identities	Gaps	Strand
724 bits(802)	0.0	407/410(99%)	1/410(0%)	Plus/Plus
Query 3		CAAGGTCTCTCCAGTGCCTTGGCCTCTGCCCCACCCAGGGCCCCCATAAA		62
Sbjct 41		TATCCTAGGCAAGGTCTCTCCNGTGCCTTGGCCTCTGCCCCACCCAGGGCCCCCATAAA		100
Query 63		GATAGGGATAtttttttttCTTTTAGAAGAGTGAAAAAGATATAGACCCAAATGAAGAG		122
Sbjct 101		GATAGGGNTATTTTTTTTCTTTTAGAAGAGTGAAAAAGATATAGACCCAAATGAAGAG		160
Query 123		AAACACCAACAAAGGAGGAGAAAGGCCTGCAGAGTCACGTGGGGGCAGAGACCAATTGGG		182
Sbjct 161		AAACACCAACAAAGGAGGAGAAAGGCCTGCAGAGTCACGTGGGGGCAGAGACCAATTGGG		220
Query 183		CCTCCGGTGGccccccACCACGAGGGGAGGAGGAAAGACGATCGGACAGGGCCAGTT		242
Sbjct 221		CCTCCGGTGGCCCCCCACCACGAGGGGAGGAGGAAAGACGATCGGACAGGGCCAGTT		280
Query 243		TCCAGTCCGCCGCTGCCCGCCCGCTGCTGGGTGAAGAAGTTTCTGAGAGCCCGCTAGCCA		302
Sbjct 281		TCCAGTCCGCCGCTGCCCGCCCGCTGCTGGGTGAAGAAGTTTCTGAGAGCCCGCTAGCCA		340
Query 303		CTGCCCTACCTGAGGCCTGGGAGCCTCCCCACCAGGACCCTGGTGTCCAGTGTCCACCT		362
Sbjct 341		CTGCCCTACCTGAGGCCTGGGAGCCTCCCCACCAGGACCCTGGTGTCCAGTGTCCACCT		400
Query 363		TATCCGGCTGAGAATTCTCCTCCGTTTTCAGTAAAGTGAAG		412
Sbjct 401		TATCCGGCTGAGAATTCTCCTCCGTTTTCAGT-AGTGAAGTCCGGATTCGAC		449

Figure 3.6. NCBI's BLAST search of the sequence obtained from SF1-pGEM®-T Vector (Sbjct) using T7 primer revealed a match to a section of the *Mus musculus* strain C57BL/6J, chromosome 2, GRCm38.p4 (Query): the region of the mouse genome that houses the SF1 promoter. Yellow indicates AvrII RE site (5' CCT AGG 3') and red indicates BspEI RE site (5' TCC GGA 3') added to the PCR-amplified SF1.

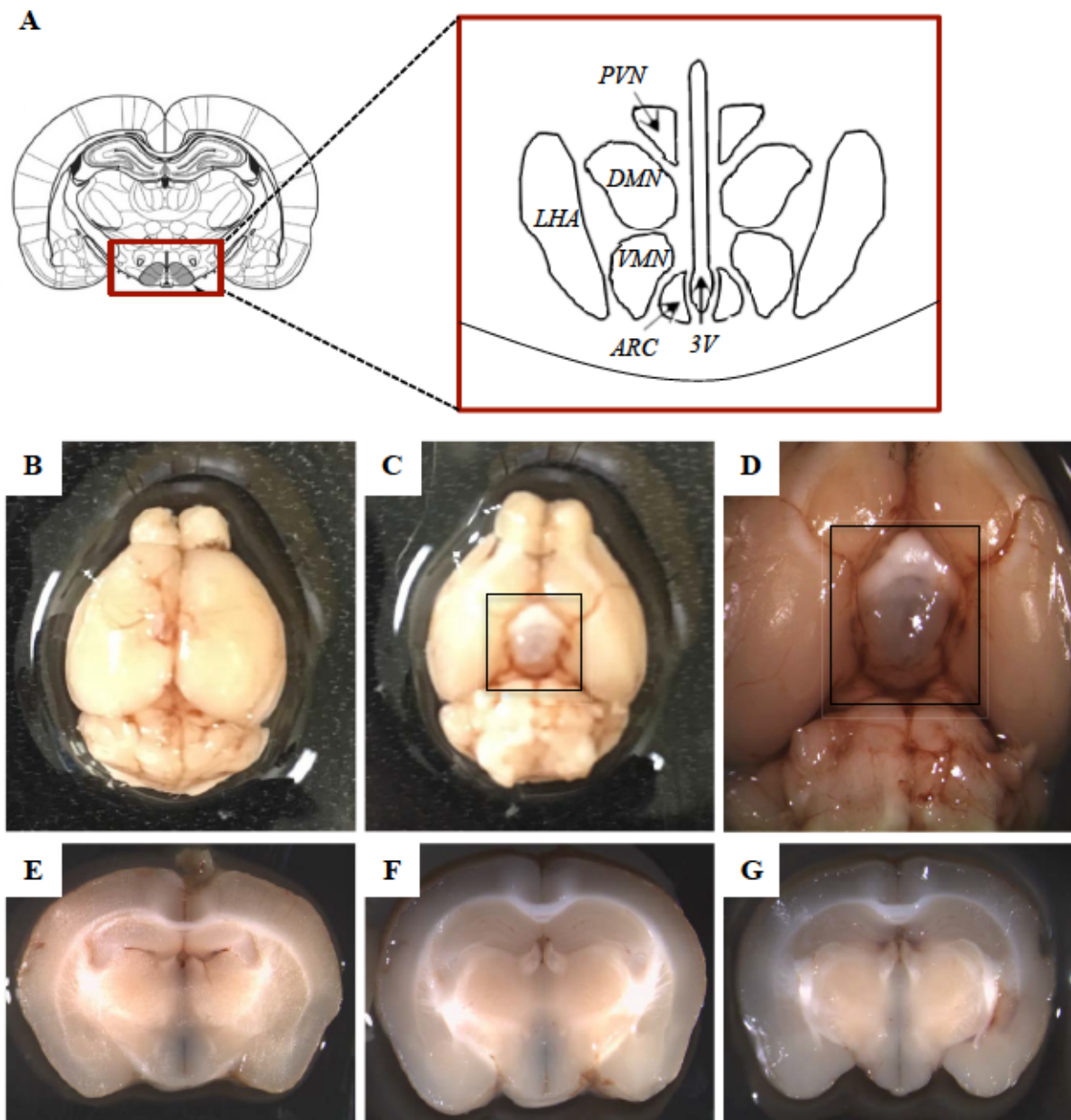


Figure 3.7. A. Coronal cross section of the brain showing the location of the hypothalamus and close-up five key hypothalamic nuclei involved in the regulation of energy metabolism. PVN; paraventricular nucleus, DMN; dorsomedial nucleus, LHA; lateral hypothalamic area, VMN; ventromedial nucleus, ARC; arcuate nucleus, 3V; third ventricle. Adapted from “Revisiting the Ventral Medial Nucleus of the Hypothalamus: The Roles of SF-1 Neurons in Energy Homeostasis”, by Y. Choi, T. Fujikawa, J. Lee, A. Reuter, & K. Kim, 2013, *Frontiers In Neuroscience*, 7. Copyright © 2013 Choi, Fujikawa, Lee, Reuter and Kim. Adapted with permission from author. B. Dorsal view of the mouse brain. C. Ventral view of the mouse brain (box indicates hypothalamus). D. Blue dye observed in the hypothalamus. E. Anterior coronal section through the hypothalamus; blue dye observed in the 3V and surrounding hypothalamic tissues. F. Middle coronal section through the hypothalamus; dye localized along the 3V. G. Posterior coronal section through the hypothalamus; dye localized further dorsal along the 3V.

included all necessary transcription factors for SF1 promoter activity will allow for the expression of GFP (control) or PACAP, specifically in the VMN of AAV9-injected mice. In order to provide Vigene with the components required to generate AAV9 expressing the control plasmid (AAV9-SF1-GFP), the pscAAV-GFP and SF1-pGEM®-T vectors were produced and Vigene successfully cloned SF1 into the pscAAV-GFP vector and packaged this construct into AAV9 such that we have the AAV9-SF1-GFP control virus to test VMN specific gene delivery.

Prior to commencing stereotaxic injections with the control virus expressing GFP (AAV9-SF1-GFP), we instead injected dye containing bromophenol blue to visualize if the published VMN coordinates (anterior/posterior -1.46mm from bregma; medial/lateral, \pm 0.39 mm from midline; and dorsal/ventral, -5.50mm from surface of the brain (Allen Institute for Brain Science, 2016)) were in fact allowing targeted delivery to the VMN. From the observed formalin-fixed hypothalamic sections, dye was observed superior to the anticipated location and therefore is potentially not reaching the VMN (Figure 3.7). We thus conclude that the coordinate for the Z-plane is lower than -5.50mm from the surface of the brain, and future injections will use the coordinate of -5.70mm from the surface of the brain in hopes of achieving injections closer to the base of the hypothalamus, specifically in the VMN. This change may appear conservative (Δ 0.2mm), but precision in the hypothalamus is imperative as the distance between the top and bottom of the 3V is only 1mm (Figure 3.8).

Although the goal of the stereotaxic injections is to reach the VMN as this would result in the greatest infection of target cells, injections into the 3V is also an option as our expression vector is driven by the SF1 promoter which is exclusively expressed in the VMN (Choi et al., 2013). Therefore, if injections were made into the 3V (a larger target than the VMN) or not entirely in the VMN, we can be confident that GFP, and in future PACAP, will



Figure 3.8. Middle coronal cross section through the hypothalamus of *Mus musculus* stereotaxically injected with 5x loading dye. Ruler shows 1mm increments.

only be expressed in the VMN. Additional injections will be conducted to ensure location accuracy prior to commencing experiments using the control virus.

Future Directions

Performing a genetic intervention to assess if the impaired thermogenic capacity observed in PACAP KO can be rescued with VMN-specific injections of PACAP is both a complex and long-term project in the Gray lab. As part of this thesis, preliminary work has been completed such that the project may progress. Here, an adenoviral construct that expresses GFP under the regulation of the SF1 promoter has been created, and a stereotaxic protocol for the injection of this virus has been developed. The remainder of this project will be completed by the Gray lab.

The long-term aim of this project is to genetically reintroduce PACAP in PACAP KO mice in the neurons of the VMN only, and assess if the impaired thermogenesis is improved (or rescued). To do so, the control virus discussed above (AAV9-SF1-GFP) will be used for two reasons: firstly, to confirm the efficacy of the ICV-VMN injections, and secondly, to behave as a control for comparisons between mice injected with the experimental virus (AAV9-SF1-PACAP) (discussed below).

To determine efficacy of the ICV-VMN injections, AAV9-SF1-GFP injected animal brains will be sectioned, and the location of GFP will be assessed using an established immunohistochemistry protocol in the Gray lab, where a primary antibody binds to GFP, followed by secondary antibody binding to amplify the signal such that the location of GFP expression can be visualized under a fluorescent microscope. Once the location of GFP expression is determined in the VMN, experimental injections may commence. First, however, construction of the experimental virus, AAV9-SF1-PACAP is required, where PACAP will replace GFP in the control virus, AAV9-SF1-GFP.

The pscAAV-SF1-GFP expression vector will be used for construction of the experimental virus. PCR amplification of PACAP from hypothalamic cDNA will be ligated with the pGEM®-T Vector (Figure 3.2) and sent to Vigene, along with isolated pscAAV-SF1-GFP plasmid where PACAP will replace GFP (Figure 3.9), and large-scale AAV9 packaging of the expression vector will be produced. This virus will be named: AAV9-SF1-PACAP.

To assess whether the cold sensitivity of PACAP $-/-$ mice is due to the absence of PACAP signaling within the VMN specifically, physiological and biochemical assessments of thermogenic markers similar to those in Chapter 2 will be used to determine if the PACAP $-/-$ phenotype can be rescued with genetic reinsertion of PACAP in the VMN. Therefore, aseptic surgical technique will be performed in order to avoid infection, and animals will be recovered post-surgery to allow for viral transfection of cells in the VMN as well as for cold acclimation prior to thermogenic assessments.

In conclusion, further elucidation of the complex pathways associated with PACAP in the VMN and their roles in regulating adaptive thermogenesis will contribute to the pool of knowledge available for pathways controlling energy expenditure. Because energy expenditure contributes immensely to whole body energy homeostasis, this knowledge may contribute to the development of safe and effective therapies for metabolic disorders, including obesity, and will be further discussed in Chapter 4.

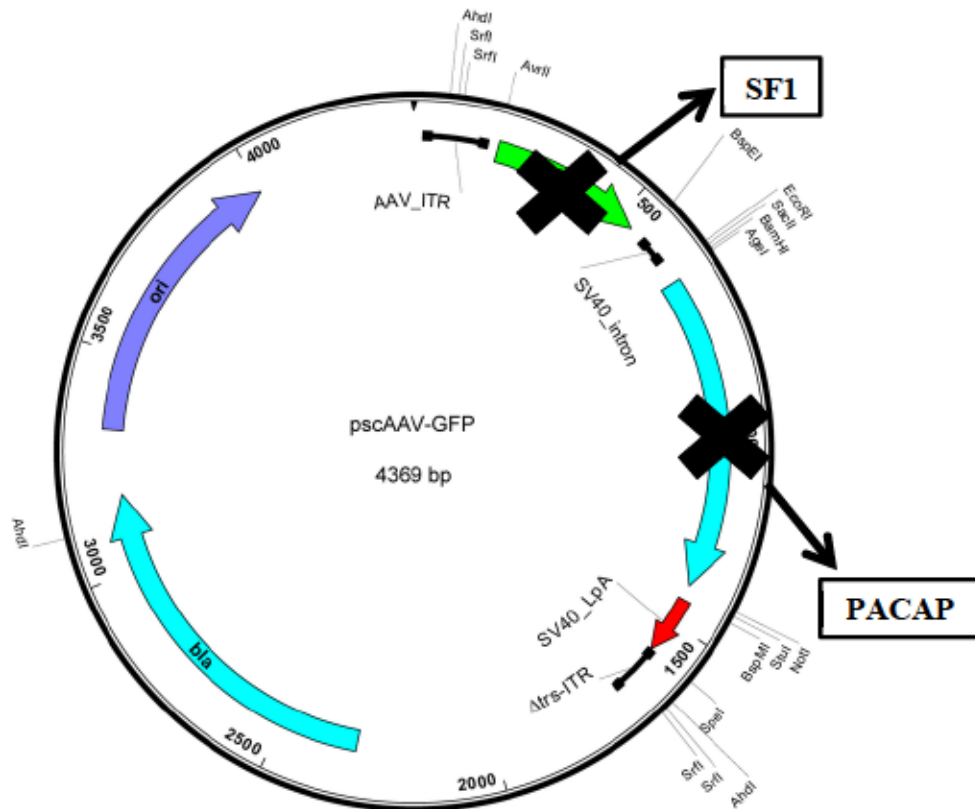


Figure 3.9. The CMV promoter replaced with the SF1 promoter, and the GFP gene replaced with the PACAP gene (pscAAV-SF1-PACAP) with the goal of expressing PACAP specifically in the VMN of the hypothalamus, a region of the brain known to specifically express SF1. Virus will be delivered to the brain via stereotaxic injection into the VMN. Adapted with permission from the author. Source: <https://www.addgene.org/32396/>. Accessed May 4, 2017.

3.5 REFERENCES

- Adams, B., Gray, S., Isaac, E., Bianco, A., Vidal-Puig, A., & Sherwood, N. (2008). Feeding and Metabolism in Mice Lacking Pituitary Adenylate Cyclase-Activating Polypeptide. *Endocrinology*, *149*(4), 1571-1580. <http://dx.doi.org/10.1210/en.2007-0515>
- Addgene: pscAAV-GFP*. (2017). *Addgene.org*. Retrieved 4 May 2017, from <https://www.addgene.org/32396/>
- Allen Institute for Brain Science. (2016). *Injections sites and stereotaxic coordinates for anterograde projectome (brain-wide)* (1st ed., p. 112). Seattle: Allen Institute for Brain Science. Retrieved from <http://help.brainmap.org/display/mouseconnectivity/Documentation>
- Animal Injection – Clodrosome: Liposomal Clodronate*. (2017). *Clodrosome.com*. Retrieved 4 May 2017, from <https://www.clodrosome.com/animal-injection/>
- Arimura, A., Somogyvári-Vigh, A., Miyata, A., Mizuno, K., Coy, D., & Kitada, C. (1991). Tissue Distribution of PACAP as Determined by RIA: Highly Abundant in the Rat Brain and Testes. *Endocrinology*, *129*(5), 2787-2789. <http://dx.doi.org/10.1210/endo-129-5-2787>
- Balthasar, N., Dalgaard, L., Lee, C., Yu, J., Funahashi, H., & Williams, T. et al. (2005). Divergence of Melanocortin Pathways in the Control of Food Intake and Energy Expenditure. *Cell*, *123*(3), 493-505. <http://dx.doi.org/10.1016/j.cell.2005.08.035>
- Bamshad, M., Song, C., & Bartness, T. (1999). CNS origins of the sympathetic nervous system outflow to brown adipose tissue. *Am J Physiol*, *276*(6 Pt 2), R1569-78.
- Bartness, T., Vaughan, C., & Song, C. (2010). Sympathetic and sensory innervation of brown adipose tissue. *Int J Obes Relat Metab Disord*, *34*, S36-S42. <http://dx.doi.org/10.1038/ijo.2010.182>
- Bellinger, L., & Bernardis, L. (2002). The dorsomedial hypothalamic nucleus and its role in ingestive behavior and body weight regulation. *Physiology & Behavior*, *76*(3), 431-442. [http://dx.doi.org/10.1016/s0031-9384\(02\)00756-4](http://dx.doi.org/10.1016/s0031-9384(02)00756-4)
- Bingham, N., Anderson, K., Reuter, A., Stallings, N., & Parker, K. (2008). Selective Loss of Leptin Receptors in the Ventromedial Hypothalamic Nucleus Results in Increased Adiposity and a Metabolic Syndrome. *Endocrinology*, *149*(5), 2138-2148. <http://dx.doi.org/10.1210/en.2007-1200>
- Bingham, N., Verma-Kurvari, S., Parada, L., & Parker, K. (2006). Development of a steroidogenic factor 1/Cre transgenic mouse line. *Genesis*, *44*(9), 419-424. <http://dx.doi.org/10.1002/dvg.20231>
- Cannon, B., & Nedergaard, J. (2004). Brown Adipose Tissue: Function and Physiological Significance. *Physiological Reviews*, *84*(1), 277-359. <http://dx.doi.org/10.1152/physrev.00015.2003>

- Cannon, B. & Nedergaard, J. (2010). Nonshivering thermogenesis and its adequate measurement in metabolic studies. *Journal Of Experimental Biology*, 214(2), 242-253. <http://dx.doi.org/10.1242/jeb.050989>
- Cano, G., Passerin, A., Schiltz, J., Card, J., Morrison, S., & Sved, A. (2003). Anatomical substrates for the central control of sympathetic outflow to interscapular adipose tissue during cold exposure. *The Journal Of Comparative Neurology*, 460(3), 303-326. <http://dx.doi.org/10.1002/cne.10643>
- Cao, W., Fan, W., & Morrison, S. (2004). Medullary pathways mediating specific sympathetic responses to activation of dorsomedial hypothalamus. *Neuroscience*, 126(1), 229-240. <http://dx.doi.org/10.1016/j.neuroscience.2004.03.013>
- Cerri, M., & Morrison, S. (2005). Activation of lateral hypothalamic neurons stimulates brown adipose tissue thermogenesis. *Neuroscience*, 135(2), 627-638. <http://dx.doi.org/10.1016/j.neuroscience.2005.06.039>
- Chechi, K., Carpentier, A., & Richard, D. (2013). Understanding the brown adipocyte as a contributor to energy homeostasis. *Trends In Endocrinology & Metabolism*, 24(8), 408-420. <http://dx.doi.org/10.1016/j.tem.2013.04.002>
- Choi, S., & Dallman, M. (1999). Hypothalamic Obesity: Multiple Routes Mediated by Loss of Function in Medial Cell Groups. *Endocrinology*, 140(9), 4081-4088. <http://dx.doi.org/10.1210/endo.140.9.6964>
- Choi, Y., Fujikawa, T., Lee, J., Reuter, A., & Kim, K. (2013). Revisiting the Ventral Medial Nucleus of the Hypothalamus: The Roles of SF-1 Neurons in Energy Homeostasis. *Frontiers In Neuroscience*, 7. <http://dx.doi.org/10.3389/fnins.2013.00071>
- Coote, J. (1995). Cardiovascular Function of the Paraventricular Nucleus of the Hypothalamus. *Neurosignals*, 4(3), 142-149. <http://dx.doi.org/10.1159/000109434>
- Cummings, K., Pendlebury, J., Sherwood, N., & Wilson, R. (2004). Sudden neonatal death in PACAP-deficient mice is associated with reduced respiratory chemoresponse and susceptibility to apnoea. *The Journal Of Physiology*, 555(1), 15-26. <http://dx.doi.org/10.1113/jphysiol.2003.052514>
- Das, M., Vihlen, C., & Legradi, G. (2006). Hypothalamic and brainstem sources of pituitary adenylate cyclase-activating polypeptide nerve fibers innervating the hypothalamic paraventricular nucleus in the rat. *The Journal Of Comparative Neurology*, 500(4), 761-776. <http://dx.doi.org/10.1002/cne.21212>
- Daya, S., & Berns, K. (2008). Gene Therapy Using Adeno-Associated Virus Vectors. *Clinical Microbiology Reviews*, 21(4), 583-593. <http://dx.doi.org/10.1128/cmr.00008-08>
- Dellovade, T., Young, M., Ross, E., Henderson, R., Caron, K., Parker, K., & Tobet, S. (2000). Disruption of the gene encoding SF-1 alters the distribution of hypothalamic

- neuronal phenotypes. *The Journal Of Comparative Neurology*, 423(4), 579-589. [http://dx.doi.org/10.1002/1096-9861\(20000807\)423:4<579::aid-cne4>3.0.co;2-#](http://dx.doi.org/10.1002/1096-9861(20000807)423:4<579::aid-cne4>3.0.co;2-#)
- Dhillon, H., Zigman, J., Ye, C., Lee, C., McGovern, R., & Tang, V. et al. (2006). Leptin Directly Activates SF1 Neurons in the VMH, and This Action by Leptin Is Required for Normal Body-Weight Homeostasis. *Neuron*, 49(2), 191-203. <http://dx.doi.org/10.1016/j.neuron.2005.12.021>
- Diané, A., Nikolic, N., Rudecki, A., King, S., Bowie, D., & Gray, S. (2014). PACAP is essential for the adaptive thermogenic response of brown adipose tissue to cold exposure. *Journal Of Endocrinology*, 222(3), 327-339. <http://dx.doi.org/10.1530/joe-14-0316>
- Dickson, L., & Finlayson, K. (2009). VPAC and PAC receptors: From ligands to function. *Pharmacology & Therapeutics*, 121(3), 294-316. <http://dx.doi.org/10.1016/j.pharmthera.2008.11.006>
- DiMicco, J., & Zaretsky, D. (2006). The dorsomedial hypothalamus: a new player in thermoregulation. *AJP: Regulatory, Integrative And Comparative Physiology*, 292(1), R47-R63. <http://dx.doi.org/10.1152/ajpregu.00498.2006>
- Dodd, G., Worth, A., Nunn, N., Korpai, A., Bechtold, D., & Allison, M. et al. (2014). The Thermogenic Effect of Leptin Is Dependent on a Distinct Population of Prolactin-Releasing Peptide Neurons in the Dorsomedial Hypothalamus. *Cell Metabolism*, 20(4), 639-649. <http://dx.doi.org/10.1016/j.cmet.2014.07.022>
- Elmqvist, J., Ahima, R., Elias, C., Flier, J., & Saper, C. (1998). Leptin activates distinct projections from the dorsomedial and ventromedial hypothalamic nuclei. *Proceedings Of The National Academy Of Sciences*, 95(2), 741-746. <http://dx.doi.org/10.1073/pnas.95.2.741>
- Enriori, P., Sinnayah, P., Simonds, S., Garcia Rudaz, C., & Cowley, M. (2011). Leptin Action in the Dorsomedial Hypothalamus Increases Sympathetic Tone to Brown Adipose Tissue in Spite of Systemic Leptin Resistance. *Journal Of Neuroscience*, 31(34), 12189-12197. <http://dx.doi.org/10.1523/jneurosci.2336-11.2011>
- Ferguson, A., Latchford, K., & Samson, W. (2008). The paraventricular nucleus of the hypothalamus – a potential target for integrative treatment of autonomic dysfunction. *Expert Opinion On Therapeutic Targets*, 12(6), 717-727. <http://dx.doi.org/10.1517/14728222.12.6.717>
- Gavini, C., Jones, W., & Novak, C. (2016). Ventromedial hypothalamic melanocortin receptor activation: regulation of activity energy expenditure and skeletal muscle thermogenesis. *The Journal Of Physiology*, 594(18), 5285-5301. <http://dx.doi.org/10.1113/jp272352>
- Gray, J., & Zolotukhin, S. (2011). Design and Construction of Functional AAV Vectors. *Adeno-Associated Virus*, 25-46. http://dx.doi.org/10.1007/978-1-61779-370-7_2

- Gray, S., Cummings, K., Jirik, F., & Sherwood, N. (2001). Targeted Disruption of the Pituitary Adenylate Cyclase-Activating Polypeptide Gene Results in Early Postnatal Death Associated with Dysfunction of Lipid and Carbohydrate Metabolism. *Molecular Endocrinology*, *15*(10), 1739-1747. <http://dx.doi.org/10.1210/mend.15.10.0705>
- Gray, S., Yamaguchi, N., Vencova, P., & Sherwood, N. (2002). Temperature-Sensitive Phenotype in Mice Lacking Pituitary Adenylate Cyclase-Activating Polypeptide. *Endocrinology*, *143*(10), 3946-3954. <http://dx.doi.org/10.1210/en.2002-220401>
- Gottschall, P., Tatsuno, I., Miyata, A., & Arimura, A. (1990). Characterization and Distribution of Binding Sites for the Hypothalamic Peptide, Pituitary Adenylate Cyclase-Activating Polypeptide. *Endocrinology*, *127*(1), 272-277. <http://dx.doi.org/10.1210/endo-127-1-272>
- Hashimoto, H., Nogi, H., Mori, K., Ohishi, H., Shigemoto, R., & Yamamoto, K. et al. (1996). Distribution of the mRNA for a pituitary adenylate cyclase-activating polypeptide receptor in the rat brain: An in situ hybridization study. *The Journal Of Comparative Neurology*, *371*(4), 567-577. [http://dx.doi.org/10.1002/\(sici\)1096-9861\(19960805\)371:4<567::aid-cne6>3.3.co;2-m](http://dx.doi.org/10.1002/(sici)1096-9861(19960805)371:4<567::aid-cne6>3.3.co;2-m)
- Hawke, Z., Ivanov, T., Bechtold, D., Dhillon, H., Lowell, B., & Luckman, S. (2009). PACAP Neurons in the Hypothalamic Ventromedial Nucleus Are Targets of Central Leptin Signaling. *Journal Of Neuroscience*, *29*(47), 14828-14835. <http://dx.doi.org/10.1523/jneurosci.1526-09.2009>
- Ikeda, Y., Luo, X., Abbud, R., Nilson, J., & Parker, K. (1995). The nuclear receptor steroidogenic factor 1 is essential for the formation of the ventromedial hypothalamic nucleus. *Molecular Endocrinology*, *9*(4), 478-486. <http://dx.doi.org/10.1210/mend.9.4.7659091>
- Ingraham, H., Lala, D., Ikeda, Y., Luo, X., Shen, W., & Nachtigal, M. et al. (1994). The nuclear receptor steroidogenic factor 1 acts at multiple levels of the reproductive axis. *Genes & Development*, *8*(19), 2302-2312. <http://dx.doi.org/10.1101/gad.8.19.2302>
- Jolivel, V., Basille, M., Aubert, N., de Jouffrey, S., Ancian, P., & Le Bigot, J. et al. (2009). Distribution and functional characterization of pituitary adenylate cyclase-activating polypeptide receptors in the brain of non-human primates. *Neuroscience*, *160*(2), 434-451. <http://dx.doi.org/10.1016/j.neuroscience.2009.02.028>
- Kim, K., Zhao, L., Donato, J., Kohno, D., Xu, Y., & Elias, C. et al. (2011). Steroidogenic factor 1 directs programs regulating diet-induced thermogenesis and leptin action in the ventral medial hypothalamic nucleus. *Proceedings Of The National Academy Of Sciences*, *108*(26), 10673-10678. <http://dx.doi.org/10.1073/pnas.1102364108>
- Labbé, S., Caron, A., Lanfray, D., Monge-Rofarello, B., Bartness, T., & Richard, D. (2015). Hypothalamic control of brown adipose tissue thermogenesis. *Front. Syst. Neurosci.*, *9*. <http://dx.doi.org/10.3389/fnsys.2015.00150>

- Lam, H., Takahashi, K., Ghatei, M., Kanse, S., Polak, J., & Bloom, S. (1990). Binding sites of a novel neuropeptide pituitary-adenylate-cyclase-activating polypeptide in the rat brain and lung. *European Journal Of Biochemistry*, *193*(3), 725-729. <http://dx.doi.org/10.1111/j.1432-1033.1990.tb19392.x>
- Larsen, P., & Mikkelsen, J. (1995). Functional identification of central afferent projections conveying information of acute "stress" to the hypothalamic paraventricular nucleus. *Journal Of Neuroscience*, *15*(4), 2609-2627.
- Leibowitz, S., Hammer, N., & Chang, K. (1981). Hypothalamic paraventricular nucleus lesions produce overeating and obesity in the rat. *Physiology & Behavior*, *27*(6), 1031-1040. [http://dx.doi.org/10.1016/0031-9384\(81\)90366-8](http://dx.doi.org/10.1016/0031-9384(81)90366-8)
- López, M., & Tena-Sempere, M. (2017). Estradiol effects on hypothalamic AMPK and BAT thermogenesis: A gateway for obesity treatment?. *Pharmacology & Therapeutics*. <http://dx.doi.org/10.1016/j.pharmthera.2017.03.014>
- Luo, X., Ikeda, Y., & Parker, K. (1994). A cell-specific nuclear receptor is essential for adrenal and gonadal development and sexual differentiation. *Cell*, *77*(4), 481-490. [http://dx.doi.org/10.1016/0092-8674\(94\)90211-9](http://dx.doi.org/10.1016/0092-8674(94)90211-9)
- Madden, C., & Morrison, S. (2008). Neurons in the paraventricular nucleus of the hypothalamus inhibit sympathetic outflow to brown adipose tissue. *AJP: Regulatory, Integrative And Comparative Physiology*, *296*(3), R831-R843. <http://dx.doi.org/10.1152/ajpregu.91007.2008>
- Majdic, G., Young, M., Gomez-Sanchez, E., Anderson, P., Szczepaniak, L., & Dobbins, R. et al. (2002). Knockout Mice Lacking Steroidogenic Factor 1 Are a Novel Genetic Model of Hypothalamic Obesity. *Endocrinology*, *143*(2), 607-614. <http://dx.doi.org/10.1210/endo.143.2.8652>
- Martínez de Morentin, P., González-García, I., Martins, L., Lage, R., Fernández-Mallo, D., & Martínez-Sánchez, N. et al. (2014). Estradiol Regulates Brown Adipose Tissue Thermogenesis via Hypothalamic AMPK. *Cell Metabolism*, *20*(1), 41-53. <http://dx.doi.org/10.1016/j.cmet.2014.03.031>
- Masuo, Y., Suzuki, N., Matsumoto, H., Tokito, F., Matsumoto, Y., Tsuda, M., & Fujino, M. (1993). Regional distribution of pituitary adenylate cyclase activating polypeptide (PACAP) in the rat central nervous system as determined by sandwich-enzyme immunoassay. *Brain Research*, *602*(1), 57-63. [http://dx.doi.org/10.1016/0006-8993\(93\)90241-e](http://dx.doi.org/10.1016/0006-8993(93)90241-e)
- Meyer, C., Willershauser, M., Jastroch, M., Rourke, B., Fromme, T., & Oelkrug, R. et al. (2010). Adaptive thermogenesis and thermal conductance in wild-type and UCP1-KO mice. *AJP: Regulatory, Integrative And Comparative Physiology*, *299*(5), R1396-R1406. <http://dx.doi.org/10.1152/ajpregu.00021.2009>
- Morrison, S., & Nakamura, K. (2011). Central neural pathways for thermoregulation. *Frontiers In Bioscience*, *16*(1), 74. <http://dx.doi.org/10.2741/3677>

- Oldfield, B., Giles, M., Watson, A., Anderson, C., Colvill, L., & McKinley, M. (2002). The neurochemical characterisation of hypothalamic pathways projecting polysynaptically to brown adipose tissue in the rat. *Neuroscience*, *110*(3), 515-526. [http://dx.doi.org/10.1016/s0306-4522\(01\)00555-3](http://dx.doi.org/10.1016/s0306-4522(01)00555-3)
- Parker, K., & Schimmer, B. (1997). Steroidogenic Factor 1: A Key Determinant of Endocrine Development and Function. *Endocrine Reviews*, *18*(3), 361-377. <http://dx.doi.org/10.1210/edrv.18.3.0301>
- Paxinos, G., & Watson, C. (1998). *The rat brain in stereotaxic coordinates* (1st ed., p. 11). Amsterdam: Academic Press/Elsevier.
- Perkins, M., Rothwell, N., Stock, M., & Stone, T. (1981). Activation of brown adipose tissue thermogenesis by the ventromedial hypothalamus. *Nature*, *289*(5796), 401-402. <http://dx.doi.org/10.1038/289401a0>
- pGEM®-T Vector Systems*. (2017). *Promega.ca*. Retrieved 4 May 2017, from <https://www.promega.ca/products/pcr/pcr-cloning/pgem-t-vector-systems/>
- Rea, P. (2015). *Essential clinical anatomy of the nervous system* (1st ed., pp. 77-87). Elsevier Inc.
- Resch, J., Boisvert, J., Hourigan, A., Mueller, C., Yi, S., & Choi, S. (2011). Stimulation of the hypothalamic ventromedial nuclei by pituitary adenylate cyclase-activating polypeptide induces hypophagia and thermogenesis. *AJP: Regulatory, Integrative And Comparative Physiology*, *301*(6), R1625-R1634. <http://dx.doi.org/10.1152/ajpregu.00334.2011>
- Resch, J., Maunze, B., Gerhardt, A., Magnuson, S., Phillips, K., & Choi, S. (2013). Intrahypothalamic pituitary adenylate cyclase-activating polypeptide regulates energy balance via site-specific actions on feeding and metabolism. *AJP: Endocrinology And Metabolism*, *305*(12), E1452-E1463. <http://dx.doi.org/10.1152/ajpendo.00293.2013>
- Ryu, V., Garretson, J., Liu, Y., Vaughan, C., & Bartness, T. (2015). Brown Adipose Tissue Has Sympathetic-Sensory Feedback Circuits. *Journal Of Neuroscience*, *35*(5), 2181-2190. <http://dx.doi.org/10.1523/jneurosci.3306-14.2015>
- Sabatier, N., Leng, G., & Menzies, J. (2013). Oxytocin, Feeding, and Satiety. *Frontiers In Endocrinology*, *4*. <http://dx.doi.org/10.3389/fendo.2013.00035>
- Saito, M., Yoneshiro, T., & Matsushita, M. (2016). Activation and recruitment of brown adipose tissue by cold exposure and food ingredients in humans. *Best Practice & Research Clinical Endocrinology & Metabolism*, *30*(4), 537-547. <http://dx.doi.org/10.1016/j.beem.2016.08.003>
- Segal, J., Stallings, N., Lee, C., Zhao, L., Socci, N., & Viale, A. et al. (2005). Use of Laser-Capture Microdissection for the Identification of Marker Genes for the Ventromedial Hypothalamic Nucleus. *Journal Of Neuroscience*, *25*(16), 4181-4188. <http://dx.doi.org/10.1523/jneurosci.0158-05.2005>

- Sheward, W., Lutz, E., Copp, A., & Harmar, A. (1998). Expression of PACAP, and PACAP type 1 (PAC1) receptor mRNA during development of the mouse embryo. *Developmental Brain Research*, *109*(2), 245-253. [http://dx.doi.org/10.1016/s0165-3806\(98\)00086-8](http://dx.doi.org/10.1016/s0165-3806(98)00086-8)
- Song, C., Vaughan, C., Keen-Rhinehart, E., Harris, R., Richard, D., & Bartness, T. (2008). Melanocortin-4 receptor mRNA expressed in sympathetic outflow neurons to brown adipose tissue: neuroanatomical and functional evidence. *AJP: Regulatory, Integrative And Comparative Physiology*, *295*(2), R417-R428. <http://dx.doi.org/10.1152/ajpregu.00174.2008>
- Stefanidis, A., Wiedmann, N., Adler, E., & Oldfield, B. (2014). Hypothalamic control of adipose tissue. *Best Practice & Research Clinical Endocrinology & Metabolism*, *28*(5), 685-701. <http://dx.doi.org/10.1016/j.beem.2014.08.001>
- Swanson, L., & Sawchenko, P. (1980). Paraventricular Nucleus: A Site for the Integration of Neuroendocrine and Autonomic Mechanisms. *Neuroendocrinology*, *31*(6), 410-417. <http://dx.doi.org/10.1159/000123111>
- Ukropec, J., Anunciado, R., Ravussin, Y., Hulver, M., & Kozak, L. (2006). UCP1-independent Thermogenesis in White Adipose Tissue of Cold-acclimated Ucp1^{-/-} Mice. *Journal Of Biological Chemistry*, *281*(42), 31894-31908. <http://dx.doi.org/10.1074/jbc.m606114200>
- Whittle, A., Carobbio, S., Martins, L., Slawik, M., Hondares, E., & Vázquez, M. et al. (2012). BMP8B Increases Brown Adipose Tissue Thermogenesis through Both Central and Peripheral Actions. *Cell*, *149*(4), 871-885. <http://dx.doi.org/10.1016/j.cell.2012.02.066>
- Woodson, K., Crawford, P., Sadovsky, Y., & Milbrandt, J. (1997). Characterization of the Promoter of SF-1, an Orphan Nuclear Receptor Required for Adrenal and Gonadal Development. *Molecular Endocrinology*, *11*(2), 117-126. <http://dx.doi.org/10.1210/mend.11.2.9881>
- Yoshida, T., Kemnitz, J., & Bray, G. (1983). Lateral hypothalamic lesions and norepinephrine turnover in rats. *Journal Of Clinical Investigation*, *72*(3), 919-927. <http://dx.doi.org/10.1172/jci111063>
- Zaretskaia, M., Zaretsky, D., Shekhar, A., & DiMicco, J. (2002). Chemical stimulation of the dorsomedial hypothalamus evokes non-shivering thermogenesis in anesthetized rats. *Brain Research*, *928*(1-2), 113-125. [http://dx.doi.org/10.1016/s0006-8993\(01\)03369-8](http://dx.doi.org/10.1016/s0006-8993(01)03369-8)
- Zincarelli, C., Soltys, S., Rengo, G., & Rabinowitz, J. (2008). Analysis of AAV Serotypes 1-9 Mediated Gene Expression and Tropism in Mice After Systemic Injection. *Molecular Therapy*, *16*(6), 1073-1080. <http://dx.doi.org/10.1038/mt.2008.76>

CHAPTER 4

Concluding Remarks for PACAP's Role in the Ventromedial Nucleus and its Association with the Melanocortin System in Regulating Adaptive Thermogenesis

4.1 SUMMARY

The work presented in this thesis was completed to address the hypothesis that: (A) PACAP acts upstream from the melanocortin system to regulate SNA to stimulate adaptive thermogenesis in BAT (Chapter 2) (Figure 4.1), and (B) that the cold sensitivity of PACAP $-/-$ mice may be due to the absence of PACAP signaling within the VMN specifically (Chapter 3) (Figure 4.1).

The objectives of this research were:

1. To determine if the impaired thermogenesis in PACAP $-/-$ mice could be rescued pharmacologically with a melanocortin agonist, Melanotan II (MTII), and thus provide evidence using a genetic model of PACAP deficiency for the connection between PACAP and the melanocortin system in regulating thermogenesis in BAT
2. To create an adenoviral construct that expresses GFP under the regulation of the SF1 promoter to act as a control vector to be used in stereotaxic surgery, thus ensuring VMN-specific expression of the vector
3. To devise a protocol for stereotaxic injections that reached the VMN in live animals

Objectives 2 and 3 were devised as preliminary steps for the following future objective:

4. To create an adenoviral construct for VMN-specific expression of PACAP to determine if the impaired thermogenesis in PACAP $-/-$ mice can be genetically rescued by transgenic expression of PACAP in the VMN only, thus determining the importance of VMN PACAP in regulating thermogenesis

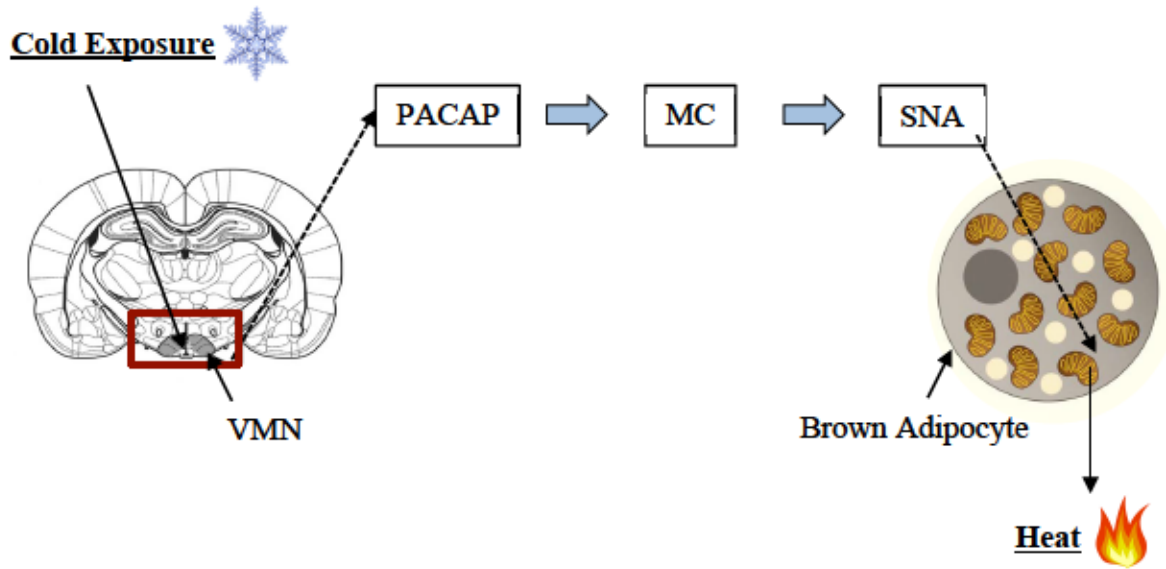


Figure 4.1. Hypothesized pathways of interaction for adaptive thermogenesis in BAT in response to cold exposure. VMN; ventromedial nucleus, PACAP; pituitary adenylate cyclase-activating polypeptide, MC; melanocortin system, SNA; sympathetic nerve activity, BAT; brown adipose tissue. Images adapted from “Revisiting the Ventral Medial Nucleus of the Hypothalamus: The Roles of SF-1 Neurons in Energy Homeostasis”, by Y. Choi, T. Fujikawa, J. Lee, A. Reuter, & K. Kim, 2013, *Frontiers In Neuroscience*, 7. Copyright © 2013 Choi, Fujikawa, Lee, Reuter and Kim. Adapted with permission from author.

Chapter 2 addressed the hypothesis and research aim 1 through the evaluation of thermogenic capacity of cold-acclimated MTII treated PACAP $-/-$ mice, using physiological (body weight and composition, metabolic rate (open circuit calorimetry), and respiratory exchange ratio (RER)), molecular (thermogenic gene expression), and histological (lipid area and cell count) analyses. Results indicate that through activation of the melanocortin system with peripheral injections of the MC4R agonist MTII, the impaired thermogenesis of cold-acclimated PACAP $-/-$ mice was partially rescued. This finding provides preliminary evidence to support the hypothesis that PACAP acts upstream from the melanocortin system in regulating SNA to BAT to induce adaptive thermogenesis during cold exposure. This preliminary evidence supports the available, but limited, literature with the use of a genetic model of PACAP $-/-$ mice and therefore adds significant value to the current pool of research. Future analyses will help support or refute the partial physiological rescue of adaptive thermogenesis with MTII treatment of cold-acclimated PACAP $-/-$ mice and will include: increasing sample size to more robustly measure gene and protein expression of thermogenic proteins in BAT, ingWAT, and gWAT depots, and performing further histological analyses of adipose tissues to identify characteristics of thermogenically active adipose tissue (such as measuring lipid content and browning in ingWAT and gWAT depots).

Chapter 3 addressed the hypothesis through research aim 2 and 3, which were vital preliminary steps for the future research aim 4. Aim 2 ensured that the constructs for the VMN-specific adeno-associated viruses were properly designed and created such that future viral injections into the VMN via stereotaxic surgery will prove safe and effective. Aim 3 further ensured safe and effective stereotaxic surgery through the development of appropriate stereotaxic injection protocols. Protocols were devised through the attendance of stereotaxic surgery workshops, as well as through visualization of the brain post-injections to

preliminarily assess the efficacy of the ICV-VMN injections. The overarching future aim of this project is to genetically reintroduce PACAP in PACAP *-/-* mice in neurons of the VMN only, and assess if the impaired thermogenesis is improved (or rescued). Changes in thermogenic capacity will be measured via physiological and biochemical assessments of thermogenic markers used in Chapter 2.

4.2 SIGNIFICANCE

Obesity is both a debilitating disease as well as a risk factor for a number of other chronic metabolic diseases; the consequences of which range from decreased quality of life to premature death (Lidell, Betz, & Enerbäck, 2014; WHO, 2016). Repercussions of the disease are high, both at the individual level with patient suffering, as well as the societal level with increased economic burden (Lidell et al., 2014, Uzogara, 2017). To provide appropriate prevention and management for this disease, the mechanisms of action resulting in the disease must initially be understood. With obesity, the disrupted mechanism in question is energy homeostasis, controlled both by energy intake and energy expenditure (Farooqi & O’Rahilly, 2006; Hinney, Vogel, & Hebebrand, 2010). Despite lifestyle interventions that suggest decreasing food intake and increasing physical activity, the prevalence of adult obesity continues to rise (Galic et al., 2010; WHO, 2016) Therefore, it has become evident that further exploration into the pathophysiology of the disease is necessary to prevent and manage this disease effectively (Galic et al., 2010; WHO, 2016). Here, the research was focused on energy expenditure, which is comprised of many systems and mechanisms, one of which is adaptive thermogenesis in BAT (Blondin et al., 2014; Lidell et al., 2014; Peirce et al., 2014). The greatest physiological stimulus regulating adaptive thermogenesis is via SNA where the release of NE acts directly at the level of brown adipocytes to generate heat in the body via the thermogenic protein, UCP1 (Lidell et

al., 2014; Peirce et al., 2014; Saito, Yoneshiro, & Matsushita, 2016). Furthermore, as proposed in this thesis, it is hypothesized that PACAP and the melanocortin system act in the VMN to regulate SNA that drives adaptive thermogenesis (Diané et al., 2014; Gray et al., 2002; Tanida, Shintani, & Hashimoto, 2011). Ultimately, understanding the role of PACAP in the VMN and its association with the melanocortin system in regulating SNA to stimulate adaptive thermogenesis in BAT will provide further knowledge regarding one of the many pathways regulating energy expenditure. Because metabolic diseases, including obesity, are examples of dysregulated energy homeostasis, determining how and where normal physiology goes awry (pathophysiology) will potentially provide therapeutic targets to help correct these detrimental diseases, either through lifestyle interventions, pharmacological interventions, or both.

For example, because activation of the sympathetic nervous system (SNS) has been shown to increase BAT activation and thermogenesis, anti-obesity pharmaceuticals such as sibutramine and ephedra were developed to stimulate the SNS (Saito, Yoneshiro, & Matsushita, 2016). However, research has shown that activating the SNS alone through the use of these pharmaceuticals is not an appropriate option for weight loss, as they are known to cause undesirable and dangerous side effects including hepatotoxicity, cardiovascular complications, and sudden death (Yen, & Ewald, 2012). As such, further research into particular mechanisms of energy metabolism will allow for the optimization of the thermogenic capacity of BAT without side effects derived with SNS activation. Potentially, this may be through selective stimulation of the SNS to BAT, other modes of BAT activation beyond the SNS, or other avenues of energy homeostasis altogether. Altogether, understanding the biological mechanisms that contribute to the health crisis of obesity is critical in developing interventions to reduce its prevalence.

Lastly, regardless as to whether appropriate lifestyle interventions or therapeutic targets are derived from this area of research, there is still an absolutely clear benefit: that is, providing evidence that the disease of obesity involves more than simply increasing one's self-control, eating less, and exercising more. Helping to eliminate this stigma by providing physiological evidence that energy metabolism is deeply seeded in hormonal control through the body's metabolic systems is an incontrovertible advancement resulting from this area of research.

4.3 REFERENCES

- Blondin, D., Labbé, S., Phoenix, S., Guérin, B., Turcotte, É., & Richard, D. et al. (2014). Contributions of white and brown adipose tissues and skeletal muscles to acute cold-induced metabolic responses in healthy men. *J Physiol*, *593*(3), 701-714. <http://dx.doi.org/10.1113/jphysiol.2014.283598>
- Choi, Y., Fujikawa, T., Lee, J., Reuter, A., & Kim, K. (2013). Revisiting the Ventral Medial Nucleus of the Hypothalamus: The Roles of SF-1 Neurons in Energy Homeostasis. *Frontiers In Neuroscience*, *7*. <http://dx.doi.org/10.3389/fnins.2013.00071>
- Diané, A., Nikolic, N., Rudecki, A., King, S., Bowie, D., & Gray, S. (2014). PACAP is essential for the adaptive thermogenic response of brown adipose tissue to cold exposure. *Journal Of Endocrinology*, *222*(3), 327-339. <http://dx.doi.org/10.1530/joe-14-0316>
- Farooqi, I. & O'Rahilly, S. (2006). Genetics of Obesity in Humans. *Endocrine Reviews*, *27*(7), 710-718. <http://dx.doi.org/10.1210/er.2006-0040>
- Galic, S., Oakhill, J., & Steinberg, G. (2010). Adipose tissue as an endocrine organ. *Molecular And Cellular Endocrinology*, *316*(2), 129-139. <http://dx.doi.org/10.1016/j.mce.2009.08.018>
- Gray, S., Yamaguchi, N., Vencova, P., & Sherwood, N. (2002). Temperature-Sensitive Phenotype in Mice Lacking Pituitary Adenylate Cyclase-Activating Polypeptide. *Endocrinology*, *143*(10), 3946-3954. <http://dx.doi.org/10.1210/en.2002-220401>
- Hinney, A., Vogel, C., & Hebebrand, J. (2010). From monogenic to polygenic obesity: recent advances. *European Child & Adolescent Psychiatry*, *19*(3), 297-310. <http://dx.doi.org/10.1007/s00787-010-0096-6>
- Lidell, M., Betz, M., & Enerbäck, S. (2014). Brown adipose tissue and its therapeutic potential. *J Intern Med*, *276*(4), 364-377. <http://dx.doi.org/10.1111/joim.12255>
- Peirce, V., Carobbio, S., & Vidal-Puig, A. (2014). The different shades of fat. *Nature*, *510*(7503), 76-83. <http://dx.doi.org/10.1038/nature13477>
- Saito, M., Yoneshiro, T., & Matsushita, M. (2016). Activation and recruitment of brown adipose tissue by cold exposure and food ingredients in humans. *Best Practice & Research Clinical Endocrinology & Metabolism*, *30*(4), 537-547. <http://dx.doi.org/10.1016/j.beem.2016.08.003>
- Tanida, M., Shintani, N., & Hashimoto, H. (2011). The melanocortin system is involved in regulating autonomic nerve activity through central pituitary adenylate cyclase-activating polypeptide. *Neuroscience Research*, *70*(1), 55-61. <http://dx.doi.org/10.1016/j.neures.2011.01.014>

Uzogara, S. (2017). Obesity Epidemic, Medical and Quality of Life Consequences: A Review. *International Journal Of Public Health Research*, 5(1), 1-12. Retrieved from <http://www.openscienceonline.com/journal/ijphr>

WHO | *Controlling the global obesity epidemic*. (2016). *Who.int*. Retrieved 2 June 2016, from <http://www.who.int/nutrition/topics/obesity/en/>

WHO | *Obesity*. (2016). *Who.int*. Retrieved 2 June 2016, from http://www.who.int/gho/ncd/risk_factors/obesity_text/en/

Yen, M., & Ewald, M. (2012). Toxicity of Weight Loss Agents. *Journal Of Medical Toxicology*, 8(2), 145-152. <http://dx.doi.org/10.1007/s13181-012-0213-7>